SAPIENZA
UNIVERSITÀ DI ROMA

UNORIENTED DUALITIES IN MASS DEFORMED TORIC GAUGE THEORIES

Scuola di Dottorato Vito Volterra
Dottorato di Ricerca in Fisica - XXXIV Ciclo

Salvatore Innoccenzo Mancani
ID number 1840861

Advisor
Prof. Fabio Riccioni

Co-Advisor
Prof. Massimo Bianchi

Academic Year 2020-2021

Unoriented dualities in mass deformed toric gauge theories
Sapienza University of Rome

This thesis has been typeset by LaTeX and the Sapthesis class.

Author's email: salvo.mancani@uniroma1.it

Abstract

This thesis focuses on a certain class of supersymmetric gauge theories. In particular, we study the interplay between relevant mass deformations of these theories and a projection known as orientifold. Using the usual tools for $\mathcal{N} = 1$ theories, such as anomaly matching and a-maximization, we look for the conditions for the theories to be conformally invariant after the projection and classify the possible outcomes into three scenarios. We find that for certain families of models the mass deformation is no longer relevant, as symmetries constrain this to be exactly marginal. Moreover, we find a web of dualities that connects these projected models and construct infinitely many non-chiral examples, along with a single dual chiral pair. The theories of interest arise as the gauge side of the AdS/CFT correspondence, while their gravity side is defined over the so-called toric geometries. Thus, projection and deformation have a geometric counterpart in the gravity theory. In this context, we use tools as brane tiling to construct our models. However, the geometric interpretation associated with our new found web of dualities is not completely understood.

This thesis is divided into six chapters. The first three introduce concepts and tools that will be used in chapters 4, 5, and 6, which represent the original part of the thesis and where it is given a classification of orientifold of orbifold models and their mass deformation, along with arguments for a new duality in the context of unoriented models. These are based on the following publications

- [1]: M. Bianchi, D. Bufalini, S. Mancani and F. Riccioni, *"Mass deformations of unoriented quiver theories", JHEP*, **07** (2020), hep-th/2003.09620;
- [2]: A. Antinucci, S. Mancani and F. Riccioni, *"Infrared duality in unoriented Pseudo del Pezzo", Phys. Lett. B*, **811** (2020), hep-th/2007.14749;
- [3]: A. Antinucci, M. Bianchi, S. Mancani and F. Riccioni, *"Suspended Fixed Points", Nucl. Phys. B*, **976** (2021), hep-th/2105.06195.

Acknowledgements

Il percorso che si conclude con la stesura di questa tesi ha richiesto una mole di energie fisiche e mentali che mai avrei immaginato. Il cambiamento e l'esperienza maturata è stata dovuta non solo ai miei sforzi, ma anche alle persone presenti. Non voglio essere banale, ma sicuramente mi hanno aiutato a trovare le motivazioni lungo la strada ed è quindi doveroso spendere alcune parole.

Per prima cosa vorrei ringraziare i miei supervisor, Fabio Riccioni e Massimo Bianchi, sia per avermi introdotto al più affascinante dei modi di vedere il mondo sia per avermi consigliato e insegnato il lavoro in questi tre anni. Ho sentito fiducia da parte loro, che è stata fondamentale nei momenti 'ora lascio tutto'.

Il confronto con colleghi e collaboratori prima ed amici poi è stato cruciale per la mia crescita. Ho imparato da, invidiato durante e apprezzato tantissimo le chiaccherate con Davide Bufalini e Andrea Antinucci e sono davvero orgoglioso di aver pubblicato dei lavori insieme a loro. Indelebili le riflessioni sul modo di vedere e di insultare il percorso di dottorato assieme ad Alfredo Grillo, e sono sicuro che continueremo a farle.

Ho amato Roma, più della mia terra natale. I ricordi che questa città mi ha dato non si limitano solamente alla sua scoperta, cosa che non ho poi fatto abbastanza, ma anche agli incontri ed alle amicizie strette. Ho ritrovato Giorgio, fin dall'inizio dell'avventura, e questi anni sono stati allegeriti da Mauro, Andrea, Chiara e Alessia, Taira, Stefano, Iris e tutta la OCERGIP 413. Sono stato il coinquilino fastidioso di Paolo, Leo e Lorenzo ma sappiate che quei tempi mi mancano. Non posso poi non ringraziare in maniera particolare Frank, Andrea e Noemi per i momenti passati assieme ed il legame che abbiamo stretto.

Ho tentato di mettere piede fuori dall'Italia e sono grato di aver trovato l'appoggio di Iolanda e Graziano, e di aver incontrato Julius, Zhenghao, Matthew, Matthew e Angie e tutta la famiglia dell'Imperial che mi ha accolto durante la mia troppo breve visita a Londra. Sono anche stato il coinquilino non così tanto fastidioso di Giorgos, Saurabh, Georgia e Lorenza. Spero di rivedervi tutti presto.

Infine, l'affetto incondizionato di Anthony, Francesco e Giuseppe, i miei cugini e sopra tutti i miei genitori ha rappresentato un'àncora durante questo percorso, fino alla fine. Vi ringrazio dal profondo.

A journey ends with this manuscript. I would have never imagined the amount of physical and mental energy it demanded. The personal experience and growth was shaped not only by my efforts but also by the people I met. I do not want to say something that one commonly says, but definitely they helped me in finding motivations along the way, so I feel I need to spend some words.

First of all, I want to thank my supervisors Fabio Riccioni and Massimo Bianchi, for having introduced me to the most fascinating way of perceiving the world and having guided in and teached me this job during the last three years. I felt their trust in me, fundamental in those 'I better give

up' moments.

I feel that discussions with collaborators, and then friends, have been crucial for personal growth. I learned from, envy during, and I am glad we had those chats and talks with Davide Bufalini and Andrea Antinucci, and I am very proud of having published with them. Together with Alfredo Grillo we shared perspective and insulted the PhD program, and I am quite sure we will keep doing this.

I loved Rome, even more than my homeland. I have enjoyed discovering the city, which I should have done more, but the memories involve also the people and friend I met. I found again Giorgio, from the beginning of this adventure, and these years have been eased off by Mauro, Andrea, Chiara and Alessia, Taira, Stefano, Iris and all from the office OCERGIP 413. I was the annoying flatmate of Paolo, Leo and Lorenzo, and I really miss those times. I particularly want to thank Frank, Andrea and Noemi for all those moments and the bond we have formed.

I went abroad and I was happy to find again Graziano and Iolanda, and to meet Julius, Zhenghao, Matthew, Matthew and Angie and the whole Imperial family who warmly welcomed me during my too short visit in London. There, I was the not-so-annoying housemate of Giorgos, Saurabh, Georgia and Lorenza, I hope I will see you again soon.

At last, for the unconditional love by old friends Anthony, Francesco and Giuseppe, my cousins and, above all, my parents, I thank you all from the heart.

Contents

Introduction

Our understanding of quantum physics relies on the dynamics of point particles, and the framework that sets the rules is quantum field theory. One of the greatest achievements of modern physics is the realization of the Standard Model (SM) along with the numerous experiments in agreement with its theoretical predictions. And yet, after roughly a century, many problems are left open and unsolved, above all the absence of gravity, as an unfinished puzzle that needs more pieces but it is not known where these can be found.

The heart of the issue is that the Standard Model is an effective description of the universe, limited to scales of energies we have been able to explore and, to a certain extent, comprehend. Alongside this aspect, in the framework of quantum field theory we have actual control over perturbative regimes, whereas the dynamics at strong coupling is simply hard to manage. The bottom line is that energy and couplings govern the physics and its description, in facts they are the parameters of a quantum field theory.

In this context, symmetry is the guiding tool and principle that allows to select models among others. While on one side a symmetry lets us formulate a theory in an elegant way and provides some physical intuition on the dynamics, on the other the more constraints that it imposes make some computations manageable. The Standard Model is in the first place a model of a certain local symmetry, known as gauge. The idea, and hope, that perhaps what is beyond the SM is determined by symmetry principles was a support for supersymmetry. Even though through the years it has not met the same experimental success of the SM, supersymmetry represents an unprecedented tool in understanding strongly coupled sectors of a quantum field theory, constraining the form of the interactions.

The paradigm of point particle could be problematic if we think of a particle as a probe for a certain system, because there is no limit on the energy scale that it can reach and this is a source for ultra-violet divergences. An attempt to deviate from this paradigm was given by Veneziano, who wrote down an amplitude trying to reproduce the phenomena of strong interaction and that was related to line objects, open strings. It became clear that the dynamics of these strings is quite rich and they also allow for closed strings. The vibration modes of both open and closed strings can reproduce the behaviour of particles, if strings are seen from a large distance. The spectrum produced by these modes not only contains the usual fields of gauge interactions, but also, surprisingly, gravity. While this sounds promising, the bosonic model of strings has an unstable

vacuum. Supersymmetry solves this problem, at the same time naturally introducing fermions in the spectrum. Demanding the resulting superstring theory to be consistent at a quantum level determines the dimension of spacetime to be 10.

In quantum corrections of string theory is hidden a novel relation between gauge interactions and gravity. In fact, contributions from open and closed strings are balanced, a fact that results in curing those ultra-violet divergences. After all, a probe with an associated length has a natural cut-off already built-in. A single framework solves many issues of modern physics, and in its foundations open strings and gauge interactions are dual to closed strings and gravity. However, together with the answers, new questions arised. The most prominent seems: where are the extra 6 dimensions in the world we see? A simple idea is that they are compact, but this has consequences. For example, strings can be wrapped along these compact directions, so that the effective theory would be 4 dimensional and whose properties depend on the details of the compact space. The spectrum given by strings wrapped around a compact space of a certain radius matches the one from strings wrapped around a space of inverse radius, a duality known as T-duality. Dualities such as this have been crucial in the development of the theory.

Apart from strings, extended objects are present as solutions of localised energy, solitons, whose tension is inversely proportional to the string coupling. These states are called Dp-branes, which decouple from strings states in the perturbative regime, while in the strong coupling limit the manageable description is based on branes. These extended objects provides a laboratory in which the duality between gauge interactions and gravity can be expressed in another way. Branes can be used as probes for a certain geometry, and strings vibrating on the brane will define a field theory: the local physics near the brane itself is determined by the property of the spacetime.

In this spirit, the AdS/CFT correspondence arose around twenty years ago and it says that a theory of gravity in a spacetime of the form 5-d Anti de Sitter $\times$ 5-d compact space is dual to a conformal supersymmetric field theory living on the boundary of the AdS part. We will give these words a context, for now the idea is that two seemingly different systems, closed strings and particles, can describe the same physics, i.e. they give the same observables. In this sense they are dual. This gauge/gravity duality relates theories on different spacetime dimensions, realizing the idea of the holographic principle that degrees of freedom inside a volume can actually be encoded on its boundary. Moreover, the two sides of the correspondence are defined at opposite regimes of couplings, meaning that actually a low curvature geometry is dual to a strongly-coupled gauge field theory, unveiling the non-perturbative regime.

The situation truly becomes interesting when branes probe a singular space. In fact, strings will smooth out the singularity, and features such as global symmetries of the gauge side of the correspondence depend on isometries of the singularity itself, properties encoded in the compact space transverse to AdS. The holographic duality is a realization of the intimate connection between geometry and physics that translates isometries on gravity side into symmetries of the gauge theory.

The development of String Theory has gone through various revolutions over the years, unfortunately never reaching the ultimate goal of obtaining the Standard Model as an effective theory at some low energy scale. In the attempts of embedding the SM into the framework of strings,

a crucial ingredient is represented by the orientifold projection. This reflects some spacetime directions and project out half of string modes, acting, roughly speaking, as a mirror. Even recent works address the SM and cosmological problems exploiting such orientifold involution. Then, it is worth studying the dynamics of field theories arising from probes of an unoriented spacetime.

In the end, the framework of String Theory is a laboratory made by tools as strings, branes, orientifold and dualities. In this thesis we focus on certain singular spaces called *toric*, whose holographic gauge dual can be systematically constructed from a set of geometric data encoded in polygons called *toric diagrams*. We investigate the consequences of the orientifold projection upon these models and in particular the fate of the conformal point in the resulting unoriented gauge theories. The orientifold projection usually breaks conformal invariance, but we will show evidences for a new scenario, where in the unoriented theory conformal invariance is restored in the infrared. This is only part of the story, as we will give arguments also for these new-found fixed point to be dual to another unoriented gauge theory. We will show that a web of dualities connects families of non-chiral models. Interestingly, before the orientifold these families are different, but related to a mother theory via relevant deformations that give mass to some fields in the spectrum. In light of the geometric connection of the AdS/CFT correspondence, the expectation is that different singular geometries are dual in some sense, if not the same, after the orientifold projection. However, a complete understading of the geometric counterpart of these field theory results is still missing.

The thesis is ideally divided into two parts, each organised as follows. The first three chapters introduce the background for constructing the unoriented theories of interest. In particular, Chapter 1 gives some basics on toric geometry and constructs a graph called *brane tiling* from geometric data of the toric polygon. The brane tiling allows to read the gauge theory associated with the given geometry. Chapter 2 focuses on $\mathcal{N} = 1$ gauge theories and their conformal point, as we play on this ground for our analysis. Chapter 3 introduces the orientifold projection and explains how to construct unoriented theories from a given brane tiling, setting the stage for the scenarios we are going to explore. The last three chapters belong to the second part of this thesis. In chapter 4 is given a systematic construction of the orientifold projection of known toric theories, many connected by mass deformations. Chapter 5 is dedicated to the mechanism that yields the new scenario for unoriented conformal theories and construct infinite-classes of non-chiral models in which this occurs. The chapter also shows that pairs of unoriented gauge theories are dual to each other. Chapter 6 presents the only chiral pair of theories that, to the best of the author's knowledge, features the new scenario and the duality. Finally, conclusions are drawn in the last dedicated chapter.

Chapter 1

Gauge/gravity duality and brane tiling

Inspired by the Bekenstein entropy of a black hole [4] that is proportional to the area of the event horizon, the holographic principle [5, 6] states that in a theory of quantum gravity in the semiclassical regime the information stored in a certain volume V_{d+1} of $(d+1)$ dimensions is encoded in its boundary A_d. The AdS/CFT correspondence, also known as holographic duality or gauge/gravity duality, is the first realization of the holographic principle and it arises naturally in the context of String Theory.

1.1 A spherical horizon

The AdS/CFT correspondence [7–10] states that a theory of gravity defined on a 10-dimensional spacetime of the form $\mathrm{AdS}_5 \times Y_5$, where AdS_5 is a 5-dimensional Anti de Sitter spacetime and Y_5 a 5-dimensional compact space, is holographically dual to a superconformal gauge theory living on the 4-dimensional conformal boundary of AdS_5. Let us clarify this statement showing the original formulation of the correspondence, following [11].

Let us first state some conventions, as capital latin letters as $M, N, \ldots$ for directions in 10-d, greeks letters as $\mu, \nu, \ldots$ for directions in 4-d and small latin letters $i, j, \ldots$ for the six extra directions. In type IIB string theory, consider a stack of N D3 branes in flat spacetime. The free parameters are the string coupling g_s and $\alpha' = l_s^2$, with l_s the string length. Being α' a dimensionful quantity, we need a length scale in the setup, or equivalently an energy scale, so that we can compare it to $\sqrt{\alpha'}$. Let us take $g_s \to 0$, the perturbative regime in string theory. We can think of the D3 branes as hyperplanes on which open strings are attached, and they do not backreact on the geometry. At low energies, i.e. $E \ll 1/\sqrt{\alpha'}$, the dynamics of open strings attached to the D3 branes is determined by a supersymmetric gauge theory living in the world-volume (WV) of the branes, with gauge group $U(N)$ and $\mathcal{N} = 4$ supersymmetry. On the other hand, the D3

branes are sources for closed strings, which propagate in flat spacetime. The complete action for massless string modes is given by

$$\mathcal{S} = \mathcal{S}_{\text{closed}} + \mathcal{S}_{\text{open}} + \mathcal{S}_{\text{int}} \ , \tag{1.1}$$

where the last term stands for the interaction between open and closed strings. In terms of metric fluctuations h, the terms in Eq. (1.1) are

$$\begin{aligned}
\mathcal{S}_{\text{closed}} &\sim -\frac{1}{2}\int d^{10}x\ \partial_M h\, \partial^M h + \mathcal{O}(\kappa) \ , \\
\mathcal{S}_{\text{open}} &\sim -\frac{1}{2\pi g_s}\int d^4x \left[\frac{1}{4}F^a_{\mu\nu}F^{a\,\mu\nu} + \frac{1}{2}\partial_\mu\phi^i\partial^\mu\phi^i + V_{\text{scalar}} + \mathcal{O}(\alpha')\right] \ , \\
\mathcal{S}_{\text{int}} &\sim -\frac{1}{8\pi g_s}\int d^4x\ \phi F^a_{\mu\nu}F^{a\,\mu\nu} + \dots \ ,
\end{aligned} \tag{1.2}$$

where $F^a_{\mu\nu}$ is the field strength under the gauge group $U(N)$, ϕ is the dilaton field, ϕ^i are the scalar fields indexed by directions transverse to the D3 branes and V_{scalar} is their scalar potential, and $\kappa = (2\pi)^{7/2}(\alpha')^2 g_s/2$. In order to ensure canonical normalization we need to rescale the dilaton field by κ, and $\mathcal{S}_{\text{int}} \sim (\alpha')^2$. Hence, if we take the particle limit of strings $\alpha' \to 0$, $\mathcal{S}_{\text{closed}}$ describes free supergravity in flat spacetime, $\mathcal{S}_{\text{open}}$ describes the bosonic part of $\mathcal{N} = 4$ YM with

$$2\pi g_s = g^2_{_{YM}} \ , \tag{1.3}$$

while open and closed strings sectors decouple[1]. The effective gauge coupling of the perturbative expansion in the YM theory is $g^2_{YM}N = \lambda$, called 't Hooft coupling. Therefore, the perturbative regime of strings is reliable for $g_sN \ll 1$. Keeping the t Hooft coupling fixed, we take the limit $N \to \infty$, known as the planar limit of the gauge theory, at which the $1/N$ expansion of the field theory is mapped to a genus expansion of the string worldsheet.

In order to explore the strong coupling limit of the gauge theory we should take $\lambda \to \infty$. In this regime, the D3 branes curve the spacetime and the metric reads

$$ds^2 = \left(1 + \frac{L^4}{r^4}\right)^{-\frac{1}{2}} \eta_{\mu\nu}dx^\mu dx^\nu + \left(1 + \frac{L^4}{r^4}\right)^{\frac{1}{2}} \left(dr^2 + r^2 ds^2_{S^5}\right) \ , \tag{1.4}$$

where the 5-dimensional sphere supports the flux of the 5-form F_5, which is quantized and gives

$$L^4 = 4\pi g_s N \alpha'^2 \ . \tag{1.5}$$

While the asymptotic region $r \gg L$ reduces to 10-dimensional flat spacetime, the region $r \ll L$,

[1] To take properly this decoupling limit, we keep the ratio r/α' fixed, where r is the distance from the D3 branes. It is called the Maldacena limit.

called near horizon geometry or throat, yields

$$\begin{aligned} ds^2 &= \frac{r^2}{L^2}\eta_{\mu\nu}dx^\mu dx^\nu + \frac{L^2}{r^2}\left(dr^2 + r^2 ds^2_{S^5}\right) \\ &= ds^2_{AdS_5} + L^2 ds^2_{S^5} \ . \end{aligned} \tag{1.6}$$

We can see that the spacetime takes the form $\mathrm{AdS}_5 \times S^5$ and L is the curvature radius of both the Anti de Sitter spacetime and the sphere. Note that in the limit $g_s N \gg 1$, $L^2 \gg \alpha'$ so the radius is much larger than the string length. Due to the redshift, all states through the throat are seen as low energy states at infinity, and hence the dynamics of closed strings in the asymptotic region $r \gg L$ decouples from the dynamics of closed strings in the near horizon region $r \ll L$. By comparing the physics at the two regimes of $g_s N$, Maldacena in [7] realised that a 4-dimensional $\mathcal{N} = 4$ SYM with gauge group[2] $SU(N)$ is dual to string theory on $\mathrm{AdS}_5 \times S^5$ with identifications

$$\begin{aligned} 2\pi g_s &= g^2_{YM} \ , \\ \frac{L^4}{\alpha'^2} &= 4\pi g_s N \ . \end{aligned} \tag{1.7}$$

The isometry of the 5-sphere is $SO(6) \cong SU(4)$, which is also the R-symmetry group of 4d $\mathcal{N} = 4$ SYM. The 't Hooft coupling $\lambda = g^2_{YM} N$ needs to be large, for the radius L to be much larger than l_s. Hence, the holographic duality is a non-perturbative statement that connects the low curvature regime of type IIB on AdS spacetime to a strongly-coupled SCFT.

1.2 Non-Spherical horizons

The original formulationo of the AdS/CFT correspondence is highly symmetric and perhaps this means also unrealistic. On the gauge side, we would like to have a field theory with the minimal number of supersymmetry, $\mathcal{N} = 1$. Based on what we said, this means that we need to deform the horizon into a space whose isometry contains an $U(1)$, which takes the role of the R-symmetry group for minimal supersymmetry. We consider then a stack of D3 branes transverse to a curved manifold. However, the physics of the dual gauge theory depends on the nature of the space around the point where the stack of branes is placed. Thus, if the manifold around that point is smooth, the physics is still $\mathcal{N} = 4$. As discussed in [12], the setup becomes interesting when the transverse space has a singularity and the branes brought to the singular point. The near horizon limit is still of the form $\mathrm{AdS}_5 \times Y_5$, and the properties of the horizon Y_5 determines the field theory of the gauge side, in particular the global symmetry. In order to have $\mathcal{N} = 1$, the holonomy group of the cone over Y_5 must be $SU(3)$, and for the cone being a Calabi-Yau (CY) three-fold, the horizon

[2] If you think that we are missing an abelian factor, you are right. We said $U(N)$ before, but $U(N) \cong SU(N) \times U(1)$, and the abelian factor corresponds to a free vector multiplet that describes the motion of the center of mass of the system of branes.

must be a 5-dimensional Sasaki-Einstein manifold. For the rest of this manuscript, we will consider orbifold singularities, obtained by quotienting the cone over the 5-sphere by a discrete subgroup of $SU(3)$[3], and deformations of these spaces. In particular, we shall consider toric CY cones, as we have more control on toric spaces. After giving definition and properties of toric spaces, we are going to introduce the machinery that allows us to read the dual SCFT from geometric data. In particular, we will construct quiver gauge theories and the so-called brane tiling.

1.3 Toric geometry

A d-dimensional toric variety is defined by a fan Σ, which is a collection of strongly rational polyhedral cones σ in R^d generated by $n \geq d$ vectors $v_i \in \mathbb{Z}_d$ such that

$$\begin{aligned} \sigma &= \left\{ \sum_{i=1}^{n} a_i v_i \mid a_i \geq 0 \right\} \\ \sigma \cap (-\sigma) &= 0 \ , \end{aligned} \tag{1.8}$$

so the apex of the cone stays at the origin and the edges are spanned by vectors v_i. To each of these vectors we associate a homogeneous coordinate $z_i \in \mathbb{C}$, and from the resulting $\mathbb{C}^n$, the set

$$V_\Sigma = \cup_I \left\{ (v_1, v_2, \ldots, v_n) \mid v_\alpha = 0 \ \ \forall \alpha \in I \right\} \ , \quad I \subseteq \{1, \ldots, n\} \ , \tag{1.9}$$

is quotiented out. The toric manifold $\mathcal{M}$ is then

$$\mathcal{M} = \frac{\mathbb{C}^n \setminus V_\Sigma}{(\mathbb{C}^\star)^{n-3} \times A} \ , \tag{1.10}$$

where A is an abelian group and $(\mathbb{C}^\star)^{n-3}$ acts as

$$\begin{aligned} &(v_1, v_2, \ldots, v_n) \sim (\lambda^{Q^1} v_1, \lambda^{Q^2} v_2, \ldots, \lambda^{Q^n} v_n) \ , \quad \lambda \in \mathbb{C}^\star \ , \\ &\sum_{i=1}^{n} Q_a^i v_i = 0 \ , \quad a = 1, \ldots, n-3 \ , \end{aligned} \tag{1.11}$$

where Q_a^i are $(n-3)$ charges called toric data. Having defined the toric variety, we want it to be a CY manifold. This happens when all the vectors v_i lie on the same hyperplane, condition that is

[3] One can construct orbifold singularities $\mathbb{C}^3/\Gamma$ with Γ an abelian [13] or non-abelian [14] subgroup of $SU(3)$ acting on $\mathbb{C}^3$. We shall work only with the abelian orbifold.

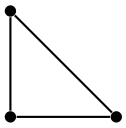

Figure 1.1a: The toric diagram of $\mathbb{C}^3$.

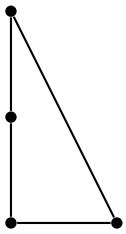

Figure 1.1b: The toric diagram of $\mathbb{C}^2/\mathbb{Z}_2 \times \mathbb{C}$.

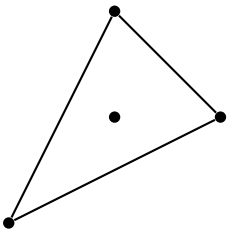

Figure 1.1c: The toric diagram of $\mathbb{C}^3/\mathbb{Z}_3$.

translated into a constraint for the charges Q_a^i

$$\sum_{i=1}^{n} Q_a^i = 0 \quad \forall a \ . \tag{1.12}$$

Moreover, this condition imposes also that the toric CY variety is non-compact. For the case of interest, a toric CY three-fold, the vectors v_i must lie on the same plane and therefore can be brought to the form $v_i = (1, w_i)$, with w_i lying on that two-dimensional lattice and spanning a graph. The dual graph is called the toric diagram and completely defines the fan Σ and, hence, the toric CY manifold. Examples of toric diagrams are displayed in Fig. 1.1a-1.1c. Note that the toric diagram is actually defined up to a $SL(2,\mathbb{Z})$ transformation, that can change the shape of the diagram but preserves the number of internal and external points, as well as the number of points in an edge. Finally, a toric CY three-fold has isometry $U(1)^3$, or an enhancement of rank 3. One of the abelian factors is identified with the R-symmetry of the dual SCFT arising in the WV of D3 branes probing a toric CY cone, while the remaining $U(1)^2$ is at the base of the construction we shall see in the next section. See [15–18] for further details on toric geometry.

1.4 Brane tiling

The configuration relevant for our purposes is made of N D3 branes placed on the tip of a toric CY cone, the singular point of the space. The toric space can be seen as a $\mathbb{T}^3$ fibration over the polytope given by the toric diagram, in particular the $\mathbb{T}^3$ degenerates to a $\mathbb{T}^2$ along the edges. We exploit the presence of the torus $\mathbb{T}^2$ in order to construct a fivebrane diagram, as we shall see. We follow closely [19], but we invite the reader to have a look at the original papers and reviews on brane tiling in order to find many more details [20–33].

1.4.1 A picture of five-branes

Consider a stack of D3 branes on the singular point of a toric CY cone, as in Tab. 1.1. The torus $\mathbb{T}^2$ of the toric space wraps, say, directions x_5 and x_7.

	0	1	2	3	4	5	6	7	8	9
D3	–	–	–	–						
CY_3					–	–	–	–	–	–

Table 1.1. D3-branes and toric CY threefold singularity.

Performing T-duality along these two directions results in a configuration with $D5$ branes, while the geometry turns into orthogonal NS5 branes as in Tab. 1.2

	0	1	2	3	4	5	6	7	8	9
D5	–	–	–	–		–		–		
NS5	–	–	–	–	–	–				
NS5'	–	–	–	–			–	–		

Table 1.2. D5-branes and NS5 branes T-dual to the configuration with D3 and CY_3.

The reason why we prefer this T-dual configuration is two-fold. First, the configuration of D3 branes at a CY singularity becomes a system of D5 and NS5 branes in flat spacetime. The information on the geometry is now encoded into the NS5s. This system of 5-branes can be complicated, but the tension of the branes are

$$\tau_{D5} \sim \frac{1}{g_s(\alpha')^3} \ , \quad \tau_{NS5} \sim \frac{1}{g_s^2(\alpha')^3} \tag{1.13}$$

and we can take the strong coupling limit where the 5-branes becomes flat and the NS5s are orthogonal to the D5. Second, we can easily count the amount of supersymmetry. In fact, since the three fivebranes do not wrap the same extra directions, supersymmetry is reduced by 1/8 and we end up with 4 supercharges. The D5 branes wrap the $\mathbb{T}^2$, so the theory living in its worldvolume is four dimensional, which means $\mathcal{N} = 1$.

Let us look closely at the system of fivebranes. We may have several parallel NS5 branes and NS5', which divide the WV of the D5 into different subregions. We identify these subregions with various gauge factors in the WV field theory. The important point is that at the junctions between the fivebranes, (p, q)-branes are formed, i.e. objects charged under both types of branes. We consider only $(N, 0)$, $(N, \pm 1)$ branes. To understand better their role, we introduce the fivebrane system as follows. Represent the $\mathbb{T}^2$ as a square with opposite boundaries identified, while the two orthogonal directions stands for the two 1-cycles of the torus. The D5s are wrapped around the graph while the NS5 wrap only 1-cycles, i.e. they are represented as arrows. Consider only one of them, it splits the graph into two regions, thus a NS5 divides the D5's WV. The NS5 charge jumps by one unit between the two regions, with the convention that the charge increases going to the right of the arrow and decreases to the left. Having a configuration of many NS5s, we obtain a web of intersecting arrows, generating the subregions we mentioned before.

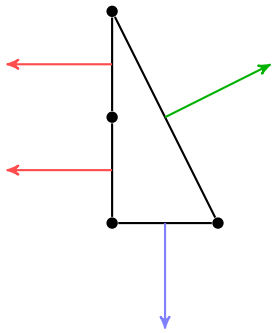

Figure 1.2a: The toric diagram of $\mathbb{C}^2/\mathbb{Z}_2 \times \mathbb{C}$ and the vectors orthogonal to the edges.

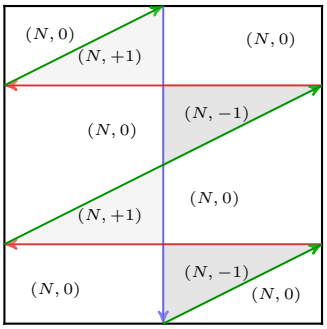

Figure 1.2b: The fivebrane diagram of $\mathbb{C}^2/\mathbb{Z}_2 \times \mathbb{C}$.

Let us clarify some points. We said that we take the strong coupling limit in order to have flat NS5 branes and produce a clear picture. In the weak coupling limit, the NS5 in the system recombine into a holomorphic curve that intersect some 1-cycles of the torus. Furthermore, the structure of the fivebrane diagram is directly related to the toric diagram, i.e. the toric geometry. Take the dual graph spanned by outgoing vectors orthogonal to the edge of the toric diagram, and embed these vectors on the planar graph representing the torus, obtaining the fivebrane diagram we have been constructing. A picture is worth a thousand words, so see Fig. 1.2a-1.2b where we work out the example of $\mathbb{C}^2/\mathbb{Z}_2 \times \mathbb{C}$.

Identified already the regiones $(N, 0)$ as gauge factors, $SU(N)$ in the 4d gauge theory, we can explore all other elements. At the intersections, massless open strings connect the two sub-parts of the D5 WV. Given the number of supersymmetries for the presence of NS5 branes, only strings in one direction are allowed, as can be seen directly from the fivebrane diagram and the vectors over it. In fact, the 4d theory is chiral[4]. Thus, at the intersection we have bifundamental chiral fields X_{ab} transforming under two gauge factors labelled with a and b. Note that the lower indices in X_{ab} denotes only the group labels and the direction from a to b, they are not gauge indices, which we are suppressing for the sake of clarity. The complete notation for X_{ab} would be $(X_{ab})_{i_a}{}^{j_b}$, where lower indices as i_a belongs to the fundamental representation, upper as j_b to the anti-fundamental.

These bifundamentals surround the regions $(N, \pm 1)$, going clockwise for $(+1)$ and counterclockwise for (-1). Note that these regions are topologically disks and at some points of the boundary massless open strings are inserted. We interpret these regions as disk amplitudes, and then as interaction terms in the 4d field theory. Then, these interaction terms are composed of bifundamental fields surrounding the disk, resulting in a trace operator whose sign is given by the direction around the disk itself,

$$\begin{aligned} (N,+1) \ : \quad & +(X_{ab})_{i_a}{}^{j_b}(X_{bc})_{j_b}{}^{l_c}\dots(X_{fa})_{k_f}{}^{i_a} = +\mathrm{Tr}\prod X_{ab}\dots \ , \\ (N,-1) \ : \quad & -(X_{ab})_{i_a}{}^{j_b}(X_{bc})_{j_b}{}^{l_c}\dots(X_{fa})_{k_f}{}^{i_a} = -\mathrm{Tr}\prod X_{ab}\dots \ . \end{aligned} \tag{1.14}$$

[4]Usually chiral. In some cases the matter content results in a non-chiral theory, and in others part of supersymmetry gets restored resulting in $\mathcal{N} = 2$. An example is $\mathbb{C}^2/\mathbb{Z}_n \times \mathbb{C}$.

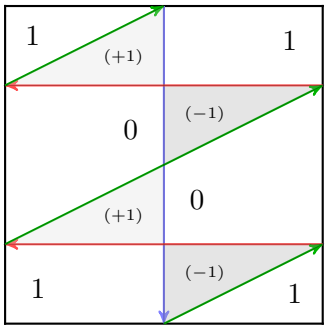

Figure 1.3: The fivebrane diagram of $\mathbb{C}^2/\mathbb{Z}_2 \times \mathbb{C}$. The gauge groups are labelled with 0 and 1.

As an example, look at the fivebrane of $\mathbb{C}^2/\mathbb{Z}_2 \times \mathbb{C}$ in Fig. 1.3, where the different gauge factors have been labelled[5] with 0 and 1. The bifundamental fields are

$$\begin{aligned} X^1_{01} &= (\square_0, \bar{\square}_1)^1 \quad , \quad X^1_{10} = (\square_1, \bar{\square}_0)^1 \\ X^2_{01} &= (\square_0, \bar{\square}_1)^2 \quad , \quad X^2_{10} = (\square_1, \bar{\square}_0)^2 \\ X_{00} = \phi_0 &= (\square_0, \bar{\square}_0) \quad , \quad X_{11} = \phi_1 = (\square_1, \bar{\square}_1) \end{aligned} \tag{1.15}$$

where the latter two fields are actually adjoints and the upper index is put to distinguish different fields with the same transformation rules. The superpotential can be read from the fivebrane diagram

$$W_{\mathbb{C}^2/\mathbb{Z}_2\times\mathbb{C}} = \phi_1 X^1_{10} X^2_{01} - \phi_1 X^2_{10} X^1_{01} + \phi_0 X^1_{01} X^2_{10} - \phi_0 X^2_{01} X^1_{10} \, . \tag{1.16}$$

One final step remains to turn the fivebrane diagram into the *brane tiling*. Shrink the disks into points, white point for $(+1)$ and black for (-1), and connect white points to black one by edges. We obtain a bipartite graph, as the edges represent the bifundamental fields. In fact, an edge is shared between two adjacent faces/gauge factors, with an orientation given by the direction from white to black points. This is the brane tiling, that encodes the information about the toric CY geometry and completely defines the dual gauge theory in the sense of the AdS/CFT correspondence. See Fig. 1.4 for the first example.

To sum up, a toric diagram specifies a certain toric geometry and from only the data in the diagram we can construct the brane tiling, which translates geometric information into the dual 4d gauge theory. The dictionary of this bipartite graph consists in: each face is a gauge factor $SU(N)_a$, each edge is a bifundamental field X_{ab} transforming under the adjacent faces, with an orientation given by the direction black to white, the nodes represent the superpotential terms.

Moreover, the bipartite nature of the graph descends from the toric condition. Being each node an interaction term, each field appears twice in the superpotential, once with positive sign and once

[5] We usually count the gauge factors starting from 0. It is for convenience, the reason will be clear when we discuss orbifold singularities and quivers in more detail.

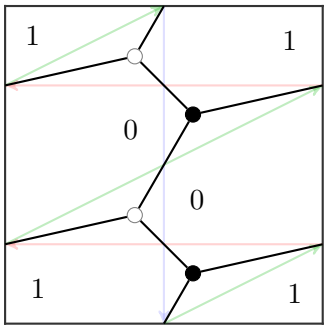

Figure 1.4: The brane tiling of $\mathbb{C}^2/\mathbb{Z}_2 \times \mathbb{C}$.

with negative sign. All interaction terms are monomial in the fields and written as trace operators. We say that they are mesonic operators, in contrast of baryonic operators usually in the form $\det \mathcal{O}$.

The global symmetry of the resulting gauge theory has several factors. Again, we divide them into mesonic and baryonic. The mesonic symmetry is the toric $U(1) \times U(1) \times U(1)_R$, which can get enhanced to a rank three group. For example, in $\mathbb{C}^2/\mathbb{Z}_2 \times \mathbb{C}$, an $SU(2)$ rotates X^i_{01}, another one rotates X^i_{10} instead. The baryonic factor is of the form $U(1)^{|G|-1}$, where $|G|$ is the number of gauge factors. This comes from the fact that each $(N, 0)$ region in the fivebrane diagram is actually a $U(N)$ group, but $U(N) \cong SU(N) \times U(1)$. The beta functions of the two factors behave differently and in the IR the $U(1)$ factor becomes weakly coupled and we consider it as a global symmetry. So, there as many global abelian factors as number of gauge factors, with the condition that they are non-anomalous, i.e. the ABJ anomaly (global)$\times$(gauge)^2 vanishes. There are finally $(|G| - 1)$ global $U(1)$ as the baryonic symmetry. The single $U(1)$ that is needed to ensure anomaly cancellation can be thought of as the center of mass of the system of branes that decouples in the IR.

1.5 The fast forward algorithm

We are going to close the circle and show how toric data are encoded in the brane tiling and how to retrieve them from the bipartite graph. Let us start by defining a perfect matching [21]: it is a set of fields that connect all nodes in the tiling exactly once. The statistical mechanics of a set of perfect matchings is called *dimer model*, for this reason we are going to use the words dimer and brane tiling interchangeably. From the brane tiling, one can define various perfect matchings and assign them a winding number around the fundamental cell of the torus, where the tiling is embedded. Choose two directions representing the two 1-cycles of the torus and a direction for the edges, say from white to black. With the example in Fig. 1.4 in mind, (h_a, h_b) will be the winding number around the two directions of the square fundamental cell, h_a goes horizontally and h_b vertically. We find 5 perfect matchings p_α, we list all of them and their winding numbers in Fig. 1.5. The winding numbers give exactly the coordinates of the toric diagram, up to a $SL(2, \mathbb{Z})$ transformation. Note that the internal point in the long side of the toric diagram has degeneracy

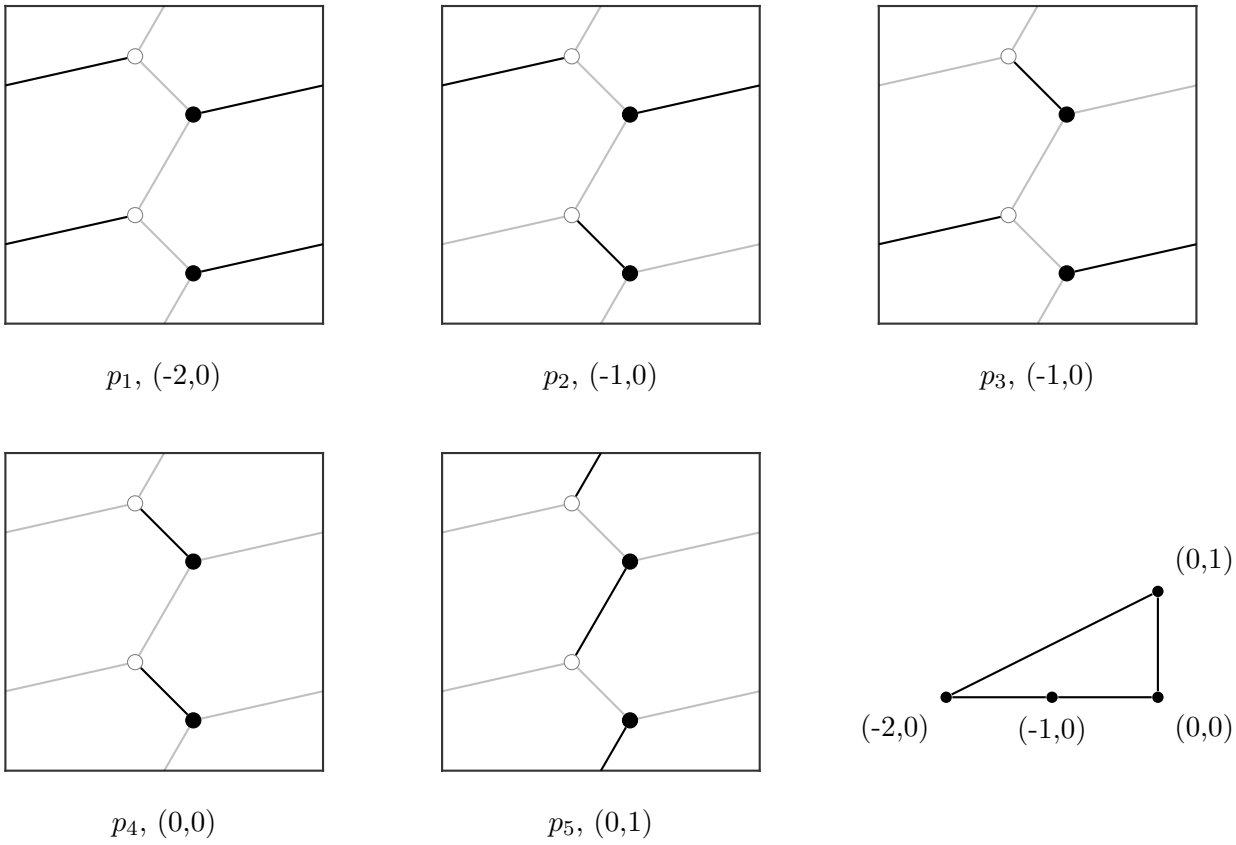

Figure 1.5. The list of all perfect matching for $\mathbb{C}^2/\mathbb{Z}_2 \times \mathbb{C}$, their winding numbers and the resulting toric diagram.

2, as two perfect matchings have the same winding numbers. Only non-extremal points may have degeneracy larger than 1, and there can be various toric diagrams with the same shape that differ for the degeneracy of these points. Associated to the same geometry, the relation between them is called toric duality and its counterpart in field theory side will be discussed in the next chapter.

1.6 Quiver gauge theories

Toric diagrams and brane tilings are powerful constructions that allow us to embed a gauge theory on a torus while storing information about the geometry. We are going to construct another way of representing a gauge theory, more convenient as the gauge group and matter content can be read more quickly but less powerful because we lose information about the geometry, and hence about the superpotential. The idea is to use a collection of nodes and arrows, called *quiver* [34–39], where each node is a gauge group $SU(N)$. For a general quiver each rank can differ one to another, whereas for a toric quiver all ranks are equal. These nodes are connected by arrows, bifundamental fields transforming in the fundamental of the outgoing node and in the antifundamental of the ingoing node. If we are starting from a brane tiling, we just need a dictionary to draw the associate

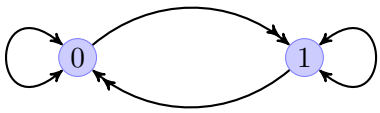

Figure 1.6: The quiver diagram for $\mathbb{C}^3/\mathbb{Z}_2$.

quiver as in Tab. 1.3.

Brane tiling	Quiver	Gauge theory
Face a	Node a	$SU(N)_a$
Edge $a\|b$	Arrow $a \to b$	$(\square_a, \overline{\square}_b)$

Table 1.3. The dictionary between tiling and quiver diagrams.

Coming back to our example $\mathbb{C}^2/\mathbb{Z}_2 \times \mathbb{C}$, from the brane tiling in Fig. 1.4 we get the quiver in Fig. 1.6. However, what we gain in convenience we lose in information as we still need to read the superpotential from the tiling to completely define the gauge theory. In case of simple examples we can guess what is the form by going around the quiver following the arrows and forming trace operators. Fig. 1.6 is a case, since it is an orbifold of $\mathbb{C}^3$ and all the terms are cubic, but in more involved instances, obtained by deformation of orbifolds, it is not granted.

1.6.1 Cancellation of gauge anomaly and fractional branes

A chiral gauge theory is physically meaningful if gauge anomalies vanish, so we need to ensure that this happens for all the cases. When dealing with toric gauge theories, all gauge factors have equal rank N, the number of D3 branes, and the matter content is such that the anomaly cancellation condition is already ensured. However, from the point of view of the quiver gauge theory, sometimes there are more choices of the ranks that cancels the anomaly and in principle the gauge theory is well-defined with all of them. In the rest of the manuscript, we assign general rank N_a to each node labelled by a and put constraints over them from gauge anomaly cancellation. It is easy to write down this condition once we have drawn the quiver as we need to account for fermions running inside a loop triangle with gauge currents attached. For each node in the quiver, say node a we add up the anomaly coefficients A_ρ associated with each arrow attached to the node, with a positive sign for outgoing arrows, being fundamental, and negative sign for ingoing arrows, begin antifundamental:

$$\sum_{\text{Outgoing } a} A_\rho - \sum_{\text{Ingoing } a} A_\rho = 0 \,, \tag{1.17}$$

where the anomaly coefficients depend on the representation. In case of bifundamental fields/arrows X_{ab}, their contribution is given by $(1 \times N_b)$, where N_b is the rank of node b. For the quiver in Fig. 1.6 the condition is trivially realised as

$$\begin{aligned} 2 \times N_1 - 2 \times N_1 = 0 \, , \\ 2 \times N_0 - 2 \times N_0 = 0 \, . \end{aligned} \tag{1.18}$$

since the theory is non-chiral and hence we can choose any N_0 and N_1. For a chiral theory, this condition put constraints on the ranks usually admitting some shifts between them. It is worth saying that this is not the only way to ensure anomaly cancellation, but it can be obtained by topological and geometric reasoning from the toric diagram and the brane tiling, considering that anomaly cancellation follows from RR charge conservation [40] and following the spirit of the correspondence, see [23, 41, 42].

The geometric meaning of shifts between the ranks, for instance a gauge factor with rank N and another with rank $N+M$, is related to the presence of M D5 branes wrapped around compact 2-cycles and hence they are stuck at the singularity, whereas N regular D3 branes can be moved away from the singular point. Fractional branes usually break conformal invariance and hence they induce a non-trivial RG-flow out of the fixed point. They are classified into three different classes, depending on the IR dynamics they trigger:

- deformation fractional branes, allowed when the toric geometry admits deformation of the complex structure. They break conformal invariance and along the flow to the infrared, the number of regular branes decreases. Tipically confinement occurs at the end of the flow.
- $\mathcal{N} = 2$ fractional branes, related to the present of internal points on the sides of the toric diagram. In these cases the geometry has a complex line of singularity rather than an isolated point, in particular $(k-1)$ internal points on a side gives rise to a line of $\mathbb{C}^2/\mathbb{Z}_k$ singularities.
- supersymmetry breaking fractional branes, which trigger a flow and in the infrared the theory has a dynamically generated superpotential that leads to supersymmetry breaking.

1.6.2 Flavour branes

We can add non-compact D7 branes to the system, which are called flavour branes. Their presence generates a D3-D7 open string sector and corresponding new matter fields. As the dynamics of the D7 is decoupled from the 4d dynamics in the WV of D3, the $U(N)$ group factors associated to the D7s are global symmetry factors. Consequentely, the additional matter fields transform in the fundamental or antifundamental of gauge factors, and antifundamental or fundamental of these global group factors. In a quiver diagram, they contribute with other nodes that we choose to draw as red squares, see Fig. 1.7 for an example of our convention. The inclusion of flavour branes on

Figure 1.7. The conventions of fields appearing in this work. On the left, two bifundamental fields transforming under gauge factors a and b, represented by blue nodes, center and right fields transforming under a gauge factor a and a flavour group α, in red. field

the brane tiling is discussed in the literature and they are nicely represented as open paths in the dimer, see [19, 43–46].

Chapter 2

The other side of the throat

2.1 The conformal point of $\mathcal{N} = 1$ gauge theory

The gauge side of the holographic correspondence is a supersymmetric gauge theory that is conformal. Determining the condition such that the theory we read from the brane tiling is conformal is then an important issue. This is simply the condition that the beta function vanish for all of the gauge couplings. For a general $\mathcal{N} = 1$ supersymmetric theory, with a single gauge group G and a list of matter superfields transforming in a representation ρ of G, the expression of the exact perturbative beta function has been given by Novikov, Shifman, Vainshtein and Zakharov in [47] as the so-called NSVZ beta function for the gauge coupling g

$$\beta_g = -\frac{g^3}{16\pi^2}\frac{3T_{\text{Adj}} - \sum_i T_{\rho_i}(1-\gamma_i)}{1 - T_{\text{Adj}}\frac{g^2}{8\pi^2}} , \tag{2.1}$$

where T_ρ is the Dynkin index of the representation ρ, γ is the associated anomalous dimension and the sum runs over all matter fields. Requesting the existence of a conformal point, i.e. imposing $\beta = 0$ implies that

$$3T_{\text{Adj}} - \sum_i T_{\rho_i}(1-\gamma_i) = 0 , \tag{2.2}$$

which not only depends on the representations but also on the anomalous dimensions γ. Note that it is easy to apply Eq. (2.2) to a quiver, with the sum running on the arrows attached to a node. Determining γ is in general quite complicated, but actually we seek for their value at the fixed point, and supersymmetry comes in our help. The lowest component of a chiral superfield is the scalar field ϕ and its dimension Δ is given by

$$\Delta = 1 + \frac{1}{2}\gamma . \tag{2.3}$$

Consider for a moment a gauge-invariant chiral primary operator $\mathcal{O}$. For a conformal theory, the superconformal algebra determines the relation between the scaling dimension $\Delta_{\mathcal{O}}$ and its R-charge $R_{\mathcal{O}}$ as

$$\Delta_{\mathcal{O}} = \frac{3}{2} R_{\mathcal{O}} = 1 + \frac{1}{2}\gamma_{\mathcal{O}} \ . \tag{2.4}$$

Moreover, for any scalar gauge-invariant operator $\mathcal{O}$, for the theory be unitary we have the bound

$$\Delta_{\mathcal{O}} \geq 1 \ \Rightarrow \ R_{\mathcal{O}} \geq \frac{2}{3} \ , \tag{2.5}$$

where the equality holds only for a free operator.

We can form a gauge-invariant chiral operator by composing matter fields, and since the R-charge of composite operators are additive, so are the anomalous dimensions. Thus, for a superconformal theory, we can think of the R-charge and anomalous dimension of matter fields related as in Eq. (2.4). We can rewrite eq. (2.6) in terms of R-charges, so the condition for a fixed point turns into a constraint on the R-charges:

$$T_{\text{Adj}} + \sum_i T_{\rho_i} \left(R_0 - 1\right) = 0 \ , \tag{2.6}$$

where R_0 is the R-charge of the scalar component. This is equivalent to demanding that the R-symmetry is not anomalous, i.e. the ABJ anomaly for R-symmetry current is zero. Note that $(R_0 - 1)$ is the R-charge of the fermionic component, since the chiral fermions enter in the triangle loop diagram associated to the anomaly, while gauginos have R-charge equal to 1.

Summing up, we require the R-symmetry to be anomaly-free, but only at the conformal point this condition is equivalent to the condition that the beta functions vanish.

The presence of matter fields we need to carefully look at global symmetries. Any of these fields can be transformed under a $U(1)$ group, i.e. rotated with a certain phase. If we have a number n_s of matter fields, the $\mathcal{N}=1$ theory has $(n_s - 1)$ non-anomalous abelian factors. The crucial point is that these phases can mix together, including the $U(1)_R$ symmetry. The consequence is that we can not uniquely define an R-symmetry, all we can do is choosing a combination of R_0 with all other abelian factors $F_{_I}$

$$R_t = R_0 + \sum_{I=1}^{n_s-1} s_{_I} F_{_I} \ , \tag{2.7}$$

where t stands for "trial". This is true but at the conformal point, where the combination in eq. (2.7) is uniquely determined, resulting in the truly conserved $U(1)_R$ symmetry, as shown by Intriligator and Wecht in [48]. The reason is again given by the supersymmetry algebra, as follows. The stress-energy tensor $T_{\mu\nu}$ and the R-symmetry current J_R are both in the same supermultiplet,

the super-stress tensor $\mathcal{T}_{\alpha\dot{\alpha}}$. For 4d conformal theories in curved space-time, the trace of the stress tensor is non-zero and reads

$$T^{\mu}_{\mu} = aE_4 + cW^2 \ , \tag{2.8}$$

where E_4 is the Euler density

$$E_4 = \frac{1}{4}\epsilon^{\mu_1\nu_1\mu_2\nu_2}\epsilon^{\rho_1\sigma_1\rho_2\sigma_2}R_{\mu_1\nu_1\rho_1\sigma_1}R_{\mu_2\nu_2\rho_2\sigma_2} \ , \tag{2.9}$$

$W_{\mu\nu\rho\sigma}$ the Weyl tensor, and a and c the central charges, which contain the 't Hooft anomalies $\mathrm{Tr}R^3$ and $\mathrm{Tr}R$ [49, 50] in the following way

$$\begin{aligned} a &= \frac{3}{32}\left(3\mathrm{Tr}R^3 - \mathrm{Tr}R\right) \ , \\ c &= \frac{1}{32}\left(9\mathrm{Tr}R^3 - 5\mathrm{Tr}R\right) \ . \end{aligned} \tag{2.10}$$

When holography holds, at large N $a = c$, i.e. $\mathrm{Tr}\, R = 0$ [10, 51–53].

Let us look at the central charge a, which in a certain sense counts the degrees of freedom and its value decreases along the RG flow, i.e. $a_{IR} < a_{IR}$ [54]. Based on the previous discussion, we should really look at the central charge a_t of the trial R_t in Eq. (2.7), so that

$$\frac{\partial a_t}{\partial s_{_I}} = \frac{3}{32}\left(9\mathrm{Tr}R_t^2F_{_I} - \mathrm{Tr}F_{_I}\right) \ , \tag{2.11}$$

$$\frac{\partial^2 a_t}{\partial s_{_I}\partial s_{_K}} = \frac{27}{16}\mathrm{Tr}R_tF_{_I}F_{_K} \ . \tag{2.12}$$

The two triangle anomalies appearing in Eq. (2.11) are related by the superconformal algebra. Since $T_{\mu\nu}$ and J_R are in the same supermultiplet, $\mathrm{Tr}R_t^2F_{_I} \propto \langle T_{\mu\nu}T_{\rho\sigma}J_{F_I}\rangle \propto \mathrm{Tr}F_{_I}$ [55], with the proportionality constant being exactly[1] 9: $9\mathrm{Tr}R_t^2F_{_I} = \mathrm{Tr}F_{_I}$ identifying the extrema of the central charge a_t. A similar reasoning gives $\mathrm{Tr}R_tF_{_I}F_{_K} \propto \langle T_{\mu\nu}J_{F_I}J_{F_K}\rangle \propto -\langle J_{F_I}J_{F_K}\rangle$, so that the extremum is a maximum. In general, being the central charge a_t a cubic function of the R-charges, the maximum is a local one.

The bottom line is that the superconformal algebra selects the unique combination R_t that defines the conserved R-symmetry at the IR fixed point. This procedure, known as a-maximization, allows us to identify the superconformal point of a 4d $\mathcal{N}=1$ theory, assigning the proper R-charges to all matter fields. Note that no superpotential was turned on in the previous discussion, but we can apply the same reasoning imposing that the symmetries are not broken by a superpotential W and that all terms[2] in W carry $R(W)=2$. So, the general procedure that we shall use in the next

[1] To see this, just study the case of a free theory, where matter fields have $R = 2/3$.

[2] To be a bit more precise, we should start with no superpotential and then add a deformation as $W = \lambda\mathcal{O}$, with

chapters is

1. impose cancellation of any gauge-anomalies;
2. impose cancellation of ABJ anomalies for any abelian factor in the global symmetry;
3. if $W \neq 0$, impose that any abelian global symmetry is preserved by the superpotential;
4. if $W \neq 0$, impose that $R(W) = 2$;
5. use any non-abelian factor in the global symmetries to impose further constraint on the R-charges;
6. choose a combination of R-charges in agreement with the previous steps. These Rs will be functions of one or more variables;
7. write down the central charge a as a function of the Rs;
8. find the maximum of the central charge a to identify the superconformal R-charges.

Before showing an example, let us give some remarks. First, one may wonder what happens in case a global abelian factor has $\mathrm{Tr}F_{_I} = 0$. From superconformal algebra, this means that this symmetry does not mix with the R-symmetry, as $\mathrm{Tr}R^2F_{_I} = 0$. This is what happens for baryonic symmetries. Second, we have implicitly assumed that at the IR fixed point no accidental symmetries are generated. A case in which this happens but we can control is the case of a gauge-invariant operator $\mathcal{O}$ that violates the unitarity bound $R \geq 2/3$. Along the flow, this operator $\mathcal{O}$ hits the unitarity bound at $R = 2/3$ and becomes free, consequently it decouples generating a further accidental abelian factor that mixes with the R-symmetry and under which only $\mathcal{O}$ is charged. In [56] it is shown how to correct the a-maximization procedure taking into account the accidental $U(1)$:

$$\begin{aligned}\widetilde{a}_t &= a_t + \frac{3}{32}\left(3\mathrm{Tr}\ R^3 - \mathrm{Tr}\ R\right)\Big|_{R=2/3} - \frac{3}{32}\left(3\mathrm{Tr}\ R_{\mathcal{O}}^3 - \mathrm{Tr}\ R_{\mathcal{O}}\right) \\ &= a_t + \frac{1}{96}\left(2 - 3R_{\mathcal{O}}\right)^2\left(5 - 3R_{\mathcal{O}}\right)\ , \end{aligned} \tag{2.13}$$

where $\widetilde{a}_t$ and a_t are the corrected and uncorrected central charges, respectively. So, after having found the maximum of a_t and the superconformal R-charges, one should check if any gauge-invariant operator decouples and, when that happens, repeat the procedure correcting the central charge.

Finally, let us show an example of how we implement a-maximization, following the procedure we have described. Consider the theory associated to orbifold $\mathbb{C}^3/\mathbb{Z}_2$, whose quiver and tiling

λ a coupling and $\mathcal{O}$ a gauge invariant operator. The coupling λ can run and with $R(W) = 2$ we are looking for a fixed point for λ.

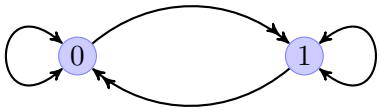

Figure 2.1a: The quiver diagram for $\mathbb{C}^3/\mathbb{Z}_2$.

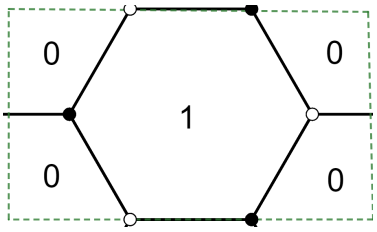

Figure 2.1b: The brane tiling for $\mathbb{C}^3/\mathbb{Z}_2$.

are drawn in Fig. 2.1a-2.1b. The gauge group is $SU(N) \times SU(N)$, with six matter fields, four bifuntamentals X^1_{01}, X^2_{01}, X^1_{10}, X^2_{10} and two adjoints ϕ_0, ϕ_1, interacting with superpotential

$$W_{\mathbb{C}^3/\mathbb{Z}_2} = \epsilon_{ij}\left(\phi_1 X^i_{10} X^j_{01} + \phi_0 X^i_{01} X^j_{10}\right) . \tag{2.14}$$

This theory is actually $\mathcal{N}=2$, but that is not a problem since we can express the fields in $\mathcal{N}=1$ multiplets. Being non-chiral, it does not suffer from gauge-anomalies, so there is no constraint for the ranks. Moreover, being the theory associated to a toric space, we expect that the global symmetry contains mesonic factors of rank 3 and only one baryonic abelian factor $U(1)_B$. We shall see that this is the case.

From the superpotential we can read an $SU(2)$ global symmetry rotating X^1_{01} and X^2_{01}, X^1_{10} and X^2_{10}. Due to this non-abelian symmetry, we count four fields, ϕ_0, ϕ_1, X^i_{01}, X^i_{10} and two superpotential terms. In order to find the number of global $U(1)_q$, we impose $q(W) = 0$ and cancellation of ABJ anomaly[3]

$$\begin{aligned} &q_{00} + q_{01} + q_{10} = 0 \\ &q_{11} + q_{10} + q_{01} = 0 \\ &2N_0 q_{00} + 2N_1 q_{01} + 2N_1 q_{10} = 0 \\ &2N_1 q_{11} + 2N_0 q_{10} + 2N_0 q_{01} = 0 \, , \end{aligned} \tag{2.15}$$

where q_{00}, q_{11} are the charges associated to the adjoint fields ϕ_0 and ϕ_1, similarly for q_{01} and q_{10}. The space of solution, which requires $N_0 = N_1 = N$, is parametrized by two variables, hence there are two abelian factors. As for the R_0-symmetry $U(1)_{R_0}$, we impose $R(W) = 2$ and anomaly-free

[3]We are using for $SU(N)$ $T_{\square} = 1$ and $T_{\text{Adj}} = 2N$.

condition and the $\mathbb{Z}_2$ symmetry[4] $R_{01}=R_{10}$ as

$$\begin{aligned} &R_{00}+2R_{01}=2\\ &R_{11}+2R_{01}=2\\ &2NR_{00}+4NR_{01}+2N=0\\ &2NR_{11}+4NR_{01}+2N=0\ , \end{aligned} \tag{2.16}$$

and two of them are redundant. In total, the global symmetry is $SU(2)\times U(1)\times U(1)\times U(1)_{R_0}$, and a possible choice of charges is given in Tab. 2.1.

	$SU(2)$	$U(1)$	$U(1)_{R_0}$	$U(1)_B$
ϕ_0	**1**	+1	0	0
ϕ_1	**1**	+1	0	0
X^i_{01}	$\square$	-1	+1	+1
X^i_{10}	$\square$	0	+1	-1

Table 2.1. Charge table of $\mathbb{C}^3/\mathbb{Z}_2$.

Note that $\mathrm{Tr}U(1)_B=0$, so that the abelian factor is baryonic. Moreover, the mesonic factor is $SU(2)\times U(1)\times U(1)_{R_0}$ as we should have expected being the theory toric. We need now to choose a combination of the $U(1)$ non-baryonic factors, construct the central charge a and maximize over it. The most general combination for R-charges is given by a solution of Eq. (2.16), hence

$$\begin{aligned} &R_{00}=R_{11}\ ,\\ &R_{00}+2R_{01}=2\ . \end{aligned} \tag{2.17}$$

Note that we can choose only one R-charge, signaling that only one $U(1)$ is mixing with $U(1)_{R_0}$. The 't Hooft anomalies read

$$\mathrm{Tr}\,R=2(N^2-1)(R_{00}-1)+4N(R_{01}-1)+2N=-2(R_{00}-1)\ , \tag{2.18}$$

$$\begin{aligned} \mathrm{Tr}\,R^3&=2(N^2-1)(R_{00}-1)^3+4N(R_{01}-1)^3+2N\\ &=2(N^2-1)(1-2R_{01})^3+4N(R_{01}-1)^3+2N\ . \end{aligned} \tag{2.19}$$

We take the large N limit to meet the holography condition, so that $\mathrm{Tr}R=0$. The central charge

[4] We have not used it before because we would have missed the baryonic factor.

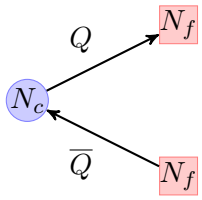

Figure 2.2. The quiver for SQCD with gauge group $SU(N_c)$ and N_f flavours.

a has a maximum at

$$R_{00} = R_{01} = \frac{2}{3}\,, \tag{2.20}$$

$$a_{\mathbb{C}^3/\mathbb{Z}_2} = \frac{3}{32}\left(3\mathrm{Tr}R^3 - \mathrm{Tr}R\right) = \frac{1}{2}N^2\,. \tag{2.21}$$

Finally, the gauge-invariant operators that can be constructed from the fundamental fields are $\mathrm{Tr}\phi_0^2$, $\mathrm{Tr}\phi_1^2$, $\mathrm{Tr}X_{01}^i X_{10}^j$ and all of their scaling dimension Δ is above the unitarity bound, hence none of them decouple. From now on, we will drop the zero in $U(1)_{R_0}$ as it will be clear from the context[5] if we are dealing with the superconformal R-charge or not.

2.2 Seiberg duality

We took a quite general detour in explaining how to determine the conformal fixed point of an $\mathcal{N}=1$ gauge theory with general gauge group G and matter fields in some representation, but the result is quite powerful. We can achieve an equally , if not even more, powerful result by looking at a simple model, the prototypical $\mathcal{N}=1$ supersymmetric theory: SQCD. Let us consider $G = SU(N_c)$ with N_f flavours, so N_f quark Q in the fundamental representation and N_f anti-quark $\widetilde{Q}$ in the antifundamental, and no superpotential. Take $N_f > N_c$, so that we can define baryons and mesons as gauge-invariant operators parametrizing the classical moduli space. The global symmetry is $SU(N_f) \times SU(N_f) \times U(1)_B \times U(1)_R$, see the quiver drawn in Fig. 2.2 and charges in Tab.2.2. The NSVZ beta function Eq. (2.1) read

	$SU(N_f)$	$SU(N_f)$	$U(1)_B$	$U(1)_R$
Q	$\overline{\square}$	$\mathbf{1}$	+1	$\frac{N_f-N_c}{N_f}$
$\bar{Q}$	$\mathbf{1}$	$\square$	-1	$\frac{N_f-N_c}{N_f}$

Table 2.2. Charge table of SQCD with gauge group $SU(N_c)$ and N_f flavours.

[5] A hint is for example whether there are other non-baryonic $U(1)$s around or not.

$$\beta_g = -\frac{g^3}{16\pi^2}\frac{6N_c - 2N_f\,(1-\gamma)}{1 - 2N_C\frac{g^2}{8\pi^2}}\ , \tag{2.22}$$

where $\gamma = \gamma_Q = \gamma_{\overline{Q}}$ is the anomalous dimension of the quarks and in perturbation theory

$$\gamma = -\frac{g^2}{8\pi^2}\frac{N_c^2-1}{N_c} + \mathcal{O}\left(g^4\right)\ . \tag{2.23}$$

Inserting in the beta function and expanding β_g we get

$$\beta_g = -\frac{g^3}{8\pi^3}\left(3N_c - N_f\right) - \frac{g^5}{64\pi^4}\left[3N_c(2N_c - N_f) + \frac{N_f}{N_c}\right] + \mathcal{O}\left(g^7\right)\ . \tag{2.24}$$

Suppose the gauge coupling is small, then the sign of the beta function is given by $(N_f - 3N_c)$. When $N_f > 3N_c$, $\beta_g > 0$ and the gauge coupling goes to zero in the IR, where the theory is free. Asymptotic freedom can be reached with the opposite behaviour, $\beta_g < 0$ and $N_f < 3N_c$, but in the IR the gauge coupling tends to increase. The second term in Eq. (2.24) may cancel the first, possibly signaling the presence of a fixed point. In order to see what happens, choose N_f slightly lower than $3N_c$,

$$N_f = 3N_c - \epsilon N_c\ , \qquad 0 < \epsilon < 1\ , \tag{2.25}$$

and looking at Eq. (2.24) we get

$$\beta_g = -\frac{g^3}{8\pi^2}\left[N_c\epsilon - \frac{g^2}{8\pi^2}3\left(N_c - 1\right) + \mathcal{O}(\epsilon) + \mathcal{O}\left(g^4\right)\right]\ . \tag{2.26}$$

There is a perturbative fixed point at

$$g_\star^2 = \frac{8\pi^2}{3}\frac{N_c}{N_c^2-1}\epsilon\ , \tag{2.27}$$

known as the Banks-Zaks fixed point [57].
We could have found a conformal point from the exact NSVZ with

$$\gamma = \frac{N_f - 3N_c}{N_f}\ . \tag{2.28}$$

Since the only other abelian factor is baryonic, the $U(1)_R$ is determined by anomaly cancellation only

$$2(R_Q - 1)N_f = -2N_c\ \Rightarrow\ R_Q = \frac{N_f - N_c}{N_f} \tag{2.29}$$

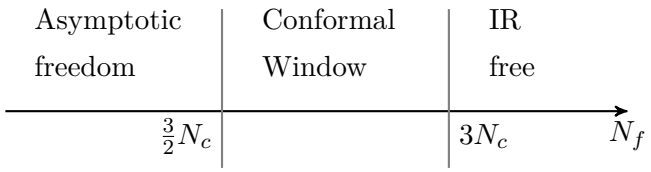

Figure 2.3. The conformal window and outer regions for SQCD with gauge group $SU(N_c)$ and N_f flavours.

and no need for a-maximization. Note that Eq. (2.4) gives the right γ. The gauge-invariant meson $M = Q\overline{Q}$ has $R_M = 2R_Q$ and dimension

$$\Delta_M = 3\frac{N_f - N_c}{N_f} \geq 1 \;\Rightarrow\; N_f \geq \frac{3}{2}N_c \,, \tag{2.30}$$

and the situation is summarized in Fig. 2.3, where

$$\frac{3}{2}N_c < N_f < 3N_c \tag{2.31}$$

is called the conformal window. There, we may expect that mesons and baryons describe the macroscopic theory of SQCD, but this expectation is too naive, as the 't Hooft anomalies do not coincide with those of quarks and gauginos. On the other hand, when N_f is slightly larger than $3/2N_c$, namely close to border but inside the conformal window, the anomalous dimension $\gamma \sim \mathcal{O}(1)$ and we lose perturbative control of the theory, a signal that we should carefully look into this region. It was Seiberg [58] who suggested that there is always a non-trivial fixed point in the conformal window, providing also a solution for the anomaly matching problem. He considered a theory with $G = SU(\widetilde{N}_c)$, N_f quark q and antiquark $\bar{q}$ and N_f^2 mesons $\widetilde{M}$, with global symmetry $SU(N_f) \times SU(N_f) \times U(1)_B \times U(1)_R$, quiver drawn in Fig. 2.4 and charges in Tab 2.3. The discussion just presented still holds, so a Banks-Zaks fixed point perturbatively emerges at $\widetilde{g}_\star$ inside a conformal window $3/2\widetilde{N}_c < N_f < 3\widetilde{N}_c$, with $R_q = R_{\bar{q}} = (N_f - \widetilde{N}_c)/N_f$ and $R_{\widetilde{M}} = 2/3$. However, this model admits the superpotential term with coupling λ

	$SU(N_f)$	$SU(N_f)$	$U(1)_B$	$U(1)_R$
$\overline{q}$	$\square$	$\mathbf{1}$	$\frac{N_c}{\widetilde{N}_c}$	$\frac{N_f-\widetilde{N}_c}{N_f}$
q	$\mathbf{1}$	$\overline{\square}$	$-\frac{N_c}{\widetilde{N}_c}$	$\frac{N_f-\widetilde{N}_c}{N_f}$
$\widetilde{M}$	$\overline{\square}$	$\square$	0	$2\frac{\widetilde{N}_c}{N_f}$

Table 2.3. Charge table of SQCD with gauge group $SU(\widetilde{N}_c)$, N_f flavours and a meson $\widetilde{M}$.

$$\widetilde{W}_\lambda = \lambda \mathrm{Tr}\, q\widetilde{M}\bar{q} \,. \tag{2.32}$$

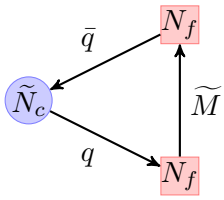

Figure 2.4. The quiver for SQCD with gauge group $SU(\widetilde{N}_c)$, N_f flavours and a meson M.

Turning on this deformation and imposing anomaly-free R-symmetry and that $R(\widetilde{W}_\lambda) = 2$ yield

$$R_q = R_{\bar{q}} = \frac{N_f - \widetilde{N}_c}{N_f} \,,$$
$$R_{\widetilde{M}} = 2\frac{\widetilde{N}_c}{N_f} \tag{2.33}$$

which is not compatible with the fixed point at $\widetilde{g}_\star$ and $\lambda = 0$: the deformation is relevant and the Banks-Zaks fixed point unstable. The solution of the matching problem relies on the fact that at some $\lambda = \lambda_\star$ there is a non-trivial fixed point with the previous assignment of R-charges. Let us compare the scaling and anomalous dimensions of the mesons in the two theories, M in $SU(N_c)$ and $\widetilde{M}$ in $SU(\widetilde{N}_c)$

$$\Delta_M = 3\frac{N_f - N_c}{N_f} \quad , \quad \Delta_{\widetilde{M}} = 3\frac{\widetilde{N}_c}{N_f} \,,$$
$$\gamma_M = 4 - 6\frac{N_c}{N_f} \quad , \quad \gamma_{\widetilde{M}} = 6\frac{\widetilde{N}_c}{N_f} - 2 \,. \tag{2.34}$$

Looking at the dimesions of the mesons, it is intuitive to put $\widetilde{N}_c = N_f - N_c$. Baryons on the two sides share the same dimension too. With this identification, the conformal windows of the two theories are the same, a hint that they provide different descriptions of the same IR physics. However, outside this region their behaviour is exchanged and where one is asymptotically free the other is IR free, and vice versa.

To sum up, we have a theory A on one side, SQCD with $G = SU(N_c)$ and N_f flavours, and on the other side a theory B SQCD with $G = SU(\widetilde{N}_c)$ and N_f flavours, N_f^2 mesons $\widetilde{M}$, interacting with $\widetilde{W} = q\widetilde{M}\bar{q}$. For $\widetilde{N}_c = N_f - N_c$, the scaling dimension of gauge invariant operators of the two theories are the same and they share the same conformal window. Outside of this window, A and B have instead different behaviour. Finally, the 't Hooft anomalies between A and B match, see Tab. 2.4. Seiberg duality states that inside the conformal window the theory A, called electric, flows to the same superconformal fixed point of theory B, the magnetic. Outside the conformal window, consider the electric theory close to $N_f = 3/2N_c$, where the theory is strongly coupled in the IR. At those scale we lose perturbative control, but the magnetic theory provides a weakly coupled description for the infrared physics, since 't Hooft anomalies are the same. Hence, the

electric theory can be seen as the UV completion of the magnetic.

Global symmetry	't Hooft anomaly
$SU(N_f)^3$	N_c
$SU(N_f)^2U(1)_B$	N_c
$SU(N_f)^2U(1)_R$	$-\frac{N_c^2}{N_f}$
$U(1)_B^2U(1)_R$	$-2N_c^2$
$U(1)_BU(1)_R^2$	0
$U(1)_R$	$-N_c^2-1$
$U(1)_R^3$	$-2\frac{N_c^4}{N_f^2}+N_c^2-1$

Table 2.4. 't Hooft anomalies for the Seiberg dual electric and magnetic theory.

Seiberg duality has allowed to establish a plethora of infrared connections between seemingly different theories. As examples, a theory with gauge group $Sp(N_c)$ and N_f fundamentals, the magnetic theory is $Sp(N_f-N_c-4)$, N_f fundamentals and an antisymmetric meson transforming in the $U(N_f)$ flavour group [59]. The magnetic dual of a theory with gauge group $SO(N_c)$ with N_f quarks in the vector representation is a theory with $SO(N_f-N_c+4)$, N_f quarks and a symmetric meson in the symmetric of the $U(N_f)$ flavour symmetry group [60]. See [61–63] for other cases with various matter fields and superpotentials.
Finally, in the context of gauge theory dynamics of systems of D-branes at CY-singularities, Seiberg duality has proven to play a crucial role in understanding very peculiar RG-flows as cascade of dualities [64, 65]. The prototypical example for this mechanism is the conifold theory, whose gauge group is in general[6] $SU(N+M)_0 \times SU(N)_1$, and matter fields X^1_{01}, X^2_{01}, X^1_{10}, X^2_{10} that interact with superpotential

$$W_c = \epsilon_{ij}\epsilon_{kl}X^i_{01}X^k_{10}X^j_{01}X^l_{10}\ . \tag{2.35}$$

The shift in the ranks signals the presence of M fractional branes in the gravity picture, while N is the number of regular branes. From the beta functions of the two gauge factors, one can see that the gauge couplings run in opposite direction, so one gauge factor reach a strongly coupled regime, while the other remains weakly coupled. The strong sector can be effectively described by its magnetic phase, with dual quark and mesons $M^{ij} = X^i_{01}X^j_{10}$ that interact as in Eq. (2.32). The gauge group of the Seiberg dual phase is $SU(N-M)_0 \times SU(N)_1$. The beta function still have opposite sign, but it is now the factor 1 that goes to strong coupling. Repeating this steps, ranks decrease and the two gauge factors show this alternate behaviour. The IR dynamics depends on

[6] Actually, with rank shifted by a quantity M we should refer to this as deformed conifold.

the relation between N and M. For instance, if $N = kM$, in the deep IR one factor confines and the remaining one is a pure gauge theory, leading to gauge condensation and chiral symmetry breaking. See [65] for a detailed description of this cascade.

2.3 Connection to geometry

We should keep in mind that the SCFTs we are interested in represent only one side of the construction, as they stand as the gauge side of the holographic correspondence. There is another part of the story, where gravity is the protagonist. As said in the previous chapter, global symmetry connects the two sides. After having briefly reviewed tools and features of 4d $\mathcal{N} = 1$ superconformal gauge theories, heavily dependent on global symmetry, we shall explore this connection.
A gauge theory that is dual to a theory of gravity defined on a geometry whose transverse space to the D3 branes is toric is completely defined by the brane tiling, as we saw in the previous chapter. This means that matter content, gauge group and superpotential can be read from the bipartite graph. However, the former two can be encoded in a quiver, which is not enough to contain the information about the interaction. In fact, the relevant data for the geometry is stored in the superpotential. In order to see this, suppose we have a quiver theory with gauge group $G = \prod_{a=1}^{n} SU(N)_a$, E bifundamental matter fields X_{ab} and a superpotential with V terms that respects the toric condition, i.e. all terms W_i are monomial in the fields and each field enter twice, once with positive sign and once with negative sign. Look closely to anomaly-free condition for R and $R(W) = 2$

$$\begin{aligned} \sum_{X_{ab}\in W_i} R_{ab} &= 2 \,, \\ \sum_{X_{ab}\in G_a} (R_{ab} - 1) &= -2 \,, \end{aligned} \tag{2.36}$$

and sum the first over all superpotential terms and the second over all groups factors, obtaining

$$\begin{aligned} \sum_{W_i} \left(\sum_{X_{ab}\in W_i} R_{ab} \right) &= 2V \,, \\ \sum_{G_a} \left(\sum_{X_{ab}\in G_a} (R_{ab} - 1) \right) &= -2n \,. \end{aligned} \tag{2.37}$$

Since each bifundamental field connects two nodes in the quiver and appears in two W_i, we can

rewrite them as

$$\begin{aligned} 2\sum_{X_{ab}} R_{ab} &= 2V \ , \\ 2\sum_{X_{ab}} (R_{ab}-1) &= 2\sum_{X_{ab}} R_{ab} - 2E = -2n \ , \end{aligned} \tag{2.38}$$

obtaining

$$n - E + V = 0 = 2 - 2g \ . \tag{2.39}$$

The last equality states that if we want to draw the interaction terms on a certain surface, exploiting a tessellation with n nodes, E arrows and V faces, the surface must have genus $g = 1$ and the Euler characteristic must vanish. Hence, that surface is a torus. This closes the circle, as in the previous chapter we started from geometric data of the toric CY cone to construct a bipartite graph on a torus.

2.3.1 Isoradial embedding

Let us go back to Eq. (2.36) and multiply both by π

$$\begin{aligned} \sum_{R_{ab}\in \text{node}} R_{ab}\pi &= 2\pi \ , \\ \sum_{R_{ab}\in \text{face}} R_{ab}\pi &= (E|_f - 2)\pi \ , \end{aligned} \tag{2.40}$$

where $E|_f$ is the number of edges around that face. We can think of the combination πR_{ab} as angles, since going around a node gives 2π and summing the internal angles of a face/polygon gives $(E|_f - 2)\pi$. In [24], the authors notice this fact and used the concept of isoradial embedding of the brane tiling, where each face of the tiling is embedded inside an unit circle, see Fig. 2.5. Connecting the centres of the circles to the nodes, we obtain a graph of rhombi, called rhombus lattice. An edge/bifundamental field is associated with each rhombus, in particular with one of the diagonals. It is natural to identify πR_{ab} with the angle under this diagonal, which gives a geometric basis under the interpretation of Eq. (2.40) as angles around a node and inside a face. Note that if $R = 0$ or $R = 1$ the rhombus closes and becomes degenerate.
Requesting that the global R-symmetry is anomaly-free not only determines that the gauge theory is embedded in a torus as a tiling, but also the shape of the tiles. On the other hand, the tiling was obtained from the toric diagram, hence from purely geometric information. The true non-anomalous R-symmetry takes the role of bridge between the two descriptions, geometry and gauge theory.

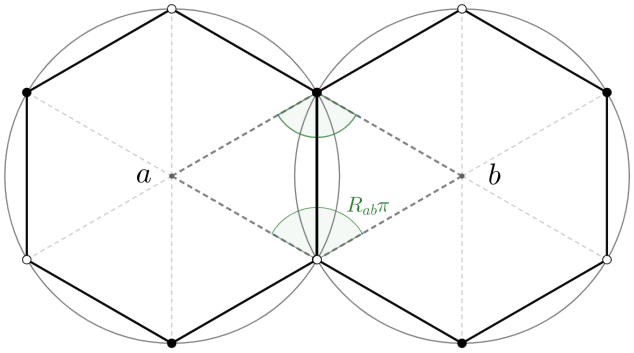

Figure 2.5. Isoradial embedding of the brane tiling, where faces are embedded into circles and each edge has an associated angle related to the R-charge of the field.

2.3.2 Toric duality

In Sec. 1.5 we mentioned the fact that non-extremal points in the toric diagram may have various degeneracies, while keeping the same shape of the toric polygon. All of them are associated to the same geometry. However, two toric diagrams with different degeneracies give different configuration of perfect matchings and bipartite graph, so the two gauge theories defined from fivebranes and brane tilings are different as well. One can actually pass from one fivebrane to the other by moving the NS5 across each other and reaching a new possible configuration. These toric phases give rise to Seiberg dual gauge theories that, in the conformal window, flows to the very same fixed point and there they share the same 't Hooft anomalies and central charge a. As we are going to see in the next section, this means that the Seiberg dual theories are associated to the same geometry. Hence, toric duality accounts for Seiberg duality [22, 66].

2.3.3 Volume minization

Exploring the geometric connection between the two sides of AdS/CFT, we are slowly going back to the construction in the previous chapter. Remember that the gravity side is defined on a geometry of the form $AdS_5 \times Y_5$, where Y_5 is a Sasaki-Einstein space, which is the base of the toric CY cone. Constructing a foliation of Y_5, whose leaves are compact, there is always a $U(1)$ isometry acting on Y_5. The space has a constant norm Killing vector, called Reeb vector, whose orbits are related to the action of the $U(1)$. When it acts freely, the space is called regular, while if the action is locally free the space is called quasi-regular. Finally, if the orbit of the Reeb vector does not close the geometry is said to be irregular. The importance of the Reeb vector relies on the fact that it represents the gravity dual of R-symmetry of the SCFT. In [67] it is shown that the Reeb vector of a given toric Y_5 can be determined only from toric data, without knowing the metric and, most importantly, the volume of the space can be computed with a procedure dual to a-maximization, which has been referred to volume minimization, and it works as follows.
Consider a toric cone defined by vectors $v_a = (1, w_a)$, with $a = 1, \ldots, d$ and $v_{d+1} = v_1$, where w_as have two components and define the toric diagram. The Reeb vector is of the form $b = (3, x, y)$,

where (x, y) can be seen as coordinates in the toric diagram. Defining (v, u, z) as

$$(v, u, z) = \det \begin{pmatrix} v^{(1)} & v^{(2)} & v^{(3)} \\ u^{(1)} & u^{(2)} & u^{(3)} \\ z^{(1)} & z^{(2)} & z^{(3)} \end{pmatrix} , \tag{2.41}$$

the volume of the space is given by

$$\text{Vol}_Y = \frac{\pi^3}{3} \sum_{a=1}^{d} \frac{(v_{a-1}, v_a, v_{a+1})}{(b, v_{a-1}, v_a)(b, v_a, v_{a+1})} \tag{2.42}$$

as a function of the components of b, and whose minimum yields the volume of Y_5 at the base of the CY cone and the precise components of the Reeb vector.
Thus, the Reeb vector determines the volume of Y_5 and it is the dual of the R-symmetry, which in turn determines the central charge a, the degrees of freedom of the gauge theory. While the volume is minimised by b, the central charge is maximized by R. In [68] it is proposed the inverse relation

$$\text{Vol}_Y = \frac{\pi^3}{4} \frac{N^2}{a} , \tag{2.43}$$

that represents the connection between geometry and field theory we have been seeking.

2.4 Deformations

We have built a machinery that allows us to generate many toric theories. From a field theory point of view, it is clear that we can deform the theory adding suitable operators to the superpotential. When these trigger a flow, the nature of the end is not guaranteed, as confinement may occur or the effective theory may develop a new conformal fixed point. We are going to introduce two types of deformations, higgsing/un-higgsing and mass deformation, and see that, under particular conditions, we end up with a different toric model.

2.4.1 Mass Deformation of toric theories

Consider again the orbifold model $\mathbb{C}^3/\mathbb{Z}_2$ of Fig. 2.1a-2.1b, recall the superpotential is

$$W_{\mathbb{C}^3/\mathbb{Z}_2} = \epsilon_{ab} \left(\phi_0 X_{10}^a X_{01}^b + \phi_1 X_{01}^a X_{10}^b \right) . \tag{2.44}$$

Deform the theory with a relevant term for the two adjoint fields, as

$$\Delta W = m^2 \left(\phi_0^2 - \phi_1^2 \right) , \tag{2.45}$$

which introduces a mass scale and triggers an RG flow. Moreover, the theory is no-longer toric, as can be seeon from the superpotential $W + \Delta W$. Integrating the massive fields out by computing F-terms and redefining fields properly, we obtain

$$W = \epsilon_{ab}\epsilon_{cd} X^a_{01} X^c_{10} X^b_{01} X^d_{10} \ . \tag{2.46}$$

Note that each field appears twice, with opposite sign: the toric condition. From the discussion in Sec. 2.3, we can embed this superpotential in a torus, using a tessellation with four-side polygons. Moreover, exploiting the $SU(2) \times SU(2)$ and $\mathbb{Z}_2$ symmetry we find that all R-charges[7] must be $1/2$. In terms of isoradial embedding this means that the related angles are $\pi/2$ and all faces on the torus are squares, as in Fig. 2.6a. In this way, we obtain a brane tiling for the resulting theory after the deformation and, from the fast forward algorithm in Sec. 1.5, the related toric diagram that specify the toric CY cone, see Fig. 2.6b. The final toric space is the conifold, the CY over the space $T^{1,1}$, whose associated field theory has been constructed for the first time in [69]. There, the authors give the geometric interpretation of the mass deformation in the original $\mathbb{C}^3/\mathbb{Z}_2$: in the cone over $S^5/\mathbb{Z}_2$, the deformation amounts to blowing up the orbifold singularity, replacing it by a 3-sphere. The geometry results in a S^3 bundle over S^2, which is in fact the geometry of $T^{1,1}$. In terms of toric geometry, the effect of mass deformation is to move a vertex, compare the two figures Fig. 1.1b-2.6b.
Let us focus on the brane tiling. Integrating a pair of massive fields out result in collapsing the corresponding edges in the dimer, and exagons turn into squares, compare Fig. 2.1b with 2.6a. In [70] it is shown that in the in the context of brane tiling, one can give mass to pairs of adjoint or vector-like fields and, after having integrated them out of the theory and suitable redefined the fields as

$$\begin{aligned} X'_{ab} &= X_{ab} + \frac{1}{m} \sum_k c^{(ab)}_k X_{ak} X_{kb} \ , \\ \phi'_a &= \phi_a + \frac{1}{m} \sum_k c^a_k X_{ak} X_{ka} \ , \end{aligned} \tag{2.47}$$

where $c^{(ab)}_k$ and c^a_k are some coefficients that ensure the restoration of toric symmetry, the effective field theory below the mass scale is associated to a toric geometry.

2.4.2 Higgsing a toric model

Mass deformation is not the only tool we have to deform a theory. Consider a supersymmetric gauge theory from the toric setup we described, with superpotential W. If we give non-zero VEV to one of the bifundamental fields we can obtain another toric theory. For instance if $\langle X_{ab} \rangle = v$ [71], we are taking out from the dimer the edge corresponding to X_{ab} and consequently the two

[7] In this case we do not need a-maximization, for the huge amount of symmetry determines the unique non-anomalous R-symmetry.

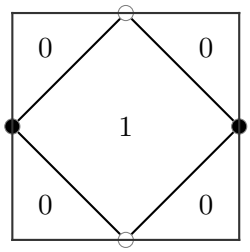

Figure 2.6a: The brane tiling of the conifold $\mathcal{C}$.

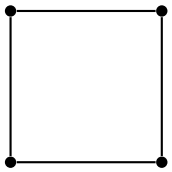

Figure 2.6b: The toric diagram of the conifold $\mathcal{C}$.

adjacent faces a and b merge into one, providing only one gauge group, which we denote a. In the case X_{ab} enters in the superpotential in a cubic term, its non-zero VEV generates quadratic terms as

$$W = \ldots + \langle X_{ab} \rangle X_{bc} X_{ca} - \langle X_{ab} \rangle X_{bd} X_{db} + \ldots \tag{2.48}$$

and the fields X_{bc}, X_{ca}, X_{bd} and X_{db} become massive, generating in turn an energy scale for the new theory. After integrating them out, one obtain the effective theory at low energy with $a = b$. The dimer will change accordingly, in a different way from a mass deformation.

The reverse method is called unhiggsing. Starting from the dimer, we unhiggs a field drawing a new edge that connects a white node with a black node and splits a face into two parts. This a new gauge factor arises and new terms in the superpotential, which can be read from the resulting dimer.

This method was a tool to obtain non-orbifold singularities from deformation of orbifold ones and their associated gauge theories, before the advent of brane tiling. We will encounter some examples in Chapter 4.

Chapter 3

Reflecting the throat

Open and unoriented strings, whose systematic construction was addressed long ago [72–75], have proven to be an unprecedented tool in the exploration of gauge field dynamics. Perhaps the investigation of unoriented singularities has been less systematic, even though it has a crucial role for Standard Model embedding [76–80], but recently some attention has been devoted to unoriented models [81–86]. In the case of unoriented singularities, an orientation reversing action σ on the CY is combined with world-sheet parity Ω that entails an action γ_Ω on the Chan-Paton factors or, equivalently, on the D-branes. The geometric counterpart of the construction, known as orientifold, involve orientifold-planes or O-planes for short.
We shall consider orientifold projections of gauge theories associated with toric CY singularities. This unoriented involution involves the action of the world-sheet parity operator Ω, general spacetime reflections σ and a suitable $\mathbb{Z}_2$ symmetry such as the left moving fermion number $(-1)^{F_L}$. The original theory before the projection will be called the *parent theory*, whose gauge group is composed by several $SU(N_a)$ gauge factors. After the orientifold projection, one can end up with a theory that includes also $SO(N_a)$ or $USp(N_a)$ gauge factors[1] and matter in symmetric or antisymmetric representations. We now discuss how to perform such orientifold projection on the diagrams discussed in the previous chapter.

3.1 Orientifolding the brane tiling

As the brane tiling encodes information about the geometry and gives the dual gauge theory, it may be as well a tool for implementing the orientifold. Since the projection involves spacetime reflection and a $\mathbb{Z}_2$ symmetry, in [81] the symmetry of the brane tiling is exploited to read the projected gauge theory, studying the possible $\mathbb{Z}_2$ involutions of the torus. These are classified, but not all of them are compatible with the request that a common supersymmetry with the stack of D3 branes is preserved, the interesting ones either have fixed loci or implement a transformation

[1] In the literature it is sometimes used $Sp(N_a/2)$ whose rank is $N_a/2$. Clearly, N must be even in this case.

with no fixed points called glide [81, 87]. We focus only on the former, where fixed loci may be either four fixed points or a fixed line. These fixed loci are associated with orientifold planes in the system of branes, hence they carry a positive or negative RR charge as the charge of the O-planes. In [39] it is discussed the introduction of O-planes in the system of D3 branes, and O3 or O7 are allowed. On the other hand, we saw in the first chapter that the brane tiling is constructed in the double T-dual configuration of D5 branes, so the orientifold planes are O5, points on or 1-cycles of the torus. The projection given in the two cases are different.

3.1.1 Four fixed points on the dimer

An inversion of both coordinates of the torus generates four fixed points. This operation preserves angles in the tiling and the mesonic global symmetry $U(1)^2 \times U(1)_R$. All elements of the tiling, namely faces, edges and nodes, are mapped to the others with respect to the fixed points. We label a face/gauge factor with a and its image under the orientifold with a'. If $a \neq a'$, for instance a group $SU(N_1)$ is mapped to another group $SU(N_2)$. This, by consistency, requires $N_1 = N_2$ in the parent theory, while in the orientifold theory we keep one factor, say $SU(N_1)$. On the other hand, when $a = a'$, a fixed point lies on the face with label a and the group $SU(N_a)$ is identified with itself. The orientifolded theory has a factor $SO(N_a)$ if the charge τ_a carried by the point is positive, $USp(N_a)$ if negative. To take into account the fact that the orientation of open strings is inverted by the orientifold plane, representations are conjugated under the involution as

$$\begin{aligned} \Box_a &\longleftrightarrow \overline{\Box}_{a'} \,, \\ \overline{\Box}_a &\longleftrightarrow \Box_{a'} \,, \end{aligned} \tag{3.1}$$

so that for a generic bifundamental field

$$(X_{ab})_{i_a}{}^{j_b} = (\Box_a, \overline{\Box}_b)_{i_a}{}^{j_b} \longleftrightarrow (\overline{\Box}_{a'}, \Box_{b'})^{i_a}{}_{j_b} = \left[(X_{ab})_{i_a}{}^{j_b}\right]^T \,. \tag{3.2}$$

When a fixed point lies on an edge, $b = a'$ and the bifundamental field is projected on a tensor representation, symmetric if the fixed point carries a positive charge τ_{ab}, antisymmetric in case of a negative τ_{ab}. Finally, white nodes in the dimer are mapped to black nodes and viceversa. Note that this means a fixed point cannot lie inside a square in a bipartite graph. The resulting superpotential is given by half the terms of the parent theory, $N_W/2$, with the constraint on the τ charges

$$\prod_{\text{fxd pts}} \tau = (-1)^{N_W/2} \,. \tag{3.3}$$

Let us provide an example of a fixed points orientifold and consider our old friend $\mathbb{C}^2/\mathbb{Z}_2 \times \mathbb{C}$. We perform such orientifold projection on its brane tiling, as drawn in Fig. 3.1, where the fixed points

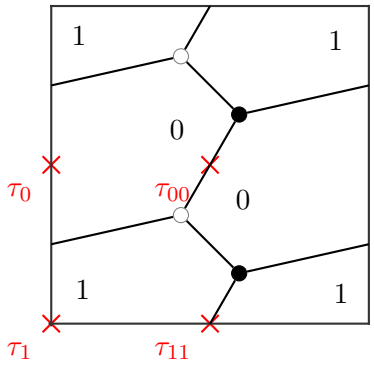

Figure 3.1: The orientifold projection with four fixed points of $\mathbb{C}^2/\mathbb{Z}_2 \times \mathbb{C}$.

are represented by red crosses.
From Fig. 3.1 we see that there are four nodes in the tiling, which represent the interaction terms of the theory. The constraint in Eq. (3.3) with $N_W/2 = 2$ demands that the product of the τs is positive, so for (τ_0, τ_{00}, τ_1, τ_{11}) we have the choices ($\pm$, $\pm$, $\pm$, $\pm$), ($\pm$, $\pm$, $\mp$, $\mp$), ($\pm$, $\mp$, $\pm$, $\mp$), ($\pm$, $\mp$, $\mp$, $\pm$). Let us focus on the last one, with the upper signs. The resulting gauge group is $SO(N_0) \times USp(N_1)$ with matter content

$$\begin{aligned} \phi_0^A &= A = \square\!\square_0 \ , \\ \phi_1^S &= S = \square\square_1 \ , \\ X_{01}^i &= \left(\square_0, \overline{\square}_1\right)^i \ , \ i = 1, 2 \ , \end{aligned} \tag{3.4}$$

where X_{01} is identified with X_{10}^i. The projected superpotential $W^{\Omega}_{\mathbb{C}^3/\mathbb{Z}_2}$ reads

$$W^{\Omega}_{\mathbb{C}^3/\mathbb{Z}_2} = -AX_{01}^2X_{10}^1 + SX_{10}^1X_{01}^2 \ . \tag{3.5}$$

3.1.2 Fixed lines on the dimer

The second projection with fixed loci inverts only one coordinate of the torus, resulting in a reflection with fixed lines. The mesonic $U(1)^2$ is broken to an $U(1)$ subgroup. Contrary to the previous case, this involution is possible only for certain complex structure, i.e. certain shape of the fundamental cell, such as reactangles and rhombi. The action over the elements of the tiling is very similar to the previous case, with the adjustment that the locus is now given by one or two lines, each carrying charge denoted by τ. When a line pass over a face a, the corresponding gauge group $SU(N_a)$ is projected into $SO(N_a)$ or $USp(N_a)$, for τ positive or negative respectively. Different edges mapped with respect to the line are identified, while edges mapped to themselves are projected into symmetric or antisymmetric representation for positive or negative τ. As for nodes, in this case the black ones are mapped to black and white to white, and it happens that a node is mapped

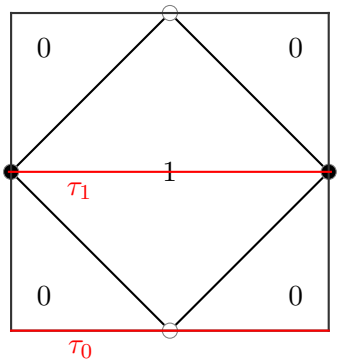

Figure 3.2: The orientifold projection with two fixed lines of the conifold $\mathcal{C}$.

to itself. As an example, the line orientifold for the conifold $\mathcal{C}$ is shown in Fig. (3.2). Denoting with τ_0 and τ_1 the charges carried by the lines passing on face 0 and 1, and choosing $\tau_0 = +$, $\tau_1 = -$ the gauge group results in $SO(N_0) \times USp(N_1)$, while fields are identified as

$$\begin{aligned} X^1_{10} &\longrightarrow X^2_{01} \ , \\ X^2_{10} &\longrightarrow X^1_{01} \ , \end{aligned} \tag{3.6}$$

hence the matter content is made by only X^1_{01}, X^2_{01} interacting as

$$W^{\Omega}_{\mathcal{C}} = X^1_{01} \left(X^2_{01}\right)^T X^2_{01} \left(X^1_{01}\right)^T - X^1_{01} \left(X^1_{01}\right)^T X^2_{01} \left(X^2_{01}\right)^T \ . \tag{3.7}$$

3.2 Orientifolding the Quiver

We discussed how to represent the gauge theory given by the brane tiling as a quiver diagram, which is a quick way to draw and read the gauge group and the matter content. While we still need to work out the superpotential from the dimer and the rules we have seen in the last section in case of an orientifold projection, we can again use the quiver diagram as an easy way to read the resulting gauge theory and the identifications under the orientifold. We need to draw the quiver in such a way the $\mathbb{Z}_2$ symmetry is explicit and draw a line that divide the quiver into two parts, mapped by the orientifold. Elements in the quiver are identified with respect to this line, which we denote by Ω. We stress that the quiver lack any of the geometric information about the torus and the Ω-line is not related with the fixed loci, its role is just to make the orientifold projection visually clear. Groups paired up by the orientifold are identified with respect to the line, while projected gauge factor are crossed by Ω. Similarly for the bifundamental fields, but the $\mathbb{Z}_2$ involution must map arrows with opposite orientation to take account of the conjugation. We show such quiver diagrams for the orientifold of $\mathbb{C}^2/\mathbb{Z}_2 \times \mathbb{C}$ and $\mathcal{C}$ in Fig. 3.3, the examples in the last section.

Figure 3.3. On the left, the quiver diagram for the orientifold projection of $\mathbb{C}^2/\mathbb{Z}_2 \times \mathbb{C}$, on the right for $\mathcal{C}$.

3.3 Orientifolding the Toric Diagram

As we have seen, projections with four fixed points on the dimer preserve the mesonic symmetry while projections with fixed lines break it. In [85], these two cases are called toric and non-toric involutions, respectively. The toric involution is described by points on an even sublattice of the toric space, while non-toric ones by fixed lines of the diagram. In [85] the authors focus on the toric diagram rather than the brane tiling and discuss the toric involution in relation with the complete resolutions of the singularity, which corresponds to dividing the toric diagram into minimal triangles. So, each point on the even sublattice represents an O7 plane, which wraps a compact divisor if the point stays inside the toric diagram, a non-compact one if it lies on the boundary of the diagram. A minimal triangle of the resolution corresponds to either an O3 plane or an O7 if a corner of the triangle lies on the even sublattice. These O-planes live in the resolved space. Thus, given a particular toric diagram we may have various resolutions and choices of the even sublattice, then different orientifold configurations. See Fig. 3.4 for an example in the case of $\mathbb{C}^3/\mathbb{Z}_3$.

Figure 3.4. The toric involution on the toric diagram of the resolved $\mathbb{C}^3/\mathbb{Z}_3$ orbifold theory, with the points of the even sublattice drawn in red. On the left the resolved orientifolded theory with a compact O7, while on the right the resolved unoriented theory with a non-compact O7 and an O3.

3.4 Anomaly cancellation condition

In order to have a meaningful orientifolded theory, gauge anomalies must vanish. The projection yields real groups, for which there is no gauge anomaly, and tensorial matter, for which the anomaly coefficient changes to $(N \pm 4)$ depending on symmetric or antisymmetric transformation rules. Their presence may rule out some solutions of the anomaly cancellation condition for the parent theory,

Figure 3.5. The orientifold projection of $\mathbb{C}^3/\mathbb{Z}_3$ with four fixed points.

such as $N_a = N\ \forall a$. The anomaly cancellation condition for a node a gets modified into

$$\sum_{X_{ab}} N_b - \sum_{X_{ca}} N_c + \sum_{X^S_{aa'}} (N_a + 4) - \sum_{X^S_{a'a}} (N_a + 4) + \sum_{X^A_{aa'}} (N_a - 4) - \sum_{X^A_{a'a}} (N_a - 4) = 0\ . \tag{3.8}$$

Let us show an example, the orientifold projection with four fixed points of $\mathbb{C}^3/\mathbb{Z}_3$, see Fig. 3.5. Since there are six terms in the superpotential, $\prod \tau = -1$ and the choices for $(\tau_0,\, \tau^1_{12},\, \tau^2_{12},\, \tau^3_{12})$ are $(\pm,\, \mp,\, \mp,\, \mp)$. Focusing on upper signs, the gauge group is $SO(N_0) \times SU(N_1)$, with fields X^i_{01}, $X^i_{12} = A^i$, with $i = 1, 2, 3$, while $X^i_{20} \to X^i_{01}$. The superpotential after the projection reads

$$W^{\Omega}_{\mathbb{C}^3/\mathbb{Z}_3} = \epsilon_{ijk} X^i_{01} A^j \left(X^k_{01}\right)^T\ , \tag{3.9}$$

and from Eq. (3.8), for $SU(N_1)$ we have

$$-3N_0 + 3(N_1 - 4) = 0 \quad \Rightarrow \quad N_1 = N_0 + 4\ . \tag{3.10}$$

In Chapter 1, we said that the shift between the ranks means that fractional branes are present, as D5 wrapping 2-cycles. Typically, the orientifold projection requires the presence of fractional branes, and for chiral theories this usually affects conformal invariance, as we are about to see.

3.5 Conformal invariance of unoriented theories

We demand what is the fate of the conformal point after the orientifold projection. In Eq. (2.1), we write the one-loop exact beta function for a generic $\mathcal{N} = 1$ gauge theory. When it vanishes, the numerator is related to the anomaly-free condition for R-symmetry. Let us focus on it

$$3T_{\text{Adj}} - \sum_i T_{\rho_i} (1 - \gamma_i) = 0\ . \tag{3.11}$$

It is easy to generalise it for an unoriented theory, with real groups and tensorial matter, as

$$\begin{aligned}\beta_a^{(SO/USp)} &\propto 3(N_a-2) - \sum_{X_{ab},X_{ba}} N_b(1-\gamma_{ab}) - \sum_{S/A}(N_a \pm 2)(1-\gamma_{S/A}) \ , \\ \beta_a^{(SU)} &\propto 3(2N_a) - \sum_{X_{ab},X_{ba}} N_b(1-\gamma_{ab}) - \sum_{S/A}(N_a \pm 2)(1-\gamma_{S/A}) \ . \end{aligned} \tag{3.12}$$

Going back to the previous example, $\left(\mathbb{C}^3/\mathbb{Z}_3\right)/\Omega$ with $(+,\,-,\,-,\,-)$ for $(\tau_0,\,\tau_{12}^1,\,\tau_{12}^2,\,\tau_{12}^3)$ and $N_0 = N_1 - 4$, we have

$$\begin{aligned}\beta_0 &\propto 3(N_0-2) - 3N_1(1-\gamma_{01}) \\ &= -18 + 3N_1\gamma_{01} \ , \\ \beta_1 &\propto 6N_1 - 3N_0(1-\gamma_{01}) - 3(N_0-2)(1-\gamma_{12}) \\ &= +18 + 3N_1(\gamma_{01}+\gamma_{12}) - 6\gamma_{12} - 12\gamma_{01} \ , \end{aligned} \tag{3.13}$$

and they vanish if the anomalous dimensions are of order $(1/N)$. Note that this holds together with the condition that the superpotential in Eq. (3.9) is marginal, i.e. $2\gamma_{01}+\gamma_{12}=0$. In the large N limit, the γs vanish, βs as well and the model behaves as a free theory. This can be seen from anomaly condition for R-symmetry and $R(W)=2$, as

$$\begin{aligned} &2R_{01} + R_{12} = 2 \ , \\ &(R_{01}-1)3N_1 + (N_0-2) = 0 \ , \\ &(R_{01}-1)3N_0 + (R_{12}-1)3(N_1-2) + 2N_1 = 0 \ , \end{aligned} \tag{3.14}$$

and in the large N-limit the system of equations is the same as the parent theory, whose solution is $R=2/3$. We can see this result as the effect of the orientifold projection is negligible in case of large number of D3 branes probing the unoriented singularity.
However, let us see another example, the orientifold projection with a fixed line of the chiral orbifold of the conifold $\mathcal{C}/\mathbb{Z}_2$, see Fig. 3.6. Let us choose a positive charge for the fixed line, $\tau_0=+1$. The projection results in gauge group $SO(N_0)\times SU(N_1)\times SO(N_2)$, with $N_0=N_2$ for anomaly condition and N_1 unconstrained. The superpotential reads

$$W^{\Omega}_{\mathcal{C}/\mathbb{Z}_2} = \epsilon_{ab}\epsilon_{cd} X^a_{01} X^c_{12} \left(X^b_{01}\right)^T \left(X^d_{12}\right)^T \ . \tag{3.15}$$

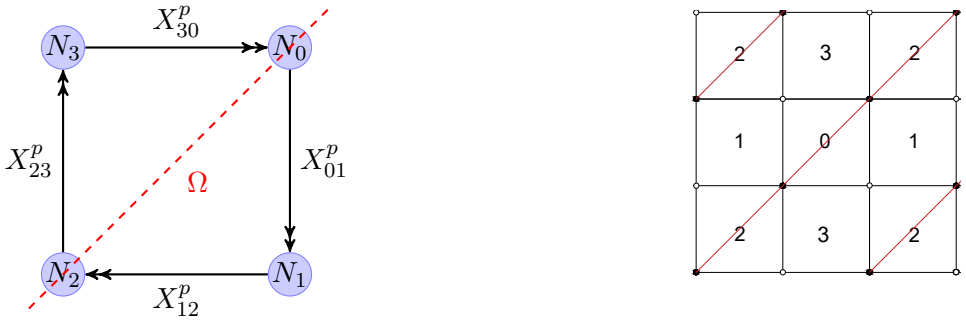

Figure 3.6. The orientifold involution with a fixed line of $\mathcal{C}/\mathbb{Z}_2'$, whose quiver is drawn on the left and the dimer on the right.

From the R symmetry we write

$$\begin{aligned} &R_{01} + R_{12} = 1 \ , \\ &(R_{01} - 1)2N_1 = -(N_0 - 2\tau_0) \ , \\ &(R_{01} + R_{12} - 2)2N_0 = -2N_1 \ , \\ &(R_{12} - 1)2N_1 = -(N_0 - 2\tau_0) \ , \end{aligned} \tag{3.16}$$

which has no solution, hence there is no conformal fixed point after the orientifold projection since no anomaly-free R-symmetry is allowed. This is an example in which conformal invariance is broken by the involution. In [88] this unoriented model is discussed, in particular its flow described as a Seiberg duality cascade and its confinement in the infrared.
Upon orientifolding, the fate of the conformal point is different in these two examples. In the first case, the fixed point still exists but with R-charges corrected at subleading order. On the other hand, in the second case conformal invariance is broken by the orientifold involution. These two cases, dubbed *first scenario* and *second scenario* are not the only ones allowed, as another behaviour will be discussed in Chapter 5.

Chapter 4

Mass deformation of unoriented quivers

In the past chapters we have introduced various tools to describe the field theory side of the gauge/-gravity duality in particular dimers, quivers and the orientifold projection, along with deformations as higgsing and mass deformation. This chapter is based on [1] and explores the overlap between orientifold and mass deformations. In doing so, our focus will be on orbifold parent theories. The systematic construction from string theory was given in [39] and along this we use here dimer and toric techniques.
In presence of orientifold planes, we reach non-orbifold singularities by mass deforming or higgsing a model, and we exploit the systematic approach of [39] in order to find consistent theories. This also allow us to add flavour branes, i.e. non-compact D7, to the system following the prescription of [39] and, as a simple example, we address this more delicate problem in the prototypical case of the unoriented $\mathbb{C}^3/\mathbb{Z}_3$ orbifold [89, 90].
We also address the issue of identifying O7 planes on compact cycles using a result from algebraic geometry, the Ito-Reid theorem [91]. We conclude our analysis discussing the orientifold projection in the context of Seiberg duality and duality cascades.

4.1 The Setup

We describe the setup at the base of our analysis. We consider Type IIB Superstring Theory on a four-dimensional Minkowski space $\mathbb{R}^{1,3}$, transverse to a singular (toric [15]) non-compact Calabi-Yau (CY) three-fold, parametrized by three complex coordinates (X_1, X_2, X_3), $I = 1, 2, 3$. The singularity is probed by D3-branes on which, at low energy, a non-abelian supersymmetric gauge theory lives. The transverse CY three-fold can either be an orbifold of $\mathbb{C}^3$ of the form $\mathbb{C}^3/\Gamma$ or a non-orbifold space. On top of this setup, we further consider the action of Orientifolds via O-planes and, later on, flavour branes.

4.1.1 D3-Branes at Toric Calabi-Yau Singularities

Consider the case of an abelian orbifold of the form $\mathbb{C}^3/\Gamma$ with $\Gamma = \mathbb{Z}_n$. On each complex coordinate (X_1, X_2, X_3) of the transverse space, the orbifold group acts as

$$g: \quad X_I \mapsto \omega^{k_I} X_I, \qquad \omega = e^{\frac{2\pi i}{n}} , \tag{4.1}$$

where g is the generator of $\mathbb{Z}_n$ and k_I must satisfy the supersymmetry-preserving CY condition[1]

$$\sum_{I=1}^{3} k_I = 0 \bmod n , \tag{4.2}$$

where $0 \leq k_I \leq (n-1)$. The quotient $\mathbb{C}^3/\mathbb{Z}_n$ has only one fixed point at the origin, which is the singularity. There we place the D3-branes, as we are interested in the dynamics of their WV. A 4d theory can arises also on D5- and D7-branes wrapping respectively collapsed two- or four-cycles of the resolved CY three-fold. At low energy, the dynamics of open strings living on their world-volume is governed by a supersymmetric quiver gauge theory whose gauge group is a product of $U(N_a)$, $a = 1, \ldots, n$ groups. The strings with endpoints connecting different fractional branes give rise to bifundamental fields $(\square_a, \overline{\square}_b)$ denoted by X_{ab}, where $\square_a(\overline{\square}_a)$ is the fundamental (antifundamental) representation of the gauge group $U(N_a)$. A more detailed discussion of the spectrum in the orbifold case is presented in [39]. The quiver for the simple example of the $\mathbb{C}^3/\mathbb{Z}_3$ orbifold is shown in Fig. (4.1). Note that the gauge theories arising from orbifold may be chiral (as $k_I = (1, 1, n-2)$) or non-chiral (as $k_I = (1, n-1, 0)$). While the latter are non-anomalous by construction, the former need the RR tadpoles to vanish for the theory to be anomaly-free, thus giving constraints on the ranks of the gauge groups. Furthermore, even if for $\mathbb{C}^3/\mathbb{Z}_n$ the sum of all the beta functions is zero, i.e. $\sum_a \beta_a = 0$, each gauge factor may have a non-zero β_a.

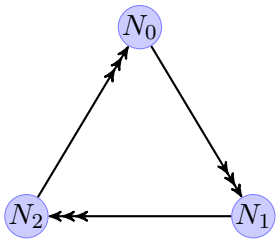

Figure 4.1. The quiver of the $\mathbb{C}^3/\mathbb{Z}_3$ orbifold theory with $k_I = (1, 1, 1)$. The bifundamental fields are arrows connecting nodes representing $U(N)$ gauge groups. The condition of anomaly cancellation gives $N_0 = N_1 = N_2$ and, as a result, $\beta_0 = \beta_1 = \beta_2 = 0$.

The above example is only one of infinitely many possibilities where fractional D3-branes are placed at CY singularities. We focus on the case of toric CY spaces, i.e. admitting at least a $U(1) \times U(1)$ isometry in addition to the $U(1)_R$ R-symmetry.
Strings on the fractional branes do not see the singular space $\widehat{Y}$, but they effectively live on a

[1] If you are keeping track of footnotes, this clarifies the reason why we start counting nodes from 0 instead of 1.

smooth resolved space Y, related to the former by a blow-down morphism $Y \to \widehat{Y}$. For $\widehat{Y} = \mathbb{C}^m/\Gamma$ orbifold theories, one can determine some useful geometrical properties of the resolved space by introducing the concept of *age grading* [14, 91, 92]. Consider an element $g \in \Gamma$, that is such that $g^n = 1$. The *age* of the element g is defined as

$$\text{age}(g) = \frac{1}{n}\sum_{I=1}^{m} k_I \ . \tag{4.3}$$

From the age, one can organize the elements of Γ in various conjugacy classes: null or baby classes have age = 0, junior classes have age = 1 and senior classes with age = 2. According to the Ito-Reid Theorem [91], each conjugacy class is associated with the dimension of de Rham cohomology groups of the crepant[2] resolution, according to

$$\dim H^{2k}(Y) = \text{number of age } k \text{ conjugacy classes of } \Gamma \tag{4.4}$$

while all odd cohomology groups are trivial[3]. The conjugacy classes of age k are then related to the existence of $2k$-cycles in the smooth space Y. In particular, a non-trivial senior class implies the existence of a compact 4-cycle. A more general and detailed discussion is presented, for instance, in [14]. As an example, the crepant resolution of $\mathbb{C}^3/\mathbb{Z}_4$ is addressed in [92]. This classification helps identifying the cycles wrapped by a D-brane or an O-plane.

4.1.2 Adding Flavour Branes

In the setup with D3-branes transverse to a singular toric CY and O-planes we may add stacks of M non-compact D7-branes which act as flavour branes. Their presence generates a non-dynamical D7-D7 open string sector, and a dynamical D3-D7 sector which adds new matter fields to the spectrum and to the superpotential. The group $U(M)$ is seen as a global symmetry by strings living on the D3. Under an orbifold quotient by $\mathbb{Z}_n$, the flavour groups becomes $U(M_\alpha)$, $\alpha = 0, \ldots, n-1$. We denote the new matter fields as $q_{a\alpha} = (\square_a, \overline{\square}_\alpha)$ for fields transforming in the fundamental of $U(N_a)$ of the a-th fractional brane and in the anti-fundamental of $U(M_\alpha)$ of the α-th flavour brane (i.e. starting from the D3-brane and ending on the D7-brane) while $\tilde{q}_{\alpha a} = (\square_\alpha, \overline{\square}_a)$ for open strings with the opposite orientation. They enter in the super-potential with terms of the form

$$W_{37} = (\tilde{q}_{\alpha a})^{i_a}_{i_\alpha} (M_{ab})^{i_b}_{i_a} (q_{b\alpha})^{i_\alpha}_{i_b} \ , \tag{4.5}$$

where $M_{ab} = (X_{ac})^{i_c}_{i_a}(X_{cd})^{i_d}_{i_c} \ldots (X_{fb})^{i_b}_{i_f}$ is a composite operator and the indices i_a run over the N_a colours of the a-th gauge group, while the indices i_α run over the M_α flavours of the α-th flavour

[2] We recall that a crepant resolution is a resolution that preserves the Calabi-Yau condition, namely the first Chern class of the tangent bundle of Y vanishes.

[3] This implies that the singularity, as most of the toric CY singularities, is 'isolated' in that it does not admit complex (marginal) deformations, i.e.. We will later on discuss relevant mass deformations which trigger RG-flows.

groups.
When the D7's wrap non-compact cycles, they are much heavier than the D3's and thus backreact on the geometry, in which case the toricity may not be preserved. This can be further seen from the super-potential where the new terms coming from the D3-D7 sector break the toric condition. In [43] the possibility of representing flavour branes as open paths in the dimer is presented and one can read the field theory after this deformation, but one can no longer define a tiling on a torus for the resulting theory, but on other geometries [46].
We can add flavour branes to the quiver as new nodes and links for the global symmetry groups and 3-7 fields. The D3-D7 open strings sector contains chiral multiplets $\mathbf{C}^{\dot{a}}$ which transform in $Spin(4)$ with weights $\pm(\frac{1}{2},\frac{1}{2})$. Under the orbifold projection by $\mathbb{Z}_n$, $\mathbf{C}^{\dot{a}}$ transform as

$$\mathbf{C}^{\dot{a}} \mapsto \omega^{\pm\frac{1}{2}(k_I+k_J)}\mathbf{C}^{\dot{a}} = \omega^{\pm s}\mathbf{C}^{\dot{a}} \ , \tag{4.6}$$

where $\omega = e^{i2\pi/n}$, $I \neq J \neq K = 1,2,3$, we have used the supersymmetry preserving condition $k_1+k_2 = -k_3 \bmod n$ and we have defined $s = (k_I+k_J)/2$. For a supersymmetric embedding of the D7 branes it must be $(\omega^{\pm s})^n = 1$, thus k_K must be even. Moreover, s determines the connection between gauge and global groups, as a colored node a is connected to a flavour node $\alpha+s$. Note that we can embed different D7-branes on the same divisor $X_K = 0$ but with different Chan-Paton factors [43]. There are various choices, but here we show only one of them for $\mathbb{C}^3/\mathbb{Z}_3$. Under an orientifold projection, flavour groups are projected to $SO/USp(M_\alpha)$ while D3-D7 strings are identified as,

$$\begin{aligned}
&\Omega : \qquad \square_\alpha \leftrightarrow \overline{\square}_{n-\alpha} \ , \\
&\widehat{\Omega} : \qquad \square_\alpha \leftrightarrow \overline{\square}_{n-\alpha-1} \ , \\
&q_{a\alpha} = (\square_a, \overline{\square}_\alpha) \leftrightarrow (\square_{\alpha'}, \overline{\square}_{a'}) = \tilde{q}_{\alpha' a'} \ .
\end{aligned} \tag{4.7}$$

4.2 Unoriented Toric Singularities and their Mass Deformation

In this Section, we try to unify the machineries of dimers and of [39]. After that, we will present several examples with small number of nodes. We will revisit by-now prototypical examples, like $\mathbb{C}^3$ and $\mathbb{C}^3/\mathbb{Z}_3$, as well as new ones. We will try and emphasize the connection between orbifold and non-orbifold singularities via mass-deformations or Higgsing that preserve toricity, where possible. The super-potential W consists of mesonic operators as $(X_{ab})^{i_b}_{i_a}(X_{bc})^{i_c}_{i_b}\dots(X_{fa})^{i_a}_{i_f}$. For convenience of notation, we just write $X_{ab}X_{bc}\dots X_{fa}$. The same holds when 3-7 fields $q_{a\alpha}$ and $\tilde{q}_{\alpha a}$ are involved. In this way, we use upper indices $I = 1,2,3$ or $p = 1,2$ to denote the different fields in a multiplet as $X^{I\,(p)}_{ab}$, which enter with different combinations in mesonic operators. We use the extended notation only when needed for clarity.

4.2.1 Orientifolding the D3 branes picture

All of the discussion in the previous chapters was mainly based on the brane tiling, i.e. the system of 5-branes, but we always keep in mind that the gauge theory arises in the D3 brane WV, with these probing the singular point of a toric CY cone. The case of unoriented projections of abelian orbifolds of the form $\mathbb{C}^3/\mathbb{Z}_n$ or $\mathbb{C}^3/\left(\mathbb{Z}_n \times \mathbb{Z}_m\right)$ in presence of either O3 or O7 planes was systematically addressed in [39], only from string amplitudes considerations. They used quivers to represent the theory arising from unoriented singularities, so the diagrams are similar and we can easily compare. The only difference with our setup relies on the orientifold action, that is encoded into four charges $(\epsilon_0, \epsilon_1, \epsilon_2, \epsilon_3)$ with a clear physical interpretation: ϵ_0 is the RR charge of the orientifold plane, while the three ϵ_I, $I = 1, 2, 3$, determine the $\mathbb{Z}_2$ action of the orientifold plane on the complex direction X_I of the CY transverse to the D3 branes. Thus, we can leave

$$\begin{aligned} O3^{\pm} &: \quad (\pm, -, -, -) \ , \\ O7^{\pm} &: \quad (\pm, +, +, -) \ . \end{aligned} \tag{4.8}$$

Note that for an O7 the ϵ_I charges has different signs, while O3 only $\epsilon_I = -$. Using the conventions of [39], when a node on the quiver is crossed by the Ω-line the corresponding gauge group is projected down to USp or SO if $\epsilon_0 = +1$ or $\epsilon_0 = -1$, respectively[4].
For orbifold theories $\mathbb{C}^3/\mathbb{Z}_n$, the possible orientifold projections are classified by parity of n. In case of odd n, there is always at least one node on top of the orientifold line, that for convenience and without loss of generality we denote by 0, while nodes a and $n-a$ are reflected into each other. For even n, configurations with all nodes away from the orientifold line are allowed, which we denote as $\widehat{\Omega}$, in such a way that nodes a and $n-a-1$ are reflected into each other (up to renumbering of the nodes). Thus

$$\begin{aligned} \Omega &: \quad \square_a \longleftrightarrow \overline{\square}_{n-a} \ , \\ \widehat{\Omega} &: \quad \square_a \longleftrightarrow \overline{\square}_{n-a-1} \ , \end{aligned} \tag{4.9}$$

hence fields are identified as in the previous sections. When a field $X^I_{aa'}$ connects a node and its image a', it gives rise to the symmetric representation if $\epsilon_0\epsilon_I = +1$ or to the antisymmetric representation if $\epsilon_0\epsilon_I = -1$. In these conventions, quivers associated to non-orbifold singularities can be related to orbifold ones via mass deformation or higgsing/un-higgsing.
It is important to stress that the orientifold charges (ϵ_0, ϵ_I) for orbifold theories, which have a more direct geometric interpretation, and the τ charges defined on the dimer are in principle different, and in fact they also act in different ways. The mesonic moduli space is spanned by gauge-invariant mesonic operators and a subclass of them can be regarded as the transverse coordinates to the D3 branes. On the dimer, they are constructed with fields lying on closed oriented paths (see [81]) and

[4]Note the opposite convention w.r.t. the brane tiling machinery. Not even physicists are perfect.

the product of τ charges they intersect gives the orientifold action on the mesonic operators. For the unoriented projection of $\mathbb{C}^3$ and $\mathbb{C}^3/\mathbb{Z}_3$ the product of pairs of τ charges, i.e. the orientifold action on mesonic operators, is exactly the same as $\epsilon_0\epsilon_I$. The relation between ϵ and τ becomes much more complicated in other cases.

4.2.2 Anomaly Cancellation Conditions

The low-energy gauge theories we have so far considered involve chiral fields, hence they can be potentially anomalous. We now rewrite the anomaly cancellation condition following the method developed in [39] for unoriented $\mathbb{C}^3/\mathbb{Z}_n$ orbifolds. Recall that for a node a in the quiver we need to count how many fields transform under the gauge group. Those which go out from the node, i.e. transform in the fundamental representation, are counted with a positive sign, while those which enter in the node, i.e. transform in the anti-fundamental representation, take a negative sign. Also chiral fields with flavour indices must be counted, if flavour branes are present. When the O-plane crosses fields which connect the node a to its image a', these are projected to their symmetric or antisymmetric representation and thus their contribution to the anomaly is $(N_a{+}4)$ and $(N_a{-}4)$ respectively, for each field. For each node a, the anomaly cancellation condition for the orbifold theory reads

$$\sum_{b=1}^{n-1} (I_{ab}N_b + J_{ab}M_b) + 4\sum_I \left(\epsilon^{(I)}_{aa'} - \epsilon^{(I)}_{a'a}\right) = 0 \,, \tag{4.10}$$

where I_{ab} and J_{ab} count with orientation how many fields start from (or end on) the node a,

$$I_{ab} = \sum_{I=1}^{3} \left(\delta_{a,\,b-k_I} - \delta_{a,\,b+k_I}\right) \,, \qquad J_{ab} = \delta_{a,\,b-s} - \delta_{a,\,b+s} \,, \tag{4.11}$$

and $\epsilon^{(I)}_{aa'}, \epsilon^{(I)}_{a'a} = \pm$ account for symmetric $(+)$ or antisymmetric $(-)$ fields, connecting nodes a and $a' = a + k_I$ (or the opposite orientation). It is important to note their relative sign in the anomaly cancellation, due to their different orientation in the spectrum[5]. In simple cases where fields along the direction I have the same orientation, $\epsilon^{(I)}_{aa'} = -\epsilon_0\epsilon_I$ and $\epsilon^{(I)}_{a'a} = \epsilon_0\epsilon_I$. The above Eq. (4.10) is a generalization of the anomaly cancellation condition used in [39], where it is was derived from the partition function of orbifold theories along the lines of [93, 94]. We will use it also for non-orbifold theories, since these can be related via mass deformations or Higgsing to orbifold theories. In this case we still use the notation $\epsilon^{(I)}_{aa'}$, where I stands for the fields in a multiplet rather than the orbifold directions. The above generalization allow us to exactly reproduce known results in the literature and to gain further physical intuition about unoriented gauge theories at general Calabi-Yau singularities, as we will see in the forthcoming sections.

[5] Actually, in [39] the anomaly cancellation condition was different, because it was assumed that fields along the direction $I = 1, 2, 3$ have always the same orientation. In the present work the general scenario is allowed, generalizing previous results. See below the example of $\mathbb{C}^3/\mathbb{Z}_4$ $(1, 1, 2)$.

4.2.3 Conformal Invariance

We also rewrite the beta functions in terms of I_{ab} and J_{ab}. The presence of both O-planes and flavour branes can alter the conformal properties of the original parent theory. It is thus an interesting question to ask which unoriented projections allow for a theory which is simultaneously anomaly-free and conformal in the perturbative regime, i.e. without the inclusion of strongly coupled sectors in the IR as done in [84, 85]. We will show that not all the orientifold projections we consider fulfill this request and we will give a physical interpretation of the results in terms of O3 and compact/non-compact O7 planes.
Recall that the β-function of an $\mathcal{N}=1$ gauge theory is

$$\beta \propto 3T_{\text{Adj}} - \sum_i T_{\rho_i}\left(1-\gamma_i\right) \ , \ , \tag{4.12}$$

where T_ρ denotes the Dynkin index of the representation ρ, γ_i is the anomalous dimension of the bi-fundamental chiral fields and the sum runs over all chiral fields transforming under the gauge group factor. To determine the anomalous dimensions of the chiral fields X_{ab}, one may use the properties of the superpotential and the fact that at the conformal point $\Delta = \frac{3}{2}R$, that has to be positive for gauge-invariant chiral fields in a unitary theory.
Starting with a superconformal quiver gauge theory, the orientifold projection may break conformal invariance. In case of an O3-plane, which acts projecting fields $X^I_{aa'}$ onto different symmetric or antisymmetric representations for different I, conformal invariance may hold. On the other hand, an O7-plane couples to the dilaton and then its presence usually breaks conformal invariance. In some cases, in order to obtain a conformal theory, we may add a suitable number of flavour branes, as shown in [39]. For quiver gauge theories with flavour branes and O-planes, the general β-function β_a at the node a reads

$$\begin{aligned}
\beta_a^{SU} &= 3N_a - \sum_I \left(\epsilon^{(I)}_{aa'} + \epsilon^{(I)}_{a'a}\right)\left(1-\gamma^{(I)}_{aa'}\right) - \frac{1}{2}\left(I^+_{ab}N_b + J^+_{ab}M_b\right) \ , \\
\beta_a^{SO/USp} &= \frac{3}{2}N_a + 3\epsilon_a - \frac{1}{2}\sum_I \left(\epsilon^{(I)}_{aa'} + \epsilon^{(I)}_{a'a}\right)\left(1-\gamma^{(I)}_{aa'}\right) - \frac{1}{4}\left(I^+_{ab}N_b + J^+_{ab}M_b\right) \ .
\end{aligned} \tag{4.13}$$

For oriented abelian orbifolds $\mathbb{C}^3/\mathbb{Z}_n$, $\gamma_{ab}=0$. The anomalous dimensions of fields in the oriented parent theory and in the unoriented one usually differ by terms of order $1/N$, which are suppressed in the large N limit. Moreover, fields transforming in the symmetric or antisymmetric representation are usually present in unoriented theories and their contribution to the beta function differs from the original fields in the parent theory. For these reasons, we allow for non-zero anomalous dimensions even in the simple case of unoriented abelian orbifolds.

In Eq. (4.13) we have used

$$I^{+}_{ab} = \sum_{I=1}^{3} \left(\delta_{a,b-k_I} + \delta_{a,b+k_I}\right) \left(1 - \gamma^{(I)}_{ab}\right) \ , \qquad J^{+}_{ab} = \delta_{a,b-s} + \delta_{a,b+s} \ , \tag{4.14}$$

and $\epsilon_a = \pm$ projects a gauge group to Sp $(+)$ or SO $(-)$. The second term on the right hand side of both expressions in Eq. (4.13) only exists if in the quiver there are fields that are cut by the orientifold action and start from the node a. The above equations are a generalization of the action of a unique orientifold charge ϵ_0 i.e. we allow different projections for gauge groups in the same theory: the same orientifold may project a gauge group to $SO(Sp)$ while another group is projected to $USp(SO)$. This generalization works also for the anomaly cancellation equation and is perfectly consistent with previous results obtained in the literature, as we will see in the examples below.

Furthermore, since for $\mathbb{C}^3/\mathbb{Z}_n$ far away from the singularity the space looks like $\mathbb{C}^3$ and the theory is conformal, the sum of all the beta functions is zero, i.e. $\sum_a \beta_a = 0$, which corresponds to a constant complex dilaton S. In fact, for $\mathbb{C}^3/\mathbb{Z}_n$ the gauge kinetic function at each node, f_a, sum up to S. Note that, as observed in [39], $U(1)$ and $O(2)$ group factors are free in the IR and so decouple from the dynamics at large distances. The vanishing of their β functions cannot be achieved and should be relaxed. Similarly $O(1) = \mathbb{Z}_2$ has no proper β function.

4.2.4 Unoriented Projections of D3-branes on $\mathbb{C}^3$

The first prototypical example is the unoriented projection of $\mathbb{C}^3$ [81, 85]. The parent gauge theory is $\mathcal{N} = 4$ Super Yang-Mills (SYM) theory with super-potential

$$W = \mathrm{Tr}\ \Phi_1[\Phi_2, \Phi_3] \ , \tag{4.15}$$

where Φ_I are adjoint fields, which parametrize the three complex directions transverse to the stack of D3-branes. The toric diagram of this theory is a triangle with no internal point and consequently there are two different involutions given by an O3 or a non-compact O7.

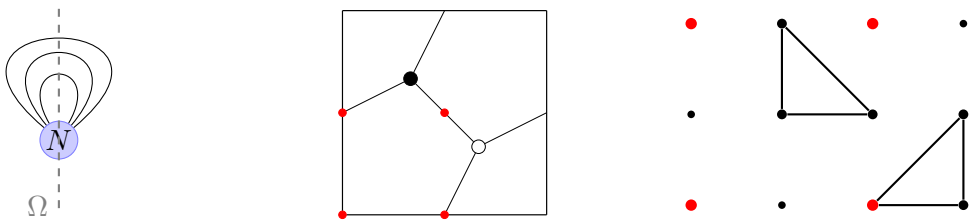

Figure 4.2. The unoriented quiver (left) and the dimer (center) of $\mathbb{C}^3$, while the unoriented toric diagram (right) with the two orientifolds O3 and O7, see Section 3.3 for a summary of the orientifold on the toric diagram.

Following the quiver description presented in [39], the orientifold charges for an O3$^{\pm}$, $(\pm,-,-,-)$ give $\mathcal{N}=4$ SYM with $USp(SO)(N)$ gauge group and the three fields transforming in the (anti)symmetric representation; the orientifold charges for a O7$^{\pm}$, $(\mp,+,+,-)$ yield a $\mathcal{N}=2$ gauge theory with either $USp(N)$ and two antisymmetric fields and one symmetric, or $SO(N)$ with two symmetric fields and one antisymmetric. The superpotential of the parent theory is easily read from the dimer and, after the unoriented projection, the product of the τ charges on the dimer must be negative due to the constraint given by Eq. (3.3). The first of various choices[6] is $(\tau_0,\tau_1,\tau_2,\tau_3)=(\mp,\pm,\pm,\pm)$, which gives $\mathcal{N}=4$ SYM. In fact, the three mesonic operators on the dimer flip their signs under O3$^{\pm}$. For this model the relation with the orientifold charges is $\epsilon_0=-\tau_0=\pm$, $\epsilon_1=\tau_0\tau_1=-$, $\epsilon_2=\tau_0\tau_2=-$, $\epsilon_3=\tau_0\tau_3=-$, and corresponds to an O3$^{\pm}$. On the other hand, the action of an O7 is encoded in such choices of τ charges as $(\pm,\pm,\pm,\mp)$ or permutation of the last three signs. The three diagrams are drawn in Fig. (4.2). Finally, note that O3 yields a conformally invariant theory with canonical dimensions and R-charges for the three adjoint chiral fields.

4.2.5 Orientifold of $\mathcal{N}=1$ Orbifold $\mathbb{C}^3/\mathbb{Z}_3$, $(1,1,1)$

In this section we analyze the second prototypical example, the unoriented projection of the chiral orbifold $\mathbb{C}^3/\mathbb{Z}_3$ [81, 85, 95], whose different descriptions are drawn in Fig. (4.3). We study the $\mathcal{N}=1$ theory with $k_I=(1,1,1)$, whose quiver is the same as the theory with $k_I=(2,2,2)$, up to relabelling the nodes. Among the conjugacy classes, summarized in Tab. (4.1), the single senior class signals the presence of a single compact 4-cycle and this information will be useful later.

$(k_1,\, k_2,\, k_3)$	Age$=\frac{1}{3}\sum_I k_I$	Conjugacy class
(0, 0, 0)	0	Baby
(1, 1, 1)	1	Junior
(2, 2, 2)	2	Senior

Table 4.1. The conjugacy classes of the orbifold model $\mathbb{C}^3/\mathbb{Z}_3$.

The super-potential is

$$W=\epsilon_{IJK}X^I_{01}X^J_{12}X^K_{20}\,, \tag{4.16}$$

which enjoys the mesonic symmetry $SU(3)$. In fact, the theory has symmetry $SU(3)\times U(1)_R$, where $U(1)_R$ is the R-symmetry of the $\mathcal{N}=1$ SCFT.

Let us perform the unoriented projection with a compact O7-plane in the resolved space, whose toric diagram is the left one shown in Fig. (4.3). Since $n=3$ is odd, there are only three equivalent projections with the O-plane on top of a node. Here, without loss of generality, we consider only

[6] The first τ lays on the face, the other three follow in clockwise order on the dimer.

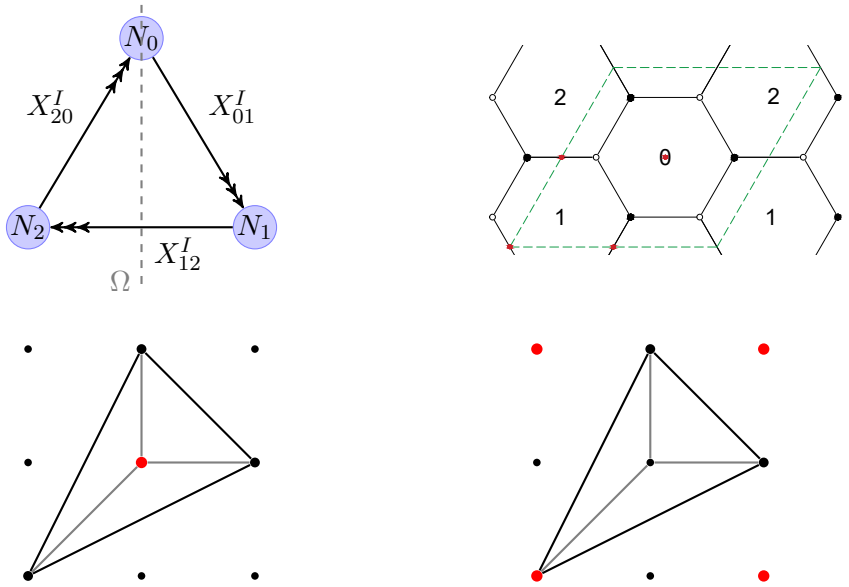

Figure 4.3. The various unoriented descriptions of $\mathbb{C}^3/\mathbb{Z}_3$. The upper row shows the quiver (left) and the Ω-line, whereas on the right side the dimer, with the four fixed points in red. In the lower row: the toric diagram and the toric involution with a compact O7 (left) and a non-compact O7 (right).

an O-plane through the node 0. This orientifold involution acts on the orbifold as

$$\overline{\square}_2 = \square_1 \,, \qquad U(N_0) \to USp/SO(N_0) \tag{4.17}$$

and the super-potential becomes

$$W^\Omega = \epsilon_{IJK} X^I_{01} X^J_{11'} X^K_{1'0} \,. \tag{4.18}$$

The anomaly cancellation condition Eq. (4.10) reads

$$N_0 = N_1 + \frac{4}{3}\sum_{I=1}^{3} \epsilon^{(I)}_{11'} = N_1 \pm 4 \,, \tag{4.19}$$

which is indeed what we would have obtained with an O3$^\pm$ placed at the origin of the singular space. According to the toric diagram, the orientifold plane is a compact O7 in the smooth resolved space, which wraps the compact 4-cycle (whose presence is signaled by the senior conjugacy class) that in the singular space corresponds to an O3$^\pm$-plane. The results are summarized in Tab. (4.2). From the dimer, we can reproduce this unoriented projection with four fixed points $\tau_i = (\pm, \mp, \mp, \mp)$ as displayed in Fig. (4.3) and negative overall product of the τ charges τ_i. Again in this case, the relation between τ charges and orientifold charges is given by $\epsilon_0 = -\tau_0$ and the relative sign of the mesonic operators under the orientifold involution $\epsilon_I = \tau_0 \tau_I$.

Orientifold	Gauge groups	Anomaly condition	$(X^1_{11'}, X^2_{11'}, X^3_{11'})$
$O3^+$	$USp(N_0) \times U(N_1)$	$N_0 = N_1 + 4$	(S, S, S)
$O3^-$	$SO(N_0) \times U(N_1)$	$N_0 = N_1 - 4$	(A, A, A)

Table 4.2. The unoriented projection $O3^{\pm}$ (on the singular space) of the orbifold model $\mathbb{C}^3/\mathbb{Z}_3$ which, in the resolved space, is a compact O7-plane. The fields $X^I_{11'}$ are projected onto symmetric or antisymmetric representation, where "A" stands for "Antisymmetric representation", while "S" for "Symmetric representation".

Let us compute the β-functions. From Eq. (4.13) and using Eq. (4.19) we obtain

$$\begin{aligned} \beta_0^{SO/USp} &= \frac{3}{2} N_1 \gamma_{01} + 2 \sum_{I=1}^{3} \epsilon^{(I)}_{11'} + 3\epsilon_0 \ , \\ \beta_1^{SU} &= \frac{3}{2} N_1 \left(\gamma_{01} + \gamma_{11'}\right) + \sum_{I=1}^{3} \epsilon^{(I)}_{11'} \left(-3 + \gamma_{11'} + 2\gamma_{01}\right) \ . \end{aligned} \tag{4.20}$$

Assuming there is a conformal point, where $1 - \gamma_{ab} = 3(1 - R_{ab})$, we have for the R-charges

$$\begin{aligned} & R_{01} \frac{9}{2} N_1 = 3N_1 - 3\epsilon_0 - 2 \sum_{I=1}^{3} \epsilon^{(I)}_{11'} \ , \\ & R_{01} \left(\frac{9}{2} N_1 + 6 \sum_{I=1}^{3} \epsilon^{(I)}_{11'} \right) + R_{11'} \left(\frac{9}{2} N_1 + 3 \sum_{I=1}^{3} \epsilon^{(I)}_{11'} \right) = 3 \left(2N_1 + 3 \sum_{I=1}^{3} \epsilon^{(I)}_{11'} \right) \ , \\ & 2R_{01} + R_{11'} = 2 \ , \end{aligned} \tag{4.21}$$

where the last equation comes from the super-potential. The solution of the system is

$$\begin{aligned} R_{01} &= \frac{2}{3} \frac{N_1 - \sum_{I=1}^{3} \epsilon^{(I)}_{11'}}{N_1} \ , \\ R_{11'} &= \frac{2}{3} \frac{N_1 + 2 \sum_{I=1}^{3} \epsilon^{(I)}_{11'}}{N_1} \ , \end{aligned} \tag{4.22}$$

from which $\gamma_{01} = -2 \frac{\sum_{I=1}^{3} \epsilon^{(I)}_{11'}}{N_1}$, $\gamma_{11'} = +2 \frac{\sum_{I=1}^{3} \epsilon^{(I)}_{11'}}{N_1}$. Note that in the large N limit we retrieve back the anomalous dimensions of the parent theory, namely, $\gamma_{11'} = \gamma_{01} = 0$ and the sum of the beta functions vanishes if $3\epsilon_0 = \sum_{I=1}^{3} \epsilon^{(I)}_{11'}$.
Note also that in the resolved space the compact O7 acts in such a way that all the three fields $X^I_{11'}$ are projected in the same way, as we can see from the anomaly cancellation condition Eq. (4.19).

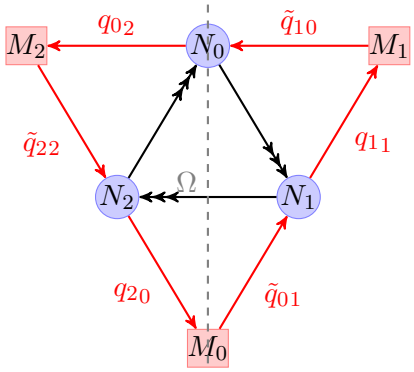

Figure 4.4. The quiver of $\mathbb{C}^3/\mathbb{Z}_3$ with the addition of flavour branes.

In [39] it is been argued that one may add non-compact flavour branes in the system as shown in Fig. (4.4). We discuss the presence of flavour branes only for this model. Since the D7-branes yield additional chiral fields, the new anomaly equations read

$$M_0 - M_1 = 3(N_1 - N_0) + 4\sum_{I=1}^{3} \epsilon_{11'}^{(I)} \,, \tag{4.23}$$

that can be solved even with the presence of O7 in the singular space and a judicious choice of M_1 and M_0. These branes enter in the super-potential with new terms such as

$$W = \epsilon_{IJK} X_{01}^I X_{12}^J X_{20}^K + \tilde{q}_{\alpha a} X_{ab}^3 q_{b\alpha} \tag{4.24}$$

wrapping the flavour branes along the divisor $X_3 = 0$. The orientifold action on the flavour groups and super-potential is

$$\begin{gathered} \overline{\square}_3 = \square_2 \,, \\ U(M_0) \to USp/SO(M_0) \,, \\ W^\Omega = \epsilon_{IJK} X_{02'}^I X_{2'2}^J X_{20}^K + \tilde{q}_{02'} X_{2'2}^3 q_{2\,0} + \tilde{q}_{10} X_{01}^3 q_{1\,1} + \tilde{q}_{1'2} X_{20}^3 q_{0\,1'} \,. \end{gathered} \tag{4.25}$$

The beta-functions, together with the anomaly-free condition, in this case read

$$\begin{aligned} 2\beta_0 &= 3N_1\gamma_{01} + 6\epsilon_0 + 4\sum_{I=1}^{3} \epsilon_{11'}^{(I)} - M_0 \,, \\ 2\beta_1 &= N_1 \left(3\gamma_{01} + \sum_{I=1}^{3} \gamma_{11'}^{(I)}\right) + 2\sum_{I=1}^{3} \epsilon_{11'}^{(I)} \left(-3 + 2\gamma_{01} + \gamma_{11'}^{(I)}\right) + M_0 \left(-2 + \gamma_{01}\right) - M_0\gamma_{01} \,. \end{aligned} \tag{4.26}$$

Imposing the vanishing of the sum of the beta functions when the anomalous dimensions are trivial, we get

$$3\epsilon_0 - \sum_{I=1}^{3} \epsilon_{11'}^{(I)} = \frac{1}{2}(M_0 + 2M_1) \ , \tag{4.27}$$

which is solved, for instance, for $\epsilon_0 = +1, \sum_{I=1}^{3} \epsilon_{11'}^{(I)} = -3$ and $M_0 = M_1 = 4$. This scenario corresponds to the presence of a O3-plane or, better, a compact O7-plane in the resolved space wrapped on a 4-cycle, whose existence is guaranteed by the Ito-Reid theorem. Note that in this case the beta functions do not vanish separately. A second choice corresponds to considering $\epsilon_0 = +1$ and $\sum_{I=1}^{3} \epsilon_{11'}^{(I)} = \pm 1$ which is related to the presence of a non-compact O7-plane.
The point of [39] is that, when the orientifold breaks conformal invariance, one may add flavour branes in order to recover such invariance. However, the presence of non-compact flavour branes breaks the toric condition and we cannot use the orientifold rules from the dimer. The tiling would not be defined on a torus and the orientifold involution gives rise to different geometries.

4.2.6 Orientifold of the First del Pezzo Surface (dP_1)

We begin the study of the unoriented projections of some non-orbifold theories with the complex cone over the first del Pezzo surface dP_1 [81, 85, 95, 96], whose different diagrams are drawn in Fig. (4.5). The anomaly cancellation condition Eq. (4.10) is derived from partition functions of orbifold theories, then in principle we are not allowed to use it for these cases. However, the dP_1 theory is related to the orbifold model $\mathbb{C}^3/\mathbb{Z}_3$ by higgsing two gauge groups [71]. From the quiver and the dimer it is easy to see that merging nodes/faces 0 and 3 into one node/face produce the diagrams of $\mathbb{C}^3/\mathbb{Z}_3$, see for example Fig. (4.6). On the toric diagram, the giggsing procedure takes out an external node, as displayed in Fig. (4.7). We will see that also the super-potential matches. Let us begin with the super-potential of dP_1, which reads

$$W = \epsilon_{pq} \left[X_{12}^q \left(X_{20} X_{01}^p - X_{23}^p X_{31} \right) + X_{12}^3 X_{23}^q X_{30} X_{01}^p \right] \ . \tag{4.28}$$

with $p, q = 1, 2$. As explained in Sec. 2.4.2, we give VEV to $\langle X_{30} \rangle = 1$ and the super-potential becomes

$$W = \epsilon_{pq} \left[X_{12}^q \left(X_{20} X_{01}^p - X_{20}^p X_{01} \right) + X_{12}^3 X_{20}^q X_{01}^p \right] \ . \tag{4.29}$$

Re-defining the fields as $X_{20} \to X_{20}^3$, $X_{01} \to X_{01}^3$ we end up with the super-potential of the $\mathbb{C}^3/\mathbb{Z}_3$ theory

$$W = \epsilon_{IJK} \left(X_{12}^I X_{20}^J X_{01}^K \right) \ . \tag{4.30}$$

The idea is to use the argument the other way around, namely from the unoriented $\mathbb{C}^3/\mathbb{Z}_3$ we un-higgs the group at node 0 and obtain the unoriented dP_1. The anomaly cancellation condition is thus inherited from the orbifold theory.

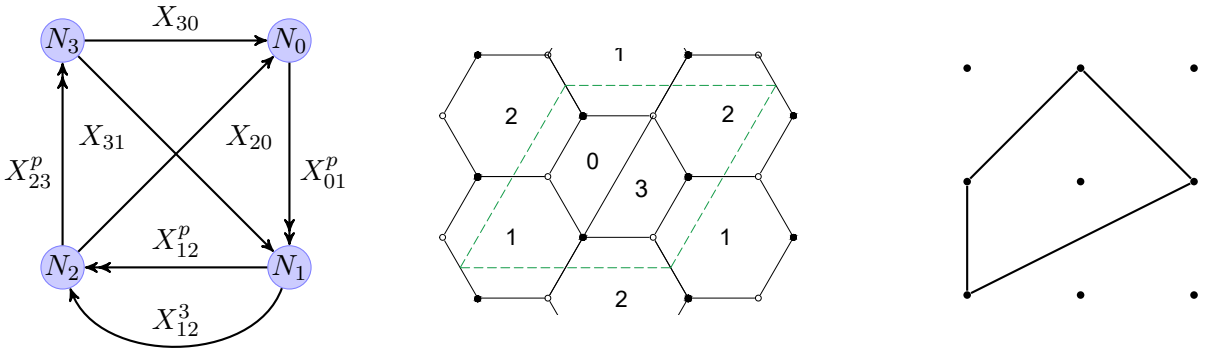

Figure 4.5. The quiver (left), the dimer (center) and the toric diagram (right) of dP_1.

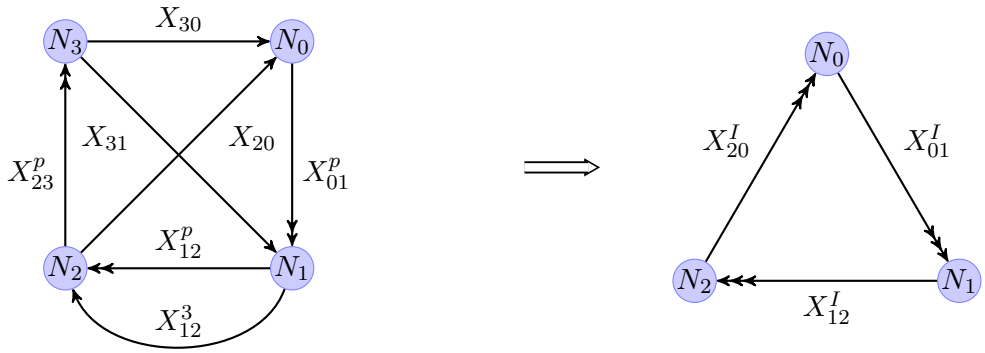

Figure 4.6. The Higgsing of nodes 0 and 3 on the quiver of dP_1 gives the quiver of $\mathbb{C}^3/\mathbb{Z}_3$.

Orientifold $\widehat{\Omega}$ of dP_1

Considering the toric diagram of this model, there are three orientifold involutions allowed, one with a compact O7, one with a non-compact O7 and an O3, and one with a non-compact O7, see Fig.(4.9). The unoriented projections from quiver and dimer are shown in Fig.(4.8). Identifications are

$$\overline{\square}_3 = \square_0 \ , \qquad \overline{\square} = \square_1 \ , \tag{4.31}$$

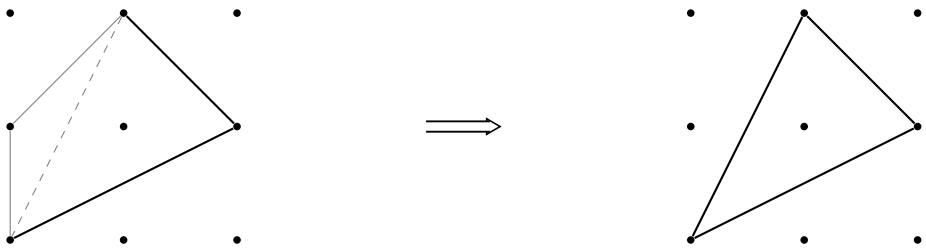

Figure 4.7. Higgsing dP_1 (left) takes out an external node from the toric diagram, resulting in $\mathbb{C}^3/\mathbb{Z}_3$ (right).

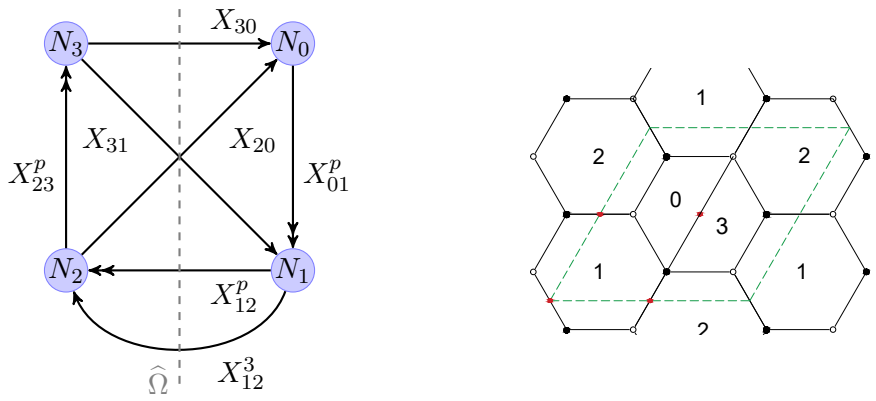

Figure 4.8. The orientifold projection $\widehat{\Omega}$ of dP_1, whose quiver is on the left and dimer on the right.

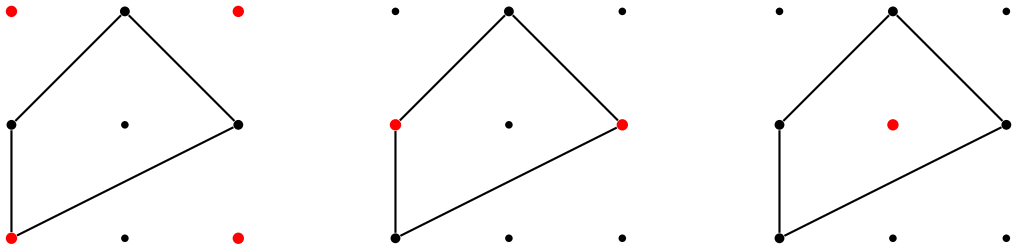

Figure 4.9. The various orientifold projections of toric diagram of dP_1. The left figure shows the orientifold with a non-compact O7 and O3, in the center a non-compact O7 and on the right a compact O7.

the superpotential reads

$$W = \epsilon_{pq}\left[X^q_{11'}\left(X_{1'0}X^p_{01} - X^p_{1'0'}X_{0'1}\right) + X^3_{11'}X^q_{1'0'}X_{0'0}X^p_{01}\right] \tag{4.32}$$

and the anomaly-cancellation equations are

$$\begin{aligned} \epsilon_{0'0} &= -\frac{1}{3}\sum_{I=1}^{3}\epsilon^{(I)}_{11'}\,, \\ N_1 &= N_0 - \frac{4}{3}\sum_{I=1}^{3}\epsilon^{(I)}_{11'}\,, \end{aligned} \tag{4.33}$$

which requires $\left(\epsilon^{(1)}_{11'}, \epsilon^{(I)}_{11'}, \epsilon^{(I)}_{11'}\right) = (\pm,\pm,\pm)$ and $\epsilon_{0'0} = \mp$. This agrees with Eq. (3.3), from which the overall product of the signs must be negative. The possible choices are summarized in Tab. (4.3).

Orientifold	Anomaly condition	$X_{0'0}$	$(X^1_{11'}, X^2_{11'}, X^3_{11'})$
$\widehat{\Omega}^+$	$N_1 = N_0 + 4$	S	(A, A, A)
$\widehat{\Omega}^-$	$N_1 = N_0 - 4$	A	(S, S, S)

Table 4.3. The orientifold involutions $\widehat{\Omega}$ of dP_1 with gauge groups $U(N_0) \times U(N_1)$.

The beta functions of this model read

$$\begin{aligned} 2\beta_0 &= N_0\left(2+2\gamma_{01}+\gamma_{0'0}+\gamma_{1'0}\right)+2\epsilon_{0'0}\left(-7+\gamma_{0'0}+2\gamma_{1'0}+4\gamma_{01}\right)\ , \\ 2\beta_1 &= N_0\left(\gamma_{0'1}+2\gamma_{01}+2\gamma_{11'}+\overline{\gamma}_{11'}\right)+2\epsilon_{0'0}\left(9+\gamma_{11'}+2\overline{\gamma}_{11'}\right)+2\epsilon_{11'}^3\left(\overline{\gamma}_{11'}-\gamma_{11'}\right)\ , \end{aligned} \tag{4.34}$$

where γ_{ab} are the anomalous dimensions of X_{ab} and $\overline{\gamma}_{11'}$ is the anomalous dimension the third field $X^3_{11'}$. Note that the parent theory is conformal [97–99] if $N_0 = N_1 = N_2 = N_3$, but the unoriented theory suffers from gauge anomalies.

4.2.7 Orientifold of the Chiral Orbifold $\mathbb{Z}_2'$ of the Conifold $\mathcal{C}$ ($\mathcal{C}/\mathbb{Z}_2'$)

We now pass to study the chiral orbifold of the Conifold, denoted by $\mathcal{C}/\mathbb{Z}_2'$ [81, 85, 95, 96], and its orientifold. The theory has two dual phases, called "electric" and "magnetic", with the same toric diagram drawn in Fig. (4.10). Later, we will compare our results with those in $\mathbb{C}^3/\mathbb{Z}_4$ and its mass deformation, with and without the orientifold.

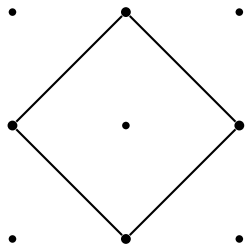

Figure 4.10. The toric diagram of $\mathcal{C}/\mathbb{Z}_2'$.

Electric Phase of $\mathcal{C}/\mathbb{Z}_2'$

The super-potential reads

$$W = \epsilon_{pq}\epsilon_{p'q'}X^p_{01}X^{p'}_{12}X^q_{23}X^{q'}_{30}\ , \tag{4.35}$$

with $p, q = 1, 2$ and $p', q' = 1, 2$ indices of $SU(2) \times SU(2)'$, the group of mesonic symmetry enjoyed by the model. By looking at the quiver present in Fig. (4.11) we see that, up to equivalence, we have two possible unoriented projections: the first denoted by Ω which passes through the nodes 0 and 2, while the second is denoted by $\widehat{\Omega}$ and passes only through fields.

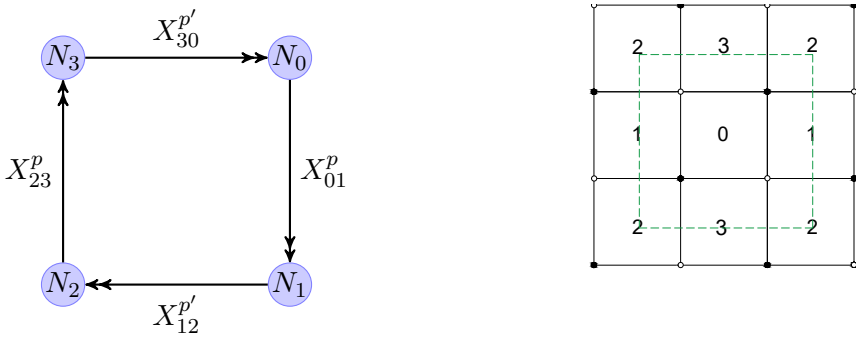

Figure 4.11. The quiver of the eletric phase of $\mathcal{C}/\mathbb{Z}_2'$ is shown on the left, while the corresponding dimer is on the right.

Orientifold Ω of the Electric Phase of $\mathcal{C}/\mathbb{Z}_2'$

This orientifold acts as

$$\overline{\square}_3 = \square_1 \ , \qquad U(N_0) \to USp/SO(N_0) \ , \qquad U(N_2) \to USp/SO(N_2) \tag{4.36}$$

and the super-potential becomes

$$W^{\Omega} = \epsilon_{pq}\epsilon_{rs} X_{01}^{p} X_{12}^{r} X_{21'}^{q} X_{1'0}^{s} \ . \tag{4.37}$$

where the $SU(2)$ indices refer now to the diagonal subgroup to which the mesonic symmetry $SU(2) \times SU(2)'$ is broken. Indeed, this unoriented projection is obtained by a fixed line in the dimer as shown in Fig. (4.12) and it breaks the mesonic symmetries and thus it is a non-toric involution. In the super-potential there are only three terms, since two are identified being the transpose of each other. The sign of the fixed line determines the projection to SO or USp gauge groups, and we must have $\epsilon_0 = \epsilon_2$. We denote the two involutions as Ω^+ for USp and Ω^- for SO, following the sign convention for the quiver. The theory is anomaly-free if

$$N_0 = N_2 \ . \tag{4.38}$$

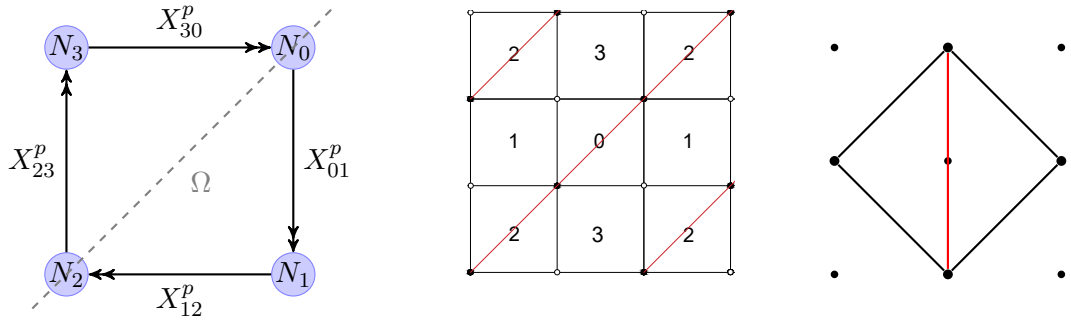

Figure 4.12. The orientifold involution Ω of $\mathcal{C}/\mathbb{Z}_2'$, whose quiver is drawn on the left and the dimer on the center, while the toric diagram is shown on the right.

In this theory, the chiral fields acquire anomalous dimensions, that appear after the mass deformation from $\mathbb{C}^3/\mathbb{Z}_4$ (see next subsection). With the anomaly-free condition, the beta functions read

$$\begin{aligned} 2\beta_0 &= 3N_0 + 6\epsilon_0 - 2N_1\,(1-\gamma_{01})\ , \\ \beta_1 &= 3N_1 - N_0(2-\gamma_{01}-\gamma_{12}), \\ 2\beta_2 &= 3N_0 + 6\epsilon_2 - 2N_1\,(1-\gamma_{12})\ , \end{aligned} \tag{4.39}$$

From the super-potential before the orientifold, each field has R-charge $1/2$ and the parent theory is conformal if all $\gamma = -1/2$. The same reasoning yields again all $\gamma = -1/2$ for the involution Ω of $\mathcal{C}/\mathbb{Z}_2'$. With these values for the anomalous dimensions, we can impose the beta functions to vanish simultaneously: from the second beta function we need that $N_0 = N_1$. Then, if we start with a conformal parent theory, after the unoriented projection we obtain

$$\begin{aligned} \beta_0 &= 3\epsilon_0\ , \\ \beta_1 &= 0\ , \\ \beta_2 &= 3\epsilon_0 \end{aligned} \tag{4.40}$$

Where we have used the fact that $\epsilon_0 = \epsilon_2$, since by construction the orientifold involution corresponds to a fixed line on the dimer. We conclude that the unoriented projection Ω breaks conformal invariance. We can still verify if the sum of the beta function vanishes. Summing the three equations above with all $\gamma = -1/2$ we get

$$\epsilon_0 = -\epsilon_2 \tag{4.41}$$

which is in contrast with the original condition $\epsilon_0 = \epsilon_2$. We conclude that this unoriented projection spoils conformal invariance, it does not allow the fractional branes to recombine into a single bulk brane and it also breaks toricity.

The results for the anomaly-free (but non toric and non conformal) theories are summarized in the

following Tab. (4.4).

Orientifold	Gauge groups	Anomaly condition
Ω^+	$USp(N_0) \times U(N_1) \times USp(N_2)$	$N_0 = N_2$
Ω^-	$SO(N_0) \times U(N_1) \times SO(N_2)$	$N_0 = N_2$

Table 4.4. The unoriented $\mathcal{C}/\mathbb{Z}_2'$.

Orientifold $\widehat{\Omega}$ of the Electric Phase of $\mathcal{C}/\mathbb{Z}_2'$

This orientifold acts as

$$\overline{\square}_3 = \square_0 \ , \qquad \overline{\square}_2 = \square_1 \tag{4.42}$$

and the super-potential reads

$$W^{\Omega} = \epsilon_{pq}\epsilon_{p'q'} X^p_{01} X^{p'}_{11'} X^q_{1'0'} X^{q'}_{0'0} \ . \tag{4.43}$$

This unoriented projection is obtained by four fixed points in the dimer as in Fig. (4.13) and it preserves the mesonic symmetries. The product of the four τ charges must be positive.

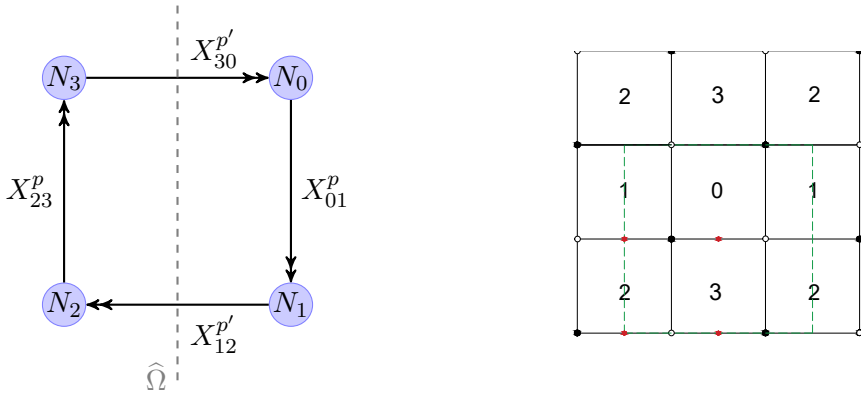

Figure 4.13. The orientifold projection $\widehat{\Omega}$ of $\mathcal{C}/\mathbb{Z}_2'$, whose quiver is drawn on the left and the dimer on the right.

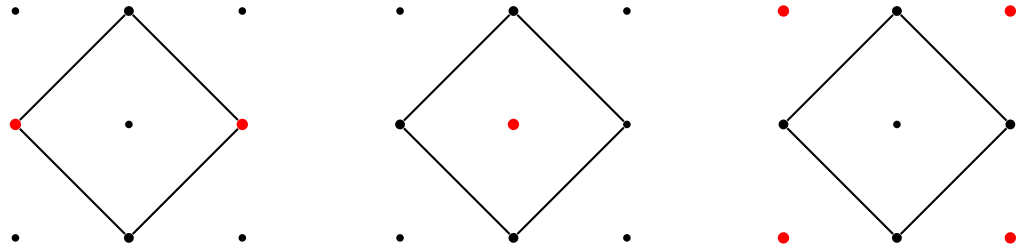

Figure 4.14. The various toric involutions $\widehat{\Omega}$ of $\mathcal{C}/\mathbb{Z}_2'$. The right figure shows the toric involution with a non-compact O7, in the center a compact O7 and on the right a O3.

The anomaly cancellation conditions read

$$\begin{aligned} N_0 &= N_1 + 2\left(\epsilon_{11'}^{(1)} + \epsilon_{11'}^{(2)}\right) \ , \\ \left(\epsilon_{0'0}^{(1)} + \epsilon_{0'0}^{(2)}\right) &= -\left(\epsilon_{11'}^{(1)} + \epsilon_{11'}^{(2)}\right) \end{aligned} \tag{4.44}$$

This means that we have various unoriented theories with gauge groups $U(N_0) \times U(N_1)$, with $N_1 = N_0$ or $N_1 = N_0 \pm 4$, summarized in Tab. (4.5).

Anomaly condition	$(X_{11'}^1, X_{11'}^2)$	$(X_{0'0}^1, X_{0'0}^2)$
$N_0 = N_1 + 4$	(S, S)	(A, A)
$N_0 = N_1 - 4$	(A, A)	(S, S)
$N_0 = N_1$	(S, A) or (A, S)	(S, A) or (A, S)
$N_0 = N_1$	(S, A) or (A, S)	(A, S) or (S, A)

Table 4.5. The various unoriented projections $\widehat{\Omega}$ of $\mathcal{C}/\mathbb{Z}_2'$, all of them with gauge groups $U(N_0) \times U(N_1)$.

Plugging in the anomaly cancellation condition, the beta functions of this model read

$$\begin{aligned} \beta_0 &= N_1\left(1 + \gamma_{01} + \gamma_{0'0}\right) + \left(\epsilon_{11'}^{(1)} + \epsilon_{11'}^{(2)}\right)\left(5 + \gamma_{0'0}\right) \ , \\ \beta_1 &= N_1\left(1 + \gamma_{01} + \gamma_{11'}\right) - \left(\epsilon_{11'}^{(1)} + \epsilon_{11'}^{(2)}\right)\left(3 - \gamma_{11'} - 2\gamma_{01}\right) \ , \end{aligned} \tag{4.45}$$

The anomalous dimensions of this unoriented theory are different from the ones of the parent theory and still non-zero.

Magnetic Phase of $\mathcal{C}/\mathbb{Z}_2'$

This theory is the magnetic dual of $\mathcal{C}/\mathbb{Z}_2'$. The node 4 is the dual of the node previously called node 0. There are four additional mesons, which are the fields $X_{31}^{pp'}$, $p, p' = 1, 2$, in Fig. (4.15). The

super-potential reads

$$W = \epsilon_{pq}\epsilon_{p'q'} X_{31}^{pp'} \left(X_{14}^{q} X_{43}^{q'} - X_{12}^{q'} X_{23}^{q} \right) \tag{4.46}$$

and the theory still enjoys an $SU(2) \times SU(2)'$ mesonic symmetry. Again, there are two inequivalent unoriented projections: the first denoted by Ω which passes trough the nodes 4 and 2, while the second is denoted by $\widehat{\Omega}$ and crosses only fields. Since the toric diagram is the same of the electric phase, the involution on the toric diagram will be the same. Note that the R-charges and then the anomalous dimensions at the conformal point are such that $\gamma_{14} = \gamma_{43} = \gamma_{23} = \gamma_{12} = -1/2$ and $\gamma_{31} = 1$.

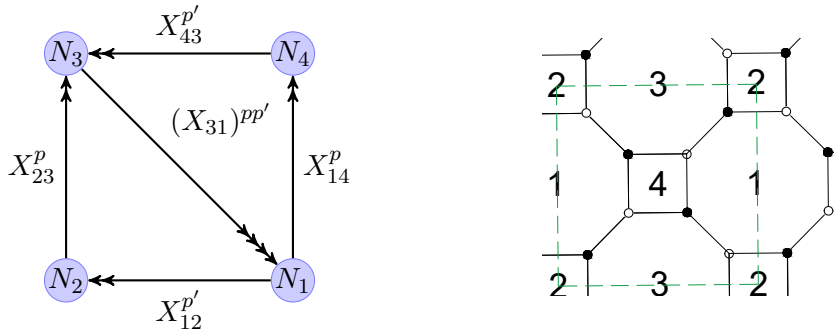

Figure 4.15. The Seiberg dual, or magnetic, phase $\mathcal{C}/\mathbb{Z}_2'$ with dualization on node 0. The quiver is shown on the left, while the corresponding dimer is on the right.

Orientifold Ω of the Magnetic Phase of $\mathcal{C}/\mathbb{Z}_2'$

This orientifold acts as

$$\overline{\square}_3 = \square_1 \ , \qquad U(N_4) \to USp/SO(N_4) \ , \qquad U(N_2) \to USp/SO(N_2) \tag{4.47}$$

and the super-potential becomes

$$W^{\Omega} = \epsilon_{pq}\epsilon_{lm} \left(X_{1'1}^{mp} X_{12}^{l} X_{21'}^{q} + X_{1'1}^{pl} X_{14}^{m} X_{41'}^{q} \right) \ . \tag{4.48}$$

The field identifications $X_{14}^{p} \leftrightarrow X_{41'}^{p'}$ and $X_{12}^{p'} \leftrightarrow X_{21'}^{p}$ leaves only one $SU(2)$ unbroken. The symmetry is thus reduced to $SU(2) \times U(1)_R$ and hence toricity is broken. We can see this also from the corresponding dimer with a fixed line shown in Fig.(4.16). We denote with ϵ the sign of the fixed line and with $\epsilon_{1'1}^{(mp)}$, $m, p = 1, 2$ the orientifold sign for the four fields $X_{1'1}^{(mp)}$. Two of the four fields are on top of the fixed line and are projected onto a symmetric or antisymmetric representation, while the other two fields are identified with each other yielding one symmetric and one antisymmetric field. We can see this from the superpotential as follows.

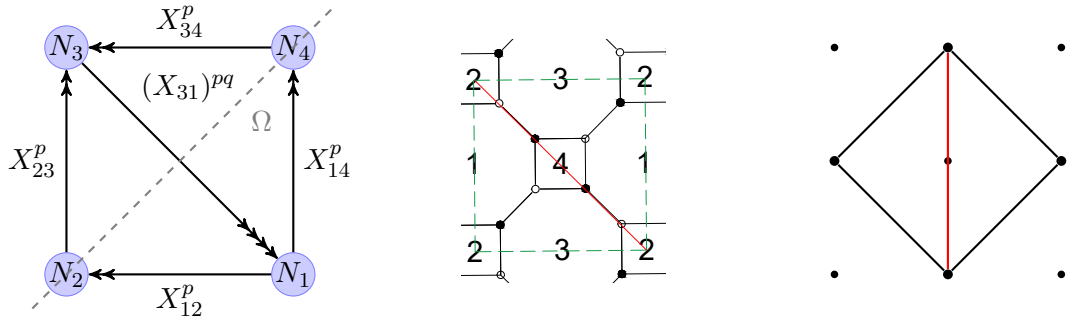

Figure 4.16. The orientifold involution Ω of the magnetic $\mathcal{C}/\mathbb{Z}_2'$, whose quiver is drawn on the left and the dimer on the center, while the toric diagram on the right.

Consider the first super-potential term and momentarily restore the gauge group indices as

$$W_1 = \epsilon_{pq}\epsilon_{lm}\left(X^{mp}_{1'1}\right)^{i_1\,j_1}\left(X^{l}_{12}\right)^{l_2}_{j_1}\mathcal{I}^{[l_2m_2]_\pm}_{(2)}\left(X^{q}_{21'}\right)_{m_2\,i_1}\,, \tag{4.49}$$

where $\mathcal{I}^{[l_2m_2]_\pm}_{(2)}$ is the two-index invariant tensor of the gauge group at the node 2 and $\pm$ indicates whether it is symmetric ($SO(N_0)$) or antisymmetric ($USp(N_0)$) in the indices l_2, m_2. Due to the presence of two ϵ_{pq} of $SU(2)$, we can only have $SO(N_2)$ with a symmetric $\left(X^{mp}_{11'}\right)^{i_1\,j_1}$ or $USp(N_2)$ with an antisymmetric $\left(X^{mp}_{11'}\right)^{i_1\,j_1}$. But a symmetric $X_{11'}$ means that we have 3 symmetric combinations $(mp)(i_1j_1)$ and 1 antisymmetric $[mp][i_1j_1]$, thus $\sum_{m,p}\epsilon^{(mp)}_{1'1} = +2$ with $SO(N_2)$, otherwise the super-potential term vanishes. On the other hand, $\sum_{m,p}\epsilon^{(mp)}_{1'1} = -2$ with $USp(N_2)$. If we let the terms to vanish, there are no F-terms for $X_{11'}$ yielding a no longer singular mesonic moduli space. Since it is unlikely that the theory becomes free after the addition of the orientifold plane, this scenario is implausible. The same line of reasoning holds for the second super-potential term. Moreover, both super-potential terms contain $X^{mp}_{11'}$, then groups at node 4 and 2 must be projected in the same way, i.e. by the single sign ϵ of the fixed line.
The anomaly cancellation condition requires that

$$N_4 + N_2 = 2\left(N_1 + \sum_{m,p=1,2}\epsilon^{(mp)}_{1'1}\right)\,, \tag{4.50}$$

with the constraint $\sum_{m,p}\epsilon^{(mp)}_{1'1} = \pm 2$. The results are summarized in Tab. (4.6).

Gauge groups	Anomaly condition	$(X^{11}_{31}, X^{12}_{31}, X^{21}_{31}, X^{22}_{31})$
$SO(N_4)\times U(N_1)\times SO(N_2)$	$N_4 + N_2 = 2N_1 + 4$	(S, S, S, A)
$USp(N_4)\times U(N_1)\times USp(N_2)$	$N_4 + N_2 = 2N_1 - 4$	(S, A, A, A)

Table 4.6. The orientifold involution Ω of the magnetic phase of $\mathcal{C}/\mathbb{Z}_2'$ without flavour branes.

With the anomaly cancellation condition, the beta functions take the form

$$\begin{aligned} 2\beta_4 &= 2N_1\left(2+\gamma_{14}\right) - 3N_2 + 6\epsilon + 6\sum_{m,p=1,2}\epsilon^{(mp)}_{1'1}\ , \\ \beta_1 &= N_1\left(-1+2\gamma_{14}+2\gamma_{1'1}\right) + N_2\left(\gamma_{12}-\gamma_{14}\right) + \sum_{m,p=1,2}\epsilon^{(mp)}_{1'1}\left(-3+\gamma_{1'1}+2\gamma_{14}\right)\ , \\ 2\beta_2 &= 2N_1(-1+\gamma_{12}) + 3N_2 + 6\epsilon\ . \end{aligned} \tag{4.51}$$

If we set $N_a = N$ for all a, i.e. the condition needed at the conformal point of the parent theory, the unoriented projection Ω of the magnetic phase of $\mathcal{C}/\mathbb{Z}_2'$ has gauge anomalies.

Orientifold $\widehat{\Omega}$ of the Magnetic Phase of $\mathcal{C}/\mathbb{Z}_2'$

This orientifold acts as

$$\overline{\square}_2 = \square_4\ , \qquad \overline{\square}_3 = \square_1 \tag{4.52}$$

and the super-potential reads

$$W^{\Omega} = \epsilon_{pq}\epsilon_{p'q'}X^{pp'}_{1'1}\left(X^{q}_{14}X^{q'}_{41'} - X^{q'}_{14'}X^{q}_{4'1'}\right) \tag{4.53}$$

This unoriented involution is obtained by four fixed points in the dimer as in Fig. (4.17) and it preserves the mesonic symmetries. The four τ charges $(\tau^1_{1'1}, \tau^2_{1'1}, \tau^1_{1'1}, \tau^2_{1'1},)$ project fields $X^{pp'}_{1'1}$ onto the symmetric (+) representation and antisymmetric (-) representantion. Their product is constrained by Eq. (3.3) and must be positive, thus also the choices for the spectrum are constrained. This reflects the choices for the $\epsilon^{(I)}_{1'1}$, since the four of them project fields as the τ charges.

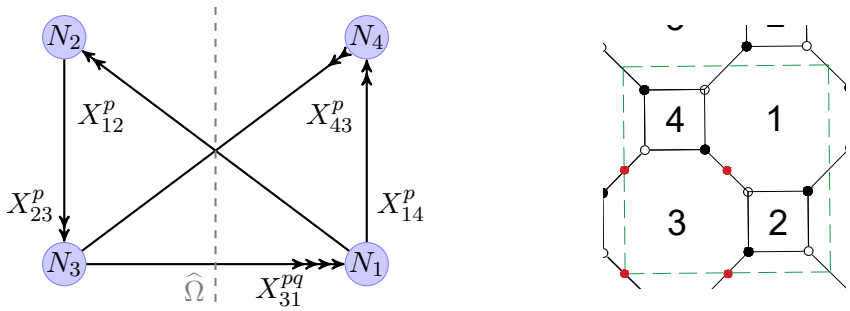

Figure 4.17. The orientifold projection $\widehat{\Omega}$ of $\mathcal{C}/\mathbb{Z}_2'$, whose quiver is drawn on the left and the dimer on the right.

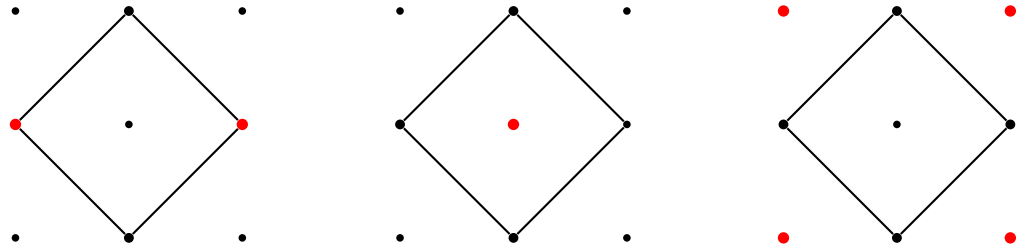

Figure 4.18. The various toric involutions $\widehat{\Omega}$ of the magnetic phase of $\mathcal{C}/\mathbb{Z}_2'$. Since Seiberg duality does not change the toric diagram, the possible involutions are the same as for the electric phase. The left figure shows the toric involution with a non-compact O7, the center toric diagram represents a toric involution with a compact O7, the right one a toric involution with an O3.

The anomaly cancellation condition reads

$$N_4 = N_1 + \sum_{I=1}^{4} \epsilon_{1'1}^{(I)} \,, \tag{4.54}$$

The various unoriented theories with gauge groups $U(N_2) \times U(N_1)$ are summarized in Tab. (4.7).

Anomaly condition	$(X_{1'1}^{11}, X_{1'1}^{12}, X_{1'1}^{21}, X_{1'1}^{22})$
$N_2 = N_1 + 4$	(S, S, S, S)
$N_2 = N_1$	(A, A, S, S)
$N_2 = N_1 - 4$	(A, A, A, A)

Table 4.7. The various unoriented projections $\widehat{\Omega}$ of the magnetic $\mathcal{C}/\mathbb{Z}_2'$, all of them with gauge groups $U(N_2) \times U(N_1)$. "A" stands for "Antisymmetric representation", while "S" for "Symmetric representation".

The beta functions of this anomaly-free model read

$$\begin{aligned} \beta_4 &= N_1 \left(1 + \gamma_{41} + \gamma_{14}\right) + 3 \sum_{I=1}^{4} \epsilon_{1'1}^{(I)} \,, \\ \beta_1 &= N_1 \left[-1 + \gamma_{14} + \gamma_{14'} + 2\gamma_{1'1}\right] + \sum_{I=1}^{4} \epsilon_{1'1}^{(I)} \left(-3 + \gamma_{1'1} + \gamma_{14} + \gamma_{14'}\right) \,. \end{aligned} \tag{4.55}$$

Note that at the conformal point of the parent theory, i.e. $N_a = N$ for all a, this unoriented theory may have gauge anomalies depending on the spectrum, see Tab. 4.7.

4.2.8 Orientifold of $\mathcal{N} = 1$ Orbifold $\mathbb{C}^3/\mathbb{Z}_4$, $(1, 1, 2)$ and its Mass Deformation

We study orientifold actions on the chiral orbifold $\mathbb{C}^3/\mathbb{Z}_4$ [39, 96] and its mass deformation to the unoriented $\mathcal{C}/\mathbb{Z}_2'$ [70]. We see that the conjugacy classes listed in Tab. (4.8) include a senior class.

This corresponds to a compact 4-cycle around which, in the smooth resolved space, an O7 plane can wrap. The crepant resolution of this model and its relation with the Generalized Kronheimer Construction can be found in [14, 92].

(k_1, k_2, k_3)	Age$= \frac{1}{4}\sum_I k_I$	Conjugacy class
(0, 0, 0)	0	Baby
(1, 1, 2)	1	Junior
(2, 2, 0)	1	Junior
(3, 3, 2)	2	Senior

Table 4.8. The conjugacy classes of the chiral orbifold model $\mathbb{C}^3/\mathbb{Z}_4$.

The associated field theory is described by the diagrams (quiver, dimer, toric) drawn in Fig. (4.19) and the super-potential reads

$$W = \epsilon_{pq}\left(X_{20}X_{01}^{q}X_{12}^{p} + X_{02}X_{23}^{q}X_{30}^{p} + X_{13}X_{30}^{q}X_{01}^{p} + X_{31}X_{12}^{q}X_{23}^{p}\right) \tag{4.56}$$

with mesonic symmetries $SU(2)\times U(1)\times U(1)_R$.

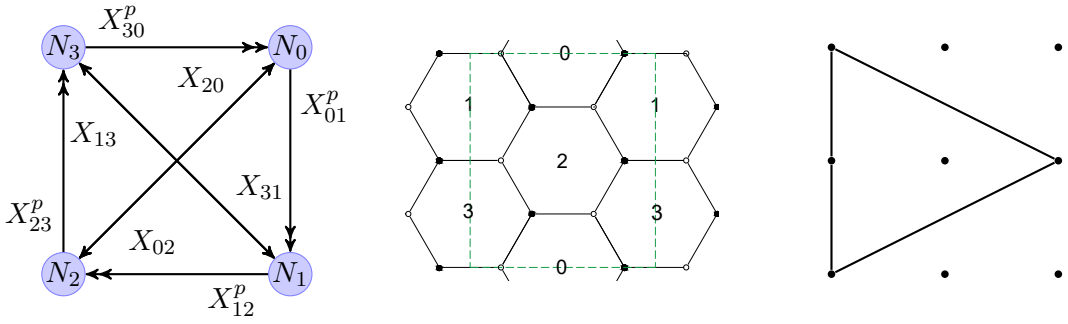

Figure 4.19. The quiver (left), the dimer (center) and the toric diagram (right) of $\mathbb{C}^3/\mathbb{Z}_4$.

The spectrum contains two vector-like fields, denoted by X_{13}, X_{31} and X_{02}, X_{20}. As discussed in [70], a pair of vector-like fields can be integrated out with a mass deformation of the theory, see Sec. 2.4.1. In general, in the low energy theory toricity is lost but, in some cases, a suitable redefinition of the fields can restore the toric symmetry. Performing this procedure for $\mathbb{C}^3/\mathbb{Z}_4$ the resulting low energy theory is the chiral orbifold of the conifold $\mathcal{C}/\mathbb{Z}_2'$. It is very simple to see this from the quivers, since Fig. (4.19) without vector-like fields it is exactly the quiver of (the electric phase of) $\mathcal{C}/\mathbb{Z}_2'$ in Fig. (4.11). It is easy to see that their superpotential, after the deformation, are the same: one starts with the super-potential of $\mathbb{C}^3/\mathbb{Z}_4$ Eq. (4.56) and adds a mass deformation

$$\Delta W = m\left(X_{31}X_{13} - X_{20}X_{02}\right)\ . \tag{4.57}$$

The F-terms of $W_D = W + \Delta W$ for the massive fields give

$$X_{02} = \frac{1}{m}\epsilon_{pq} X_{01}^q X_{12}^p \ , \qquad X_{20} = \frac{1}{m}\epsilon_{pq} X_{23}^q X_{30}^p \ ,$$
$$X_{13} = \frac{1}{m}\epsilon_{pq} X_{12}^p X_{23}^q \ , \qquad X_{31} = \frac{1}{m}\epsilon_{pq} X_{30}^p X_{01}^q \ . \tag{4.58}$$

Plugging them back in W_D the super-potential read

$$W_D = \frac{1}{m}\epsilon_{pq}\epsilon_{lm} X_{23}^q X_{30}^m X_{01}^p X_{12}^l \ , \tag{4.59}$$

which is indeed the super-potential of $\mathcal{C}/\mathbb{Z}_2'$. Note that the mesonic symmetries along the flow have been enhanced from $SU(2)\times U(1)\times U(1)$ to $SU(2)\times SU(2)\times U(1)$, after integrating out the massive fields. Furthermore, the presence of a mass scale changes the dimension of the fields.
On the toric diagram, the effect of the mass deformation corresponds to moving external nodes, as drawn in Fig. (4.20).

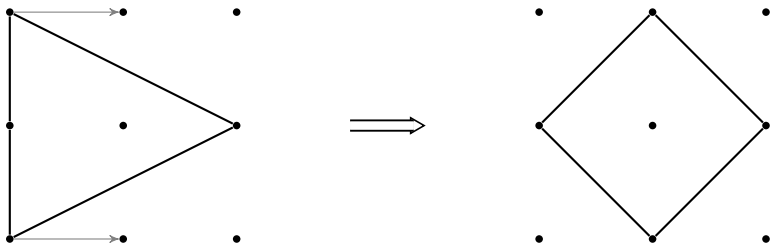

Figure 4.20. Mass deformation on $\mathbb{C}^3/\mathbb{Z}_4$ (left) moves external nodes in the toric diagram, yielding $\mathcal{C}/\mathbb{Z}_2'$ (right).

In studying the unoriented projections of these two models, it is interesting to analyze the relation between them. From the toric diagram of $\mathbb{C}^3/\mathbb{Z}_4$ shown in Fig. (4.21), we see that in the resolved space there are three different types of orientifold: one with an O3, one with a compact O7 (which wraps the compact 4-cycle) and one with a non-compact O7. On the other hand, from the quiver one can note the existence of only two orientifolds: Ω crossing two nodes, and $\widehat{\Omega}$ crossing fields, only. We study both cases in that order.

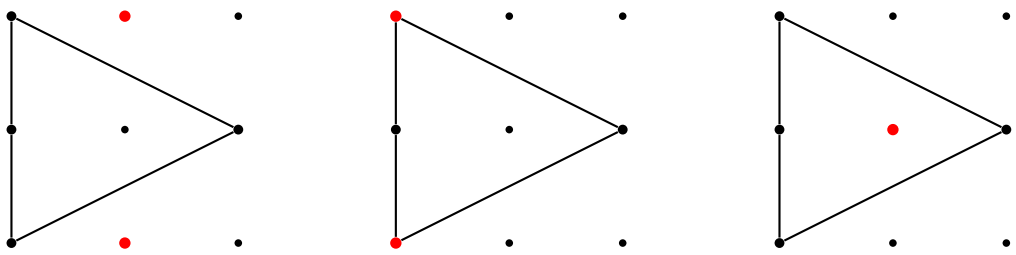

Figure 4.21. The three toric orientifold projections on the toric diagram. The right one is performed by an O3 plane, while the one on the left a non-compact O7, on the right a compact O7.

Orientifold Ω of $\mathbb{C}^3/\mathbb{Z}_4$

As it is clear from the quiver in Fig. (4.22), the unoriented projection Ω acts as

$$\overline{\square}_3 = \square_1 \ , \qquad U(N_0) \to USp/SO(N_0) \ , \qquad U(N_2) \to USp/SO(N_2) \ , \tag{4.60}$$

The superpotential reads

$$W^{\Omega} = \epsilon_{pq} \left(X_{20} X^q_{01} X^p_{12} + X_{02} X^q_{21'} X^p_{1'0} + X_{11'} X^q_{1'0} X^p_{01} + X_{1'1} X^q_{12} X^p_{21'} \right) \ . \tag{4.61}$$

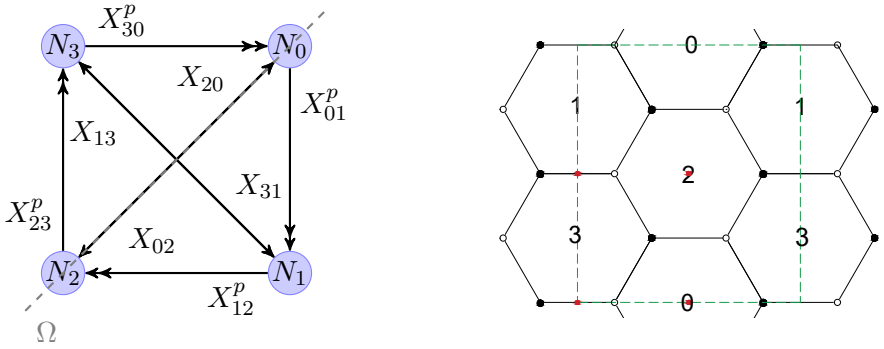

Figure 4.22. The quiver and the corresponding dimer for the orientifold projection Ω of $\mathbb{C}^3/\mathbb{Z}_4$.

The anomaly cancellation condition gives

$$N_0 = N_2 + 2 \left(\epsilon^{(3)}_{11'} - \epsilon^{(3)}_{1'1} \right) \ . \tag{4.62}$$

When $\epsilon^{(3)}_{11'} = \epsilon^{(3)}_{1'1}$, the fields $X_{11'}$ and $X_{1'1}$ are projected in the same symmetric or antisymmetric representation, with $N_0 = N_2$. When $\epsilon^{(3)}_{11'} = -\epsilon^{(3)}_{1'1}$ they are projected in opposite ways and the anomaly cancellation condition becomes $N_0 = N_2 + 4\epsilon^{(3)}_{11'}$. However, the various possible choices are constrained from the dimer and from the super-potential. Indeed, by looking at the dimer, where this unoriented projection is obtained by fixed point involution, one can note that according to Eq. (3.3), the product of the τ charges must be positive. Hence, this limits the possible cases to four choices of the unoriented theory: the gauge groups can be $USp/SO(N_0) \times U(N_1) \times USp/SO(N_2)$ while the fields $X_{11'}$, $X_{1'1}$ can transform in the (S,S) or (A,A) representation, only. The second constraint comes from the orientifold action on the super-potential, which imposes further conditions on the spectrum: by momentarily restoring the gauge group indices and considering the super-potential term with, for instance, the field $X_{11'}$:

$$W_{11'} = \epsilon_{pq} \left(X_{11'} \right)_{[i_1 j_1]_\pm} \left(X^q_{1'0} \right)^{j_1}_{l_0} \mathcal{I}^{[l_0 m_0]_\pm}_{(0)} \left(X^p_{01} \right)_{m_0}{}^{i_1} \ , \tag{4.63}$$

where $\mathcal{I}^{[l_0 m_0]_\pm}_{(0)}$ is the invariant tensor of the gauge group at the node 0 and $\pm$ indicates whether it is

symmetric ($SO(N_0)$) or antisymmetric ($USp(N_0)$) in the indices l_0, m_0. The whole super-potential term must be symmetric for the identification of groups 1 and $3 = 1'$, thus, we can only have $X^S_{11'}$ with $USp(N_0)$ or $X^A_{11'}$ with $SO(N_0)$, otherwise the term vanishes. The same line of reasoning holds for the super-potential term with $X_{1'1}$ and the invariant tensor of the group at node 2. The results are summarized in Tab. (4.9).

Gauge groups	Anomaly condition	$(X_{11'},\ X_{1'1})$
$SO(N_0) \times U(N_1) \times SO(N_2)$	$N_0 = N_2$	(A, A)
$USp(N_0) \times U(N_1) \times USp(N_2)$	$N_0 = N_2$	(S, S)
$USp(N_0) \times U(N_1) \times SO(N_2)$	$N_0 = N_2 + 4$	(S, A)
$SO(N_0) \times U(N_1) \times USp(N_2)$	$N_0 = N_2 - 4$	(A, S)

Table 4.9. The various orientifold projections Ω of $\mathbb{C}^3/\mathbb{Z}_4$. "A" stands for "Antisymmetric representation", while "S" for "Symmetric representation".

At this point it is natural to wonder if the unoriented involution Ω of $\mathbb{C}^3/\mathbb{Z}_4$ can be mass deformed to the unoriented projection Ω of $\mathcal{C}/\mathbb{Z}_2'$. For the $SO/USp(N_0) \times U(N_1) \times USp/SO(N_2)$ it is not possible to add a mass deformation term as $X_{11'}X_{1'1}$ since the two fields transform under different representations, one symmetric and the other antisymmetric: the product of the two fields vanishes, and the mass term is trivial. Besides, in this case the anomaly condition requires $N_0 = N_2 \pm 4$, in contrast to $N_0 = N_2$ for the case of O-plane for $\mathcal{C}/\mathbb{Z}_2'$.
On the other hand, the case with $SO/USp(N_0) \times U(N_1) \times SO/USp(N_2)$ has $N_0 = N_2$ and admits a mass deformation. Integrating out massive fields one obtains

$$W^{\Omega} = \frac{1}{m}\left(X^1_{12}X^2_{21'}X^2_{1'0}X^1_{01} + X^2_{12}X^1_{21'}X^1_{1'0}X^2_{01} - X^2_{12}X^2_{21'}X^1_{1'0}X^1_{01} - X^1_{12}X^1_{21'}X^2_{1'0}X^2_{01}\right) \tag{4.64}$$

and the first two terms are identified, since they are the transpose of each other. This is the super-potential in Eq. (4.37) of the unoriented projection Ω for $\mathcal{C}/\mathbb{Z}_2'$, which is obtained by a fixed line on the dimer and hence it is not toric, in agreement with the result of the mass deformation.
Let us discuss conformal invariance. Plugging in the anomaly cancellation condition, the beta functions read

$$\begin{aligned}
2\beta_0 &= 2N_1\left(-1+\gamma_{01}\right) + N_2\left(2+\gamma_{02}\right) + 6\epsilon_0 + 6\left(\epsilon^{(3)}_{11'} - \epsilon^{(3)}_{1'1}\right) \ , \\
\beta_1 &= N_1\left(2 + \frac{\gamma_{11'}+\gamma_{1'1}}{2}\right) + N_2\left(-2+\gamma_{12}+\gamma_{01}\right) + \epsilon^{(3)}_{11'}\left(-3+2\gamma_{01}+\gamma_{11'}\right) \\
&\quad + \epsilon^{(3)}_{1'1}\left(1-2\gamma_{01}+\gamma_{1'1}\right) \ , \\
2\beta_2 &= 2N_1\left(-1+\gamma_{12}\right) + N_2\left(2+\gamma_{02}\right) + 6\epsilon_2 + 2\epsilon^{(3)}_{11'}\left(-1+\gamma_{02}\right) + 2\epsilon^{(3)}_{1'1}\left(1-\gamma_{02}\right) \ .
\end{aligned} \tag{4.65}$$

Summing the above beta functions we get

$$\sum_{i=0}^{2}\beta_i = N_1\left(\gamma_{01}+\gamma_{12}+\frac{\gamma_{11'}+\gamma_{1'1}}{2}\right)+N_2\left(\gamma_{02}+\gamma_{01}+\gamma_{12}\right)+3\left(\epsilon_0+\epsilon_2\right)$$
$$+\epsilon^{(3)}_{11'}\left(-1+2\gamma_{01}+\gamma_{02}+\gamma_{11'}\right)+\epsilon^{(3)}_{1'1}\left(-1-2\gamma_{01}-\gamma_{02}+\gamma_{1'1}\right) \tag{4.66}$$

The unoriented theory is globally conformal (i.e. the sum of the above beta functions vanish) in the large N-limit, with non-zero anomalous dimensions for $\epsilon_0=-\epsilon_2$ and $\epsilon^{(3)}_{11'}=-\epsilon^{(3)}_{1'1}$.

Orientifold $\widehat{\Omega}$ of $\mathbb{C}^3/\mathbb{Z}_4$

The unoriented involution $\widehat{\Omega}$ identifies

$$\overline{\square}_3=\square_0\ ,\qquad \overline{\square}_2=\square_1 \tag{4.67}$$

and the superpotential reads

$$W^{\Omega}=\epsilon_{pq}\left(X_{1'0}X^q_{01}X^p_{11'}+X_{01'}X^q_{20'}X^p_{0'0}+X_{10'}X^q_{0'0}X^p_{01}+X_{0'1}X^q_{11'}X^p_{1'0'}\right)\ , \tag{4.68}$$

while the anomaly-free condition is

$$N_0=N_1+2\left(\epsilon^{(1)}_{11'}+\epsilon^{(2)}_{11'}\right)\ ,$$
$$\left(\epsilon^{(1)}_{0'0}+\epsilon^{(2)}_{0'0}\right)=-\left(\epsilon^{(1)}_{11'}+\epsilon^{(2)}_{11'}\right)\ . \tag{4.69}$$

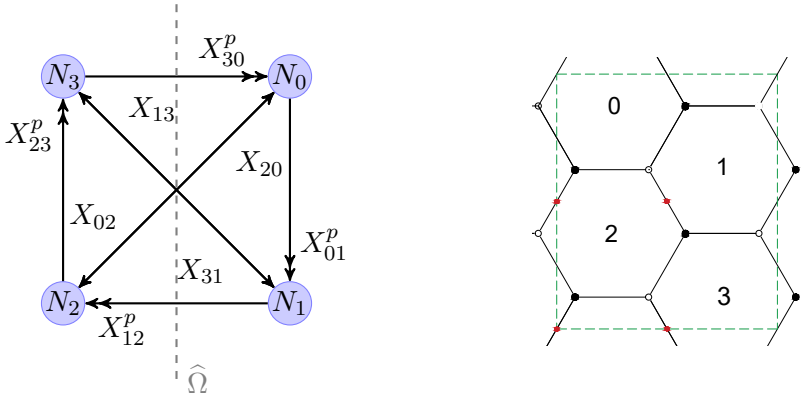

Figure 4.23. The quiver and the corresponding dimer for the orientifold involution $\hat{\Omega}$ of $\mathbb{C}^3/\mathbb{Z}_4$.

There are no constraints on the spectrum other than the anomaly cancellation condition. The different choices are summarized in Tab. (4.10) and both lines show the same possibilities as for the unoriented projection $\widehat{\Omega}$ of $\mathcal{C}/\mathbb{Z}_2'$. Thus, both choices can be mass deformed with a mass term for

$X_{01'}$, $X_{1'0}$ and $X_{0'1}$, $X_{10'}$. Integrating them out gives the toric super-potential

$$W^{\Omega} = \frac{1}{m}\epsilon_{pq}\epsilon_{lm}X^{p}_{01}X^{l}_{11'}X^{m}_{1'0'}X^{q}_{0'0} \ , \tag{4.70}$$

which is also the super-potential of $(\mathcal{C}/\mathbb{Z}_2')/\widehat{\Omega}$, obtained with a toric involution.

Anomaly condition	$(X^1_{11'}, X^2_{11'})$	$(X^1_{0'0}, X^2_{0'0})$
$N_1 = N_0$	(S,A) or (A,S)	(A,S) or (S,A)
$N_1 = N_0 \pm 4$	(S,S) or (A,A)	(A,A) or (S,S)

Table 4.10. The various unoriented projections $\widehat{\Omega}$ of $\mathbb{C}^3/\mathbb{Z}_4$ with gauge groups $U(N_0)\times U(N_1)$. "A" stands for "Antisymmetric representation", while "S" for "Symmetric representation".

Computing the beta-functions with the anomaly-free condition we have (with $\gamma_{01'} = \gamma_{1'0} = \gamma_{0'1} = \gamma_{10'}$)

$$\begin{aligned}
\beta_0 &= N_1\left(\gamma_{01} + \gamma_{01'} + \frac{\gamma^{(1)}_{0'0} + \gamma^{(2)}_{0'0}}{2}\right) + \epsilon^{(1)}_{0'0}\left(-5 - \gamma^{(2)}_{0'0}\right) + \epsilon^{2}_{0'0}\left(-5 - \gamma^{(1)}_{0'0}\right) \ , \\
\beta_1 &= N_1\left(\gamma_{01} + \gamma_{01'} + \frac{\gamma^{(1)}_{11'} + \gamma^{(2)}_{11'}}{2}\right) + \sum_{I=1}^{2}\epsilon^{(I)}_{11'}\left(-5 + 2\gamma_{01} + 2\gamma_{01'}\right) + \sum_{I=1}^{2}\epsilon^{(I)}_{11'}\gamma^{(I)}_{11'}
\end{aligned} \tag{4.71}$$

$$\begin{aligned}
\beta_0 + \beta_1 = N_1 &\left(2\gamma_{01} + 2\gamma_{01'} + \frac{\gamma^{(1)}_{0'0} + \gamma^{(2)}_{0'0} + \gamma^{(1)}_{11'} + \gamma^{(2)}_{11'}}{2}\right) \\
&+ \sum_{I=1}^{2}\epsilon^{(I)}_{11'}\left(\gamma^{(1)}_{11'} + \gamma^{(2)}_{11'} + 2\gamma_{01} + 2\gamma_{01'}\right) - \epsilon^{(1)}_{0'0}\gamma^{(2)}_{0'0} - \epsilon^{(2)}_{0'0}\gamma^{(1)}_{0'0} \ .
\end{aligned} \tag{4.72}$$

When the anomalous dimensions are trivial, both beta functions vanish if $\epsilon^{(1)}_{11'} = -\epsilon^{(2)}_{11'}$, corresponding to an O3 or a compact O7 in the smooth space, while for $\epsilon^{(1)}_{11'} = \epsilon^{(2)}_{11'}$ the theory is not conformal and the unoriented projection is given by a non-compact O7 in the resolved space.

4.2.9 Orientifold Projection of Non-chiral Orbifolds

All the examples we have discussed so far involve unoriented projection of chiral orbifolds. We are going to study also non-chiral examples [19, 100–103], related via mass deformation to well known theories as the Suspended Pinch Point (SPP), as well as the Conifold and its non-chiral orbifold. The analysis follows closely what is done for chiral examples, thus it will be less detailed.

Orientifold of $\mathcal{N}=2$ Orbifold $\mathbb{C}^3/\mathbb{Z}'_3$, $(1,2,0)$

The non-chiral orbifold $\mathbb{C}^3/\mathbb{Z}'_3$ with $k_I=(1,2,0)$ has only a junior class from the age classification, hence there are no compact 4-cycles. In fact, the toric diagram has no internal points and the unoriented projection is only given by O3 and non-compact O7 in the resolved space, see Fig. (4.24). The unoriented projection Ω acts as

$$\overline{\square}_2=\square_1\ , \qquad U(N_0)\to USp/SO(N_0)\ , \tag{4.73}$$

and the superpotential reads

$$W^{\Omega}=\phi'_0\left(X_{01'}X_{1'0}-X_{01}X_{10}\right)+\phi_1\left(X_{10}X_{01}-X_{11'}X_{1'1}\right)+\phi_{1'}\left(X_{1'1}X_{11'}-X_{1'0}X_{01'}\right)\ , \tag{4.74}$$

where ϕ_a are the adjoint fields at node a, ϕ'_0 is projected down to a symmetric or an antisymmetric representation. The anomaly cancellation condition reads

$$\epsilon_{11'}=\epsilon_{1'1}\ . \tag{4.75}$$

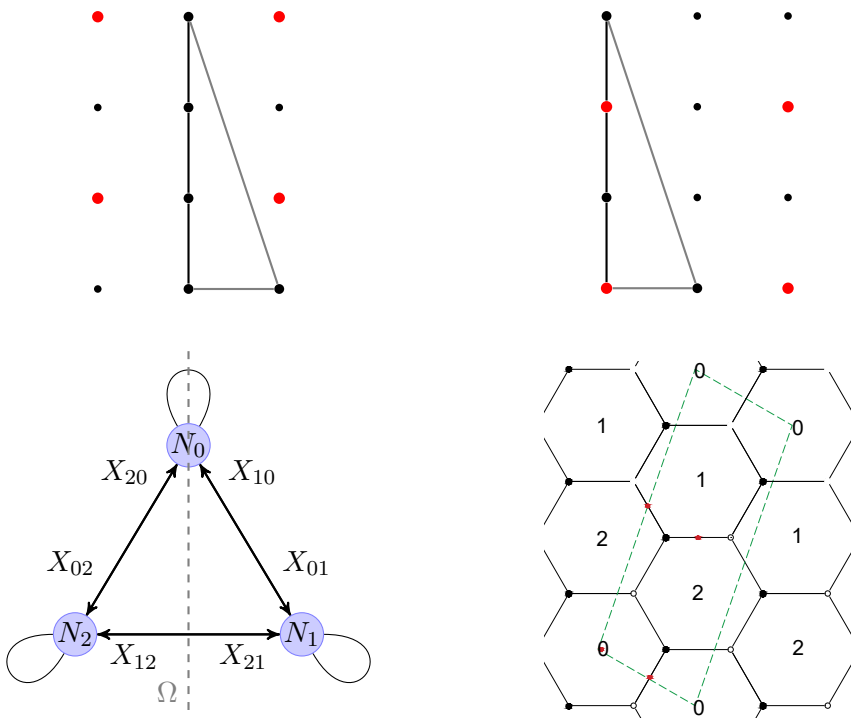

Figure 4.24. The various unoriented descriptions of $\mathbb{C}^3/\mathbb{Z}'_3$. The upper figure shows the toric diagram and the toric involution with a compact O3 (left) and a non-compact O7 (right). In the lower row: the left side show the quiver and the Ω-line, whereas on the right side the dimer and the four fixed points in red.

From the dimer, Ω is obtained by fixed point involution and the product of τ charges is negative.

Together with the anomaly-free condition, this means that a symmetric ${\phi'}_0$ requires an $USp(N_0)$ group and an antisymmetric ${\phi'}_0$ requires an $SO(N_0)$ group. The beta functions with a non-trivial anomalous dimension for the adjoint fields are

$$\begin{aligned}\beta_0 &= N_0\left(1+\frac{1}{2}\gamma_{00}\right) - N_1 + 3\epsilon_0 - \epsilon_{00}^{(3)}\left(1-\gamma_{00}\right) \ , \\ \beta_1 &= N_1\left(1+\gamma_{11}\right) - N_0 - 2\epsilon_{11'}^{(1)}\end{aligned} \tag{4.76}$$

and if we suppose $\gamma_{00} = \gamma_{11} = 0$ we get

$$\begin{aligned}\beta_0 &= N_0 - N_1 + 3\epsilon_0 - \epsilon_{00}^{(3)} \ , \\ \beta_1 &= N_1 - N_0 - 2\epsilon_{11'}^{(1)}\end{aligned} \tag{4.77}$$

and the beta functions can vanish simultaneously when all the charges have the same sign $(\epsilon_0, \epsilon_{00}, \epsilon_{11'}, \epsilon_{1'1}) = (\pm,\pm,\pm,\pm)$: this corresponds to an O3-plane. Furthermore one notes that the sum of the beta functions with the same condition, namely

$$3\epsilon_0 = \epsilon_{00}^{(3)} + 2\epsilon_{11'}^{(1)} \ , \tag{4.78}$$

In the following table we show the possible cases compatible with the anomaly cancellation condition.

Gauge groups	${\phi'}_0$	$(X_{11'}, X_{1'1'})$
$USp(N_0)\times U(N_1)$	S	(S,S) or (A,A)
$SO(N_0)\times U(N_1)$	A	(S,S) or (A,A)

Table 4.11. The orientifold involution Ω of the non-chiral orbifold $\mathbb{C}^3/\mathbb{Z}'_3$. "A" stands for "Antisymmetric representation", while "S" for "Symmetric representation".

Orientifold of the Suspended Pinch Point (SPP)

In [104] it is shown that the SPP theory and its unoriented projections [81] may be obtained via higgsing of the orbifold $\mathbb{C}^3/\left(\mathbb{Z}_2\times\mathbb{Z}_2\right)$, and in [70] it is shown the mass deformed $\mathbb{C}^3/\mathbb{Z}'_3$ model flows to the SPP. In the previous section, the same happens with mass deformation of the orientifold involution. The final superpotential reads

$$W^{\Omega} = {\phi'}_0\left(X_{01'}X_{1'0} - X_{01}X_{01}\right) + X_{11'}X_{1'1}X_{10}X_{01} - X_{1'1}X_{11'}X_{1'0}X_{01'} \ . \tag{4.79}$$

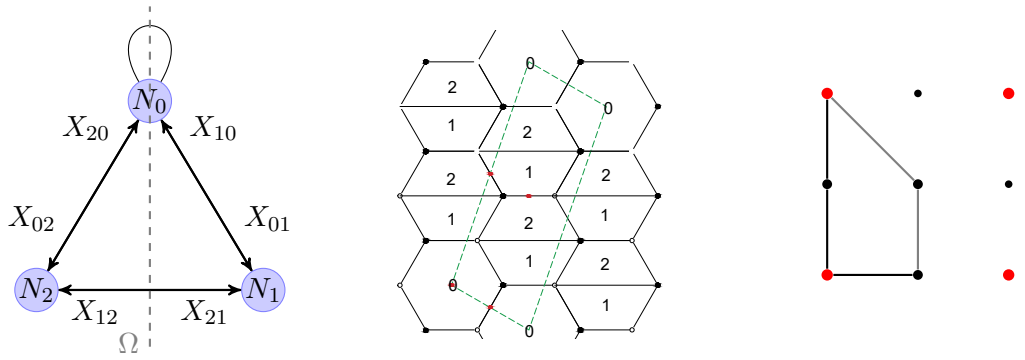

Figure 4.25. The various unoriented descriptions of the SPP: the quiver, the dimer with the four fixed points in red, and the toric diagram with toric involution corresponding to a non-compact O7 or a non-compact O7 and a O3, depending on how the toric diagram is triangulated.

The theory is anomaly free if $\epsilon_{11'} = \epsilon_{1'1}$, which is the same condition as in the previous model. From the dimer, the product of the τ charges is positive, then $USp(N_0)$ requires ${\phi'}_0$ to be antisymmetric, while $SO(N_0)$ requires a symmetric ${\phi'}_0$. The beta functions with a non-trivial anomalous dimension for the adjoint fields are

$$\begin{aligned}\beta_0 &= N_0\left(1+\frac{1}{2}\gamma_{00}\right) - N_1 + 3\epsilon_0 - \epsilon_{00}^{(3)}\left(1-\gamma_{00}\right)\ ,\\ \beta_1 &= 2N_1 - N_0 - 2\epsilon_{11'}\end{aligned} \tag{4.80}$$

and if we assume $\gamma_{00} = 0$ we get

$$\begin{aligned}\beta_0 &= N_0 - N_1 + 3\epsilon_0 - \epsilon_{00}\ ,\\ \beta_1 &= 2N_1 - N_0 - 2\epsilon_{11'}\ .\end{aligned} \tag{4.81}$$

The beta functions can vanish separately if $N_1 = \epsilon_{00} + 2\epsilon_{11'} - 3\epsilon_0$ and $N_0 = 2\left(\epsilon_{00'} + \epsilon_{11'} - 3\epsilon_0\right)$. The sum vanishes if $N_1 = \epsilon_{00} + 2\epsilon_{11'} - 3\epsilon_0$. The following table summarizes the possibilities compatible with conformal invariance. When all the fields transform in the same representation, the orientifold involution is given by an O3.

Gauge groups	${\phi'}_0$	$(X_{11'}, X_{1'1'})$
$USp(N_0)\times U(N_1)$	A	(S,S) or (A,A)
$SO(N_0)\times U(N_1)$	S	(S,S) or (A,A)

Table 4.12. The orientifold projection Ω of the SPP. "A" stands for "Antisymmetric representation", while "S" for "Symmetric representation".

Orientifold of $\mathcal{N} = 2$ Orbifold $\mathbb{C}^3/\mathbb{Z}_4'$, $(1, 3, 0)$

In this section we study the unoriented projections Ω and $\hat{\Omega}$ of the non-chiral $\mathbb{C}^3/\mathbb{Z}_4'$ model with $k_I = (1, 3, 0)$, whose conjugacy classes are only junior classes, from $(1, 3, 0)$ and $(2, 2, 0)$. There are no compact 4-cycles, in agreement with the fact that the toric diagram has no internal point and hence no compact O7 in the resolved space. The various diagrams are drawn in Fig. (4.26).

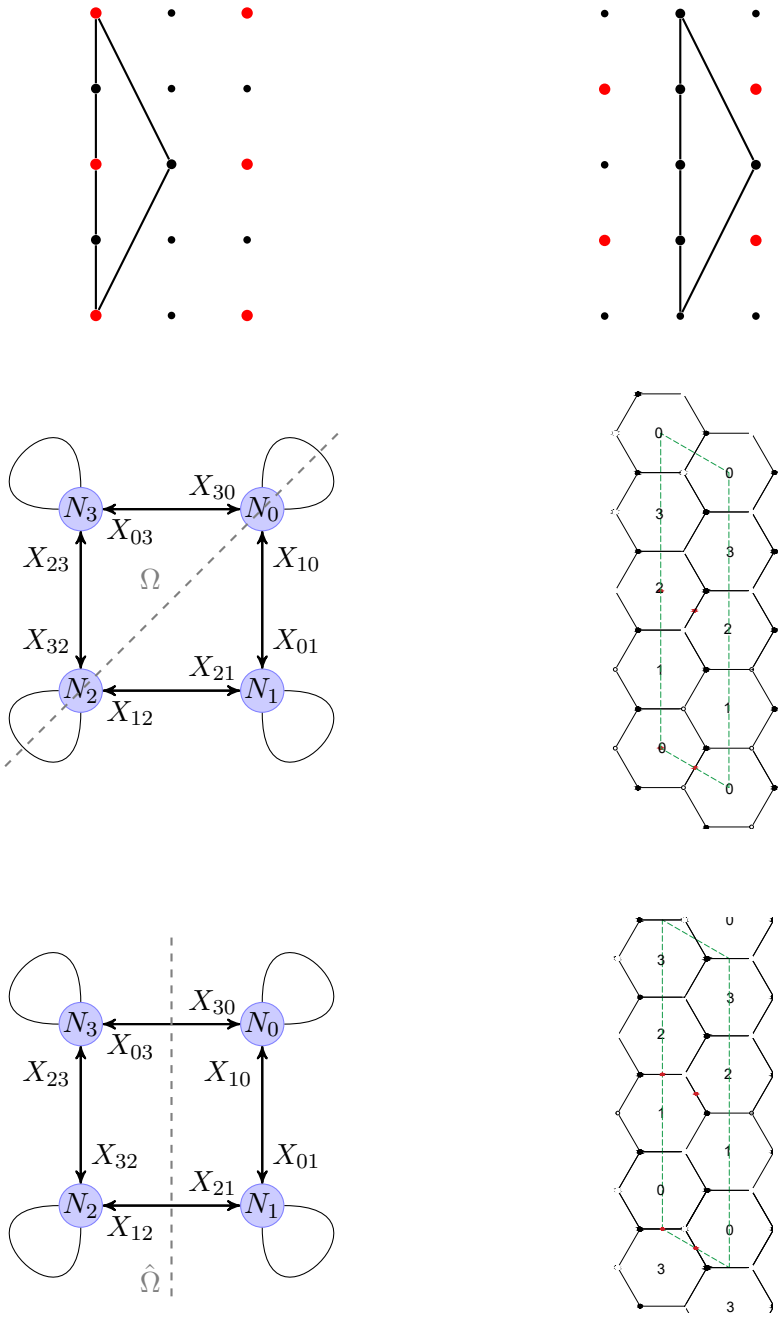

Figure 4.26. The various unoriented descriptions of $\mathbb{C}^3/\mathbb{Z}_4'$. The upper figure shows the toric diagram and the toric involution with a non-compact O7 (left) and a O3 (right). The middle row shows the orientifold involution Ω, on quiver (left) and dimer (right), while in the lower row are drawn the quiver (left) and the dimer (right) for the $\hat{\Omega}$.

Orientifold Ω of $\mathbb{C}^3/\mathbb{Z}'_4$

The action of the involution is

$$\overline{\square}_3 = \square_1 \ , \quad U(N_0) \to USp/SO(N_0) \ , \quad U(N_2) \to USp/SO(N_2) \ , \tag{4.82}$$

and the superpotential reads

$$\begin{aligned} W^{\Omega} = {} & \phi'_0 \left(X_{01}X_{10} - X_{01'}X_{1'0}\right) + \phi_1 \left(X_{12}X_{21} - X_{10}X_{01}\right) \\ & + \phi'_2 \left(X_{21'}X_{1'2} - X_{21}X_{12}\right) + \phi_{1'} \left(X_{1'0}X_{01'} - X_{1'2}X_{21'}\right) \ . \end{aligned} \tag{4.83}$$

The theory is anomaly-free without any relevant restriction on the gauge group ranks and on the spectrum. From the dimer, this orientifold configuration is given by four τ charges whose product is positive. The choices are displayed in Tab (4.13).

The beta-functions read

$$\begin{aligned} 2\beta_0 &= N_0 \left(2 + \gamma_{00}\right) - 2N_1 + 6\epsilon_0 - 2\epsilon_{00} \left(1 - \gamma_{00}\right) \ , \\ \beta_1 &= 2N_1 \left(2 + \gamma_{11}\right) - N_0 - N_2 \ , \\ 2\beta_2 &= N_2 \left(2 + \gamma_{22}\right) - 2N_1 + 6\epsilon_2 - 2\epsilon_{22} \left(2 + \gamma_{22}\right) \ . \end{aligned} \tag{4.84}$$

In case of trivial anomalous dimensions, by imposing the simultaneous vanishing of the individual beta functions we get a condition on the charges

$$3(\epsilon_0 + \epsilon_2) = \epsilon_{22} + \epsilon_{00} \tag{4.85}$$

which can be satisfied only if $\epsilon_0 = -\epsilon_2$ and $\epsilon_{00} = -\epsilon_{22}$. This corresponds to projecting the group and the adjoint fields in opposite manner.
Their sum is $\sum_a \beta_0 = 3\left(\epsilon_0 + \epsilon_2\right) + \epsilon_{00} + \epsilon_{22}$, which vanishes, again, only if $\epsilon_0 = -\epsilon_2$ and $\epsilon_{00} = -\epsilon_{22}$. This corresponds to an O3 plane, while other choices (for which $\sum_a \beta_a \neq 0$) are given by a non-compact O7.

Gauge groups	ϕ'_0	ϕ'_2
$USp(N_0) \times U(N_1) \times USp(N_2)$	S/A	S/A
$USp(N_0) \times U(N_1) \times SO(N_2)$	S/A	A/S
$SO(N_0) \times U(N_1) \times USp(N_2)$	S/A	A/S
$SO(N_0) \times U(N_1) \times SO(N_2)$	S/A	S/A

Table 4.13. The orientifold projection Ω of $\mathbb{C}^3/\mathbb{Z}'_4$. "A" stands for "Antisymmetric representation", while "S" for "Symmetric representation".

Orientifold $\hat{\Omega}$ of $\mathbb{C}^3/\mathbb{Z}'_4$

The action of the involution is

$$\overline{\square}_3 = \square_0 \ , \quad \overline{\square}_2 = \square_1 \ , \tag{4.86}$$

and the superpotential reads

$$\begin{aligned} W^{\Omega} = &\phi_0 \left(X_{01}X_{10} - X_{00'}X_{0'0}\right) + \phi_1 \left(X_{12'}X_{2'1} - X_{10}X_{01}\right) \\ &+ \phi_{1'} \left(X_{1'0'}X_{0'1'} - X_{1'1}X_{11'}\right) + \phi_{0'} \left(X_{0'0}X_{00'} - X_{0'1'}X_{1'0'}\right) \ . \end{aligned} \tag{4.87}$$

The anomaly-free condition gives

$$\begin{aligned} \epsilon_{00'} &= \epsilon_{0'0} \ , \\ \epsilon_{11'} &= \epsilon_{1'1} \ , \end{aligned} \tag{4.88}$$

which is in agreement with the constraint from the dimer, since the product of the τ charges must be positive. The choices are reported in Tab. (4.14).
The beta-functions read

$$\begin{aligned} \beta_0 &= N_0 \left(1 + \gamma_{00}\right) - N_1 - 2\epsilon_{00'} \ , \\ \beta_1 &= N_1 \left(1 + \gamma_{11}\right) - N_0 - 2\epsilon_{11'} \ , \end{aligned} \tag{4.89}$$

whose sum vanishes at large N only if $\epsilon_{00'} = -\epsilon_{11'}$, which corresponds to an O3 plane, while the other choice (for which $\sum_a \beta_a \neq 0$) are given by a non-compact O7. The same condition holds for each $\beta_a = 0$, with $N_1 = N_0 - 2\epsilon_{00'}$.

Gauge groups	$(X_{00'}, X_{0'0})$	$(X_{11'}, X_{1'1})$
$U(N_0) \times U(N_1)$	(S,S) or (A,A)	(S,S) or (A,A)
$U(N_0) \times U(N_1)$	(S,S) or (A,A)	(A,A) or (S,S)

Table 4.14. The unoriented involution $\hat{\Omega}$ of $\mathbb{C}^3/\mathbb{Z}'_4$. "A" stands for "Antisymmetric representation", while "S" for "Symmetric representation".

Orientifold of the Non-chiral orbifold of the conifold $\mathcal{C}/\mathbb{Z}_2$

In [70] it is shown that the mass deformation of the non-chiral orbifold $\mathbb{C}^3/\left(\mathbb{Z}_2 \times \mathbb{Z}_2\right)$ flows to the non-chiral orbifold of the conifold $\mathcal{C}/\mathbb{Z}_2$ [81, 105]. Also, the mass deformation of the adjoint fields in the non-chiral orbifold $\mathbb{C}^3/\mathbb{Z}'_4$ flows to $\mathcal{C}/\mathbb{Z}_2$, as well as the orientifolds Ω and $\hat{\Omega}$, whose various diagrams are drawn in Fig. (4.27). We now study them.

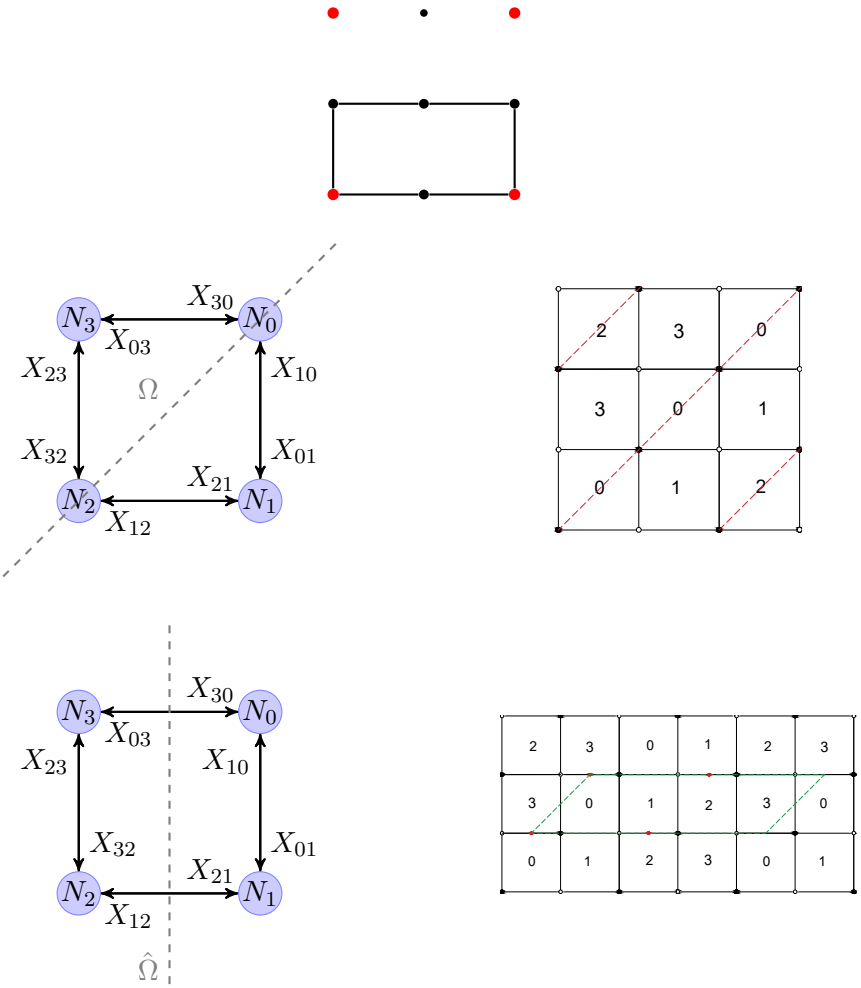

Figure 4.27. The various unoriented descriptions of the non-chiral $\mathcal{C}/\mathbb{Z}_2$. The upper figure shows a possible toric diagram from which one can notice the presence of a non-compact O7 and a O3 or only a non-compact O7, depending on how the toric diagram is triangulated. The middle row shows the orientifold involution Ω, on quiver (left) and dimer (right), while in the lower row are drawn the quiver (left) and the dimer (right) for the involution $\hat{\Omega}$.

Orientifold Ω of $\mathcal{C}/\mathbb{Z}_2$

The action of the non-toric involution is

$$\bar{\square}_3 = \square_1 \ , \qquad U(N_0) \to USp/SO(N_0) \ , \qquad U(N_2) \to USp/SO(N_2) \ , \tag{4.90}$$

and the superpotential reads

$$W^{\Omega} = X_{21}X_{12}X_{21'}X_{1'2} - X_{1'2}X_{21'}X_{1'0}X_{01'} + X_{01'}X_{1'0}X_{01}X_{10} - X_{10}X_{01}X_{12}X_{21} \ , \tag{4.91}$$

where fields factors $X_{12}X_{21}$ and $X_{01'}X_{1'0}$ absorb the $(1/m)$ coming from the mass deformation. Being non-chiral, the theory is anomaly-free. From the dimer, this orientifold configuration is

obtained by a fixed line involution, then the groups at nodes 0 and 2 are projected in the same way, i.e. $\epsilon_0 = \epsilon_2$. The only choices are $USp(N_0) \times U(N_1) \times USp(N_2)$ and $SO(N_0) \times U(N_1) \times SO(N_2)$. The beta-functions read

$$\begin{aligned} 2\beta_0 &= 3N_0 - 2N_1 + 6\epsilon_0 \ , \\ \beta_1 &= 3N_1 - N_0 - N_2 \ , \\ 2\beta_2 &= 3N_2 - 2N_1 + 6\epsilon_0 \ . \end{aligned} \tag{4.92}$$

Their sum vanishes only if $N_1 = -6\epsilon_0 - \frac{1}{2}(N_0 + N_2)$ and $N_0 + N_2 < -12\epsilon_0$, allowed only for SO groups. Individually, the beta functions do not vanish simultaneously.

Orientifold $\hat{\Omega}$ of $\mathcal{C}/\mathbb{Z}_2$

The action of the involution is

$$\overline{\square}_3 = \square_0 \ , \qquad \overline{\square}_2 = \square_1 \ , \tag{4.93}$$

and the superpotential reads

$$W^{\Omega} = X_{1'1}X_{11'}X_{1'0'}X_{0'1'} - X_{0'1'}X_{1'0'}X_{0'0}X_{00'} + X_{00'}X_{0'0}X_{01}X_{10} - X_{10}X_{01}X_{11'}X_{1'1} \ , \tag{4.94}$$

As for the previous model, the anomaly-free condition gives

$$\begin{aligned} \epsilon_{00'} &= \epsilon_{0'0} \ , \\ \epsilon_{11'} &= \epsilon_{1'1} \ , \end{aligned} \tag{4.95}$$

which is again in agreement with the constraint from the dimer, since the product of the four τ charges must be positive. The choices are reported in Tab (4.14).
The beta-functions read

$$\begin{aligned} \beta_0 &= 2N_0 - N_1 - 2\epsilon_{00'} \ , \\ \beta_1 &= 2N_1 - N_0 - 2\epsilon_{11'} \ , \end{aligned} \tag{4.96}$$

whose sum vanishes only if $\epsilon_{00'} = \epsilon_{11'} = 1$ from which $N_0 + N_1 = 4$, whereas $\beta_0 = 0 = \beta_1$ if $N_0 = N_1 = 2$.

Gauge groups	$(X_{00'}, X_{0'0})$	$(X_{11'}, X_{1'1})$
$U(N_0) \times U(N_1)$	(S,S) or (A,A)	(S,S) or (A,A)
$U(N_0) \times U(N_1)$	(S,S) or (A,A)	(A,A) or (S,S)

Table 4.15. The orientifold projection $\hat{\Omega}$ of $\mathcal{C}/\mathbb{Z}_2$.

4.3 Seiberg Duality and Orientifolds

In the preceding sections we have shown the commutativity between mass deformation and orientifold projection, as long as the deformation preserves the $\mathbb{Z}_2$ symmetry exploited by the orientifold. In the following, we ask whether a similar relation holds between Seiberg duality and orientifold. Recall that Seiberg duality relates two theories which have the same fixed point in the IR. When a duality cascade occurs, the true IR is the end of the cascade. For this reason, it is meaningful to ask whether the unoriented projection at the beginning of a duality cascade yields the same theory as the unoriented projection at the end of the cascade. Duality cascades in unoriented quiver theories have been studied in [88, 106], where each node is dualized and the theory flows from the UV to the IR. In our case, nodes are dualized following the order $(0, 2, 1, 3)$. We start again with the $\mathcal{C}/\mathbb{Z}_2'$ theory in Fig. (4.11) with $N_0 = N_2 = N + M$, $N_1 = N_3 = N$, where N is the number of regular branes and M is the number of fractional branes and $N > M$ in order to dualize the nodes. Along the cascade, the number of fractional branes diminishes.
Before proceeding any further, recall that Seiberg duality for a gauge group $USp(N_c)$ with N_f fundamentals yields a magnetic theory $USp(N_f - N_c - 4)$, N_f fundamentals and a singlet in the antisymmetric 'meson' of the $U(N_f)$ 'flavour' group [59], Seiberg duality for a gauge group $SU(N_c)$ with N_f fundamentals and antifundamentals yields a magnetic theory $SU(N_f - N_c)$, N_f fundamentals and anti-fundamentals and a singlet 'meson' in the bifundamental of the $U(N_f) \times U(N_f)$ 'flavour' groups [58], whereas the magnetic dual of $SO(N_c)$ with N_f quarks in the vector representation is a theory with $SO(N_f - N_c + 4)$, N_f quarks and a singlet 'meson' in the symmetric of the $U(N_f)$ 'flavour' group [60].
Let us denote the two ways of performing the projections as **A** and **B**.

- **A**: Orientifold + duality cascade.
  Let us perform the projection Ω in Fig. (4.12) with $\epsilon_0 = +1$, which gives $USp(N + M)$ at the node 0, $U(N)$ at the node 1 and $USp(N+M)$ at the node 2. We dualize all nodes in the order (0,2,1), with node 3 identified with 1 by the orientifold. First, at node 0 the gauge theory changes as $USp(N + M) \to USp(N - M - 4)$ and there are four additional antisymmetric mesons M^{pq}. The orientifold projection is Ω in Fig. (4.16). It is important to note that these mesons are composite in terms of the electric quarks, namely

  $$M^{pq} = (\Box_{1'}, \overline{\Box}_0)^p \, (\Box_0, \overline{\Box}_1)^q = (\overline{\Box}_1, \overline{\Box}_0)^p \, (\Box_0, \overline{\Box}_1)^q \ , \tag{4.97}$$

  which transform under two of the groups. In order to make the combination antisymmetric we get: $[i_0 j_0](l_1 m_1) + (i_0 j_0)[l_1 m_1]$, where $i_0, j_0 = 1, ...N_0$ run on the group 0 and $l_1, m_1 = 1, ...N_1$ along the group 1. This gives the proper orientifold signs for the mesons, thus $\sum_{I=1}^{4} \epsilon_{1'1}^{(I)} = -2$. Besides, in this way the theory is anomaly-free. We can proceed to dualization of the node 2, whose gauge group becomes $USp(N - M - 4)$. Furthermore, there are other mesons with "opposite orientation" to the previous ones, since they transform under two conjugate representations. Whenever that happens, we integrate them out. What remains is to dualize

node 1 (and 3), with gauge group $U(N-2M-8)$. This completes the first step in the duality cascade, and the process can be repeated several times as long as the duality is allowed. After k steps in the cascade the theory is $USp(N_0^A) \times U(N_1^A) \times USp(N_0^A)$ with

$$\begin{aligned} N_0^A &= N - (2k-1)M - 4k^2 \,, \\ N_1^A &= N - 2kM - 4k(k+1) \end{aligned} \tag{4.98}$$

and it represents the bottom of the duality cascade, namely the IR theory whose quiver is shown in Fig. (4.28), if

$$N < M(2k+1) + 4k(k+2) \tag{4.99}$$

and

$$\begin{cases} (2k-1)M + 4k^2 < N & \text{if } M < 4k \,, \\ 2kM + 4k(k+1) < N & \text{if } M > 4k \,. \end{cases}$$

When these condition holds, no more dualities are allowed and the cascade stops.

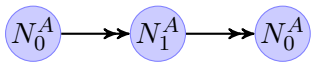

Figure 4.28. The theory at the end of the duality cascade of $(\mathcal{C}/\mathbb{Z}_2')/\Omega$. The orientifold projection is performed before the cascade.

- **B**: duality cascade + orientifold.
  We exchange now the order and study the orientifold involution at the end of a duality cascade. We start with M' fractional branes and eventually we compare this with M of the previous case. The order of dualization is (0,2,1,3), with all gauge groups $U(N)$ and again integrating out fields in two conjugate representations. The cascade stops after k' steps when

  $$2k'M' < N < M'(2k'+1) \,. \tag{4.100}$$

  The unoriented projection over nodes 0 and 2 yields an anomaly-free theory $USp(N_0^B) \times U(N_1^B) \times USp(N_0^B)$ at the IR with

  $$\begin{aligned} N_0^B &= N - (2k'-1)M' \,, \\ N_1^B &= N - 2k'M' \,, \end{aligned} \tag{4.101}$$

  whose quiver is drawn in Fig. (4.29).

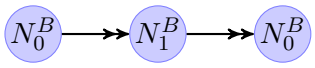

Figure 4.29. The unoriented theory at the end of the duality cascade of $\mathcal{C}/\mathbb{Z}_2'$. The orientifold projection is performed after the cascade.

Comparing the theories in **A** and **B** at the bottom of the cascades, they are equal if

$$\begin{aligned}(2k'-1)M' &= (2k-1)M + 4k^2 \,, \\ 2k'M' &= 2kM + 4k(k+1) \,,\end{aligned} \tag{4.102}$$

which leads to

$$\begin{aligned}M' &= M + 4k \,, \\ k' &= \frac{kM + 2k(k+1)}{M+4k} \,.\end{aligned} \tag{4.103}$$

The solution in terms of integers p and q reads

$$\begin{aligned}k' &= p \,, \\ k &= q + p \,, \\ M &= 2\left[\frac{p}{q}(p-1) - q - 1\right] \,, \\ M' &= M + 4(p+q) \,,\end{aligned} \tag{4.104}$$

with the condition $\frac{p}{q}(p-1) \in \mathbb{N}$ and $\frac{p}{q}(p-1) \geq q+1$.
Note that $k = k'$ is allowed only if $k = k' = 0$ or $k = k' = 1$, where the former stands for $M = M'$ and no duality cascade is triggered and the latter describe a solution with $M' = M + 4$ and the flow stops if

$$2M + 8 < N < 3M + 12 \tag{4.105}$$

and

$$\begin{cases} M + 4 < N & \text{if } M < 4 \,, \\ 2M + 8 < N & \text{if } M > 4 \,. \end{cases}$$

If we perform the same process but with an unoriented projection giving SO gauge groups instead of Sp, the path[7] **A** stops at ranks

$$\begin{aligned}N_0^A &= N - (2k-1)M + 4k^2 \,, \\ N_1^A &= N - 2kM + 4k(k+1) \,,\end{aligned} \tag{4.106}$$

[7] Along the way, the mesons are symmetric and $\sum_{I=1}^{4} \epsilon_{1'1}^{(I)} = +2$.

if

$$N < M(2k+1) - 4k(k+2) \tag{4.107}$$

and

$$\begin{cases} (2k-1)M - 4k^2 < N & \text{if } M < 4k \ , \\ 2kM - 4k(k+1) < N & \text{if } M > 4k \ , \end{cases}$$

while **B** remains the same since the orientifold projection is performed at the end of the cascade. The IR theories are the same if

$$\begin{aligned} M' &= M - 4k \ , \\ k' &= \frac{kM - 2k(k+1)}{M - 4k} \ , \end{aligned} \tag{4.108}$$

and in terms of integers p and q it is solved as

$$\begin{aligned} k' &= p \ , \\ k &= p - q \ , \\ M &= 2\left[\frac{p}{q}(p-1) - q + 1\right] \ , \\ M' &= M + 4(p-q) \ , \end{aligned} \tag{4.109}$$

with conditions $\frac{p}{q}(p-1) \in \mathbb{N}$, $\frac{p}{q}(p-1) \geq q-1$, $p - q > 1$.
In general, cascades **A** and **B** do not end at the same step since insisting that the theories are the same in the IR gives $k > k'$ in the Sp case and $k < k'$ in the SO case. Starting instead from the same theory in the UV, the IR theories are different. This is because the unoriented projection in the UV changes the degrees of freedom even before the flow along the cascade. Thus, the order of duality cascade and orientifold matters. Besides, the physical interpretation of cascade **B**, where the orientifold projection is performed in the IR, is geometrically unclear, although in the (non-perturbative) context of F-theory a certain geometric configuration could appear as an O-plane at some distance, providing a possible physical scenario.

4.4 Discussion

Let us conclude and summarise our results. We have discussed unoriented theories arising from the addition of O-planes on stacks of D3-branes probing toric Calabi-Yau singularities. We focused on $\mathbb{C}^3/\mathbb{Z}_3$ and $\mathbb{C}^3/\mathbb{Z}_4$, both chiral and non-chiral, and their non-orbifold descendants obtained by means of mass deformations [70] and higgsing/unhiggsing [71]. Examples of chiral non-orbifold theories include dP_1 [97] and the chiral $\mathbb{Z}_2$ quotient of the Conifold $\mathcal{C}/\mathbb{Z}_2'$ [107], while non-chiral models include the Suspended Pinch Point (SPP) [104] and the non-chiral $\mathbb{Z}_2$ quotient of the Conifold

$\mathcal{C}/\mathbb{Z}_2$. When possible, we have simultaneously used both quiver and dimer descriptions in order to spell out the conditions for anomaly cancellation and super-conformal invariance, sometimes retrieved at the perturbative level after the inclusion of flavour branes [39]. For the unoriented projection of $\mathbb{C}^3$ and $\mathbb{C}^3/\mathbb{Z}_3$ we have found the relation between the orientifold charges (ϵ_0, ϵ_I), which have a direct geometric interpretation, and the τ charges τ of the dimer [44, 81]. Orientifold charges are given by the action of τ charges on basic mesonic operators but a general relation was not evident before.

Moreover, by exploiting the combination of toric diagrams and the Ito-Reid Theorem [91], we have addressed the problem of the distinction between O3-planes and compact/non-compact O7-planes for orbifold singularities, in the resolved geometry. Although theories with flavour branes admit a description in terms of bipartite graph on bordered Riemann surfaces [43, 45, 46], in general the resulting super-potential does not satisfy the toric condition and it is not obvious to us how far one can go with the use of toric and dimer diagrams in the context of unoriented projection. This is one of the reasons why it has been important for us to recover a satisfactory quiver description of unoriented CY singularities: it allows the inclusion of non-compact D7-branes. The quiver description can be used, even in the presence of both flavour branes and orientifold planes, to easily compute RR-tadpole cancellation conditions [93, 94] and the vanishing of beta functions, needed in order to obtain an anomaly-free super-conformal field theory at the perturbative level. However, it should be noted that the superpotential can be unequivocally determined from the dimer diagram. We stress that the anomaly cancellation condition, initially derived for orbifold theories in [39], was used also for non-orbifold models and we justified the procedure by means of mass deformation and higgsing as long as they preserve the $\mathbb{Z}_2$ symmetry exploited by the orientifold.

We have illustrated how, in general, each quiver model admits more than one possible orientifold projection. We have not explored non-perturbative phases that can be reached using S-duality [81–85]. Yet, by generalizing the anomaly cancellation condition derived in [39], we have recovered results already present in the literature. Furthermore, we have exploited the symmetries of the invariant tensors of $SO(N)$ and $USp(N)$ and the symmetries induced by the action of the unoriented projection on the fields present in super-potential in order to further constraint the spectrum and interactions. Our analysis has also shown that some particular unoriented projections, combined with the requirement of vanishing RR tadpoles, do not admit the existence of anomaly-free super-conformal theories, barring non-perturbative sectors that may emerge at strong coupling in the IR [84, 85].

Finally, we have studied the interplay between duality cascade and unoriented projections following similar analyses [88, 99]. A first analysis shows that performing the unoriented projection in the UV or in the IR yields similar theories, in the sense that the matter content are the same, but different in the ranks of gauge groups, i.e. the degrees of freedom. The conclusion is that the two operations do not commute, even though the duality preserves the $\mathbb{Z}_2$ symmetry of the orientifold. This is a crucial difference with mass deformation, as the flow triggered by the relevant mass term is preserved under the orientifold projection.

We have almost not touched the issue of non-perturbative corrections induced by stringy instantons

[38, 89, 90, 108–112]. They may play an important role in correcting the geometry, as already observed in some cases in [106, 113, 114]. Extending these analyses to the unoriented case with flavour should be possible along the lines of [39]. In the present analysis, we have not considered at all the issue of dynamical supersymmetry breaking in unoriented theories, which was recently addressed in [115] and represents an interesting line of research.

Chapter 5

Suspended Fixed Points

The orientifold projection of a toric theory gives rise to a rich structure, as the gauge group contains symplectic and orthogonal factors, along with tensorial matter fields. After the orientifold projection, we ask what is the fate of the conformal point. The factors we have just mentioned introduce sub-leading elements in the beta function and hence it is believed that anomalous dimensions receive at most sub-leading corrections. Moreover, in order to cancel gauge anomalies, usually the ranks of the gauge factors must be shifted, signaling the presence of fractional branes. These are seen as branes wrapping compact cycles, whose size introduce a scale in the theory. Then, it is usually believed that orientifold projection breaks conformal invariance.
We have powerful tools at our disposal to determine the fixed point of a general $\mathcal{N} = 1$ gauge theory, a-maximization above all. We can implement the algorithm described in Chapter 2 for the unoriented theories and determine whether a fixed point exists or not. We find useful to compare the result with the central charge of the parent SCFT. Since the orientifold projection acts on the spacetime as a reflection and exploits a $\mathbb{Z}_2$ symmetry, we expect that the projection roughly halves the degrees of freedom, or better said, the degrees of freedom are halved at large ranks N. Recall the form of the central charge a

$$a = \frac{3}{32}\left(3\mathrm{Tr}\, R^3 - \mathrm{Tr}\, R\right) , \tag{5.1}$$

which depends on the R-symmetry. Denoting by a^Ω the central charge of the projected SCFT and by a the central charge of the parent theory, based on what we said we can classify the possible outcomes into two scenarios

1. *first scenario*, when a^Ω-maximization gives a conformal point and at large N the ratio $a^\Omega/a = 1/2$. The orientifold projection affects the anomalous dimensions γ, and consequently the R-charges, by $1/N$ terms. At large N, the $\mathbb{Z}_2$ involution has effectively reduced the degrees of freedom by half;

2. *second scenario*, when there is no conformal point, the allowed choices for the ranks for a

meaningful theory do not cancel the beta functions. In other words, one can not define a non-anomalous R-symmetry. In some cases, the flow towards the infrared of the orientifolded theory is described by a duality cascade [88], or conformal symmetry can be restored by the inclusion of flavour branes [39].

Note that from Gubser relation [68], the volume of the 5-dimensional Sasaki-Einstein manifold Y_5 is related to the central charge of the SCFT by

$$\mathrm{Vol}_Y = \frac{\pi^3}{4}\frac{N^2}{a} \,, \tag{5.2}$$

so in first scenario, assuming the orientifolded SCFT has a dual AdS side, the volume of the corresponding Y_5^Ω is inversely proportional to a^Ω. A meaningful comparison between Vol_5^Ω and Vol_5 requires that we take the spaces with the same radius. This radius[1] is proportional to the units of five-form flux supported by the compact space. However, in presence of orientifold planes the units of five-form flux is $(N/2)$ [116]. Hence, after the orientifold we should rescale the volume as

$$\mathrm{Vol}_Y^\Omega = \frac{\pi^3}{4}\left(\frac{N}{2}\right)^2\frac{1}{a^\Omega} \,. \tag{5.3}$$

Note that in first scenario the ratio $\mathrm{Vol}_Y^\Omega/\mathrm{Vol}_Y = 1/2$, as we should expect.
This Chapter, based on [3], explores a third possibility that we call *third scenario*: at large N the ratio $a^\Omega/a < 1/2$, hence the degrees of freedom are more than halved, while the volume Vol_Y^Ω results larger than a half of Vol_Y. We will see this mechanism is related to an $U(1)$ becoming anomalous and not mixing with other global abelian factors that give the superconformal R-symmetry. We focus on orientifold projection $(\mathrm{SPP}/\mathbb{Z}'_n)^\Omega$ and in general of $L^{a,b,a}$ theories. These can be obtained from mass deformation of $\mathbb{C}^2/\mathbb{Z}_{3n}\times\mathbb{C}$, which we dubbed $\mathbb{C}^3/\mathbb{Z}'_{3n}$ Surprisingly, the third scenario leads to a new unoriented duality between theories with fixed lines orientifolds in firt scenario and with fixed points orientifold in third scenario, as we shall see. The results are summarized in the chart in Fig. 5.1, which serves as a guide for the reader.

5.1 SPP and its non-chiral orbifold $\mathbb{Z}'_n$

The Suspended Pinch Point (SPP) is a (non-isolated) toric singularity, that can be realized as an affine variety in $\mathbb{C}^4$ with the relation

$$xy = z^2 w \,, \tag{5.4}$$

[1] It is actually the fourth power of the radius of the horizon that is proportional to the units of five-form flux N.

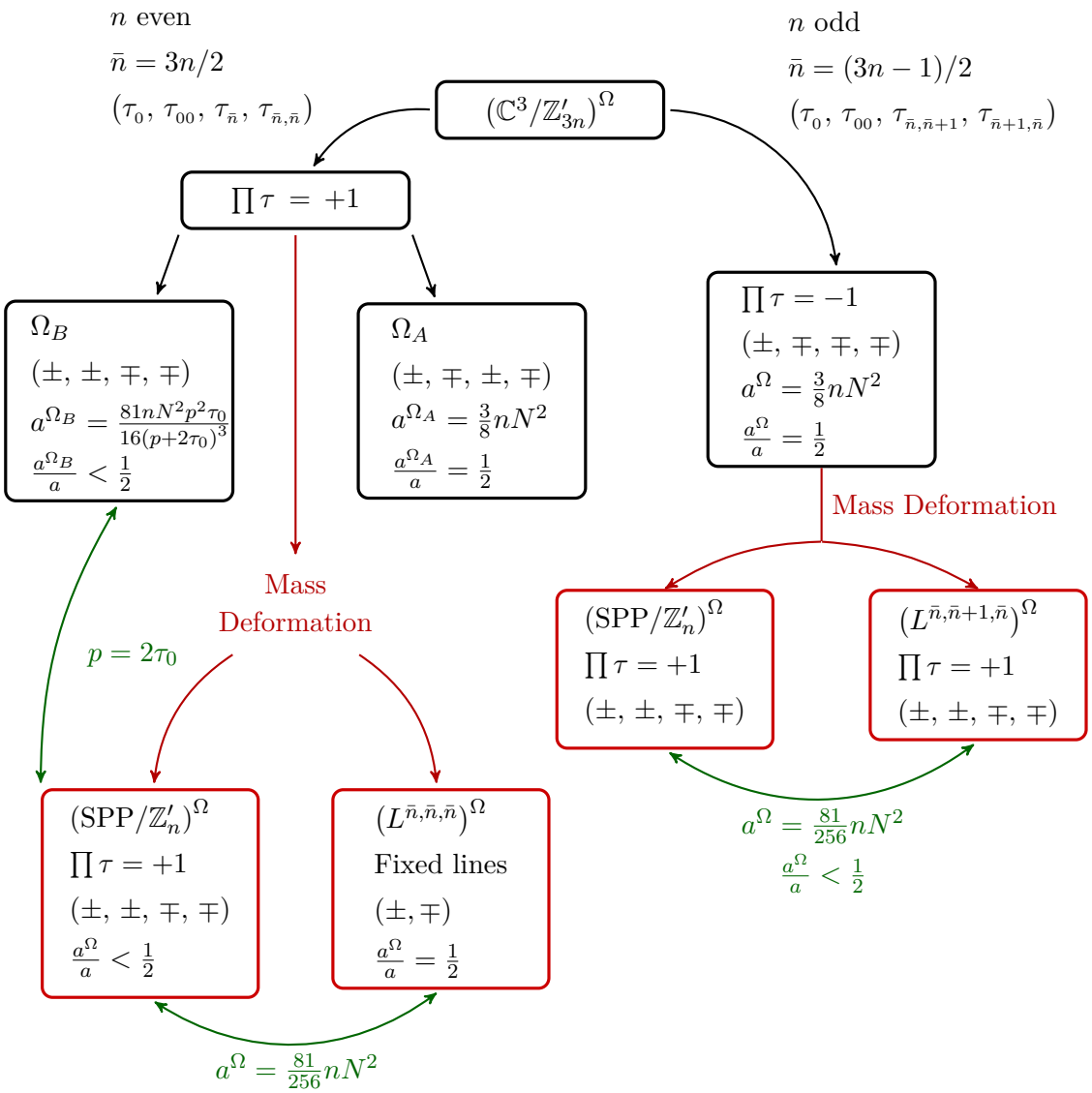

Figure 5.1. The web of unoriented dualities found between $\mathbb{C}^3/\mathbb{Z}'_{3n}$, $\mathrm{SPP}/\mathbb{Z}'_n$ and $L^{k,n-k,k}$.

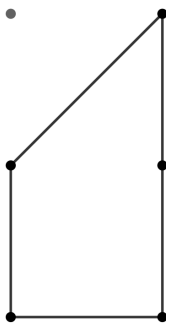

Figure 5.2. The toric diagram of the SPP singularity.

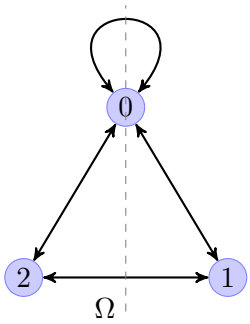

Figure 5.3a: The quiver diagram for SPP. The line Ω represents the orientifold projection.

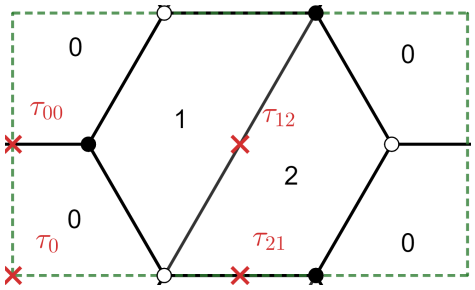

Figure 5.3b: The dimer of the SPP theory, the four fixed points of the orientifold projection are drawn in red.

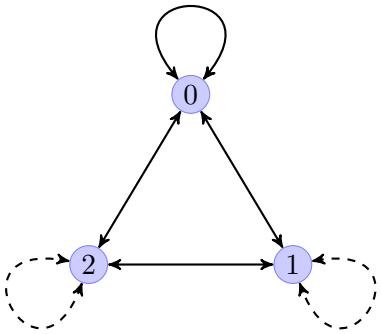

Figure 5.4a: The quiver diagram for $\mathbb{C}^3/\mathbb{Z}'_3$. Giving mass to the adjoint fields represented by dashed lines yields SPP.

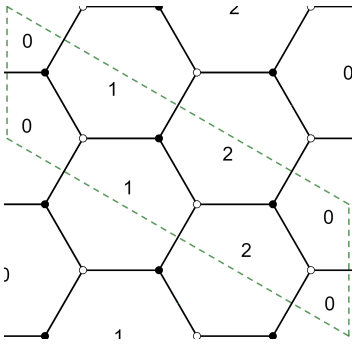

Figure 5.4b: The brane tiling for $\mathbb{C}^3/\mathbb{Z}'_3$.

with x, y, z, w $\in \mathbb{C}^4$. The singularity is represented by the toric diagram in Fig. 5.2, which has no internal points, signalling that the associated gauge theory is non-chiral. The gauge group is $U(N_0) \times U(N_1) \times U(N_2)$, while the matter content corresponds to six chiral fields denoted by X_{ij} $(i \neq j)$, transforming under the fundamental representation of $U(N_i)$ and the anti-fundamental of $U(N_j)$, together with the chiral field X_{00}, that we denote by ϕ_0,[2] in the adjoint on the group $U(N_0)$. We draw the quiver and the dimer of the theory in Figs. 5.3a and 5.3b. The superpotential reads

$$W_{\text{SPP}} = \phi_0 \left(X_{02}X_{20} - X_{01}X_{10}\right) + X_{12}X_{21}X_{10}X_{01} - X_{21}X_{12}X_{20}X_{02} \,, \tag{5.5}$$

as can be deduced from the dimer.

The SPP theory can be obtained by mass deformation of another toric theory, the non-chiral orbifold of flat space $\mathbb{C}^3/\mathbb{Z}'_3$ [70]. Its graphical representation as dimer and quiver is shown in Fig. 5.4a-5.4b. The superpotential reads

[2] In general we denote adjoint chiral fields X_{ii} by ϕ_i.

$$W_{\mathbb{C}^3/\mathbb{Z}'_3} = \phi_0 \left(X_{02}X_{20} - X_{01}X_{10}\right) + \phi_1 \left(X_{10}X_{01} - X_{12}X_{21}\right) + \phi_2 \left(X_{21}X_{12} - X_{20}X_{02}\right) \tag{5.6}$$

which reduces to the superpotential of SPP adding the mass term

$$\Delta W_{\mathbb{C}^3/\mathbb{Z}'_3} = \frac{M}{2}\left(\phi_1^2 - \phi_2^2\right) \tag{5.7}$$

and integrating the massive fields out. Plugging F-terms into the superpotential and redefining fields as

$$\begin{aligned} X'_{21}X'_{12} &= \frac{1}{M} X_{21}X_{12} \ , \\ \phi'_0 &= \phi_0 + \frac{1}{2M}\left(X_{01}X_{10} - X_{02}X_{20}\right) \end{aligned} \tag{5.8}$$

gives the superpotential of SPP.
We now review how the R-charges and the central charge a of the conformal SPP theory are determined using a-maximization. We denote the R-charges of X_{ij} by

$$R_{ij} = r_{ij} + 1 \ , \tag{5.9}$$

where r_{ij} is the R-charge of the fermionic field in the multiplet. First, we impose the constraint $R(W) = 2$, that gives

$$\begin{aligned} r_{01} + r_{10} + r_{00} &= -1 \ , \\ r_{12} + r_{21} - r_{00} &= -1 \ , \\ r_{20} + r_{02} &= r_{01} + r_{10} \ . \end{aligned} \tag{5.10}$$

This constraint implies that all the r's must satisfy $-1 < r < 1$, otherwise some field, say X_{01}, must have zero or negative R-charges and corresponding gauge-invariant operators, as $\mathrm{Tr}\, X_{01}X_{10}$, will have conformal dimension below the unitarity bound. The $\mathbb{Z}_2$ symmetry of the quiver implies $r_{12} = r_{21}$, $r_{02} = r_{01}$ and $r_{20} = r_{10}$. The condition that the beta functions vanish (which in turn is equivalent to the R-symmetry being anomaly-free) gives

$$\begin{aligned} r_{00}\left(2N_0 - N_1 - N_2\right) &= -\left(2N_0 - N_1 - N_2\right) \ , \\ r_{00}\left(N_1 - N_2\right) &= \left(2N_1 - N_0 - N_2\right) \ , \\ r_{00}\left(N_0 - N_1\right) &= \left(2N_2 - N_1 - N_0\right) \ , \end{aligned} \tag{5.11}$$

where we have used Eq. (5.10). We note that $2N_0 - N_1 - N_2 \neq 0$ would imply $r_{00} = -1$, violating unitarity. We therefore impose $N_0 = N_1 = N_2 = N$, which leaves r_{00} undetermined. Note that Eq. (5.10) is invariant under the exchange $r_{ji} \leftrightarrow r_{ij}$, then we put them equal. This is inherited

from the $\mathcal{N}=2$ $\mathbb{C}^3/\mathbb{Z}'_3$ and its superpotential before mass deformation. Hence, we have a one-parameter family of solutions, corresponding to the fact that there is one non-anomalous $U(1)$ flavour symmetry that can in principle redefine the R-charge. The superconformal R-charge is then determined by a-maximization. In particular, defining $r_{01}=x$, the a-charge[3] at leading order in N

$$a_{\text{SPP}}=\frac{9}{32}\text{Tr }R^3=\frac{9N^2}{32}\left[(-1-2x)^3+4\,(x)^3+2(-1-x)^3+3\right] \tag{5.12}$$

has a local maximum at [117]

$$r_{00}=1-\frac{2}{\sqrt{3}}\,,\qquad r_{12}=-\frac{1}{\sqrt{3}}\,,\qquad r_{01}=r_{10}=-1+\frac{1}{\sqrt{3}}\,, \tag{5.13}$$

which gives the superconformal a-charge

$$a_{\text{SPP}}=\frac{3\sqrt{3}}{8}N^2\,. \tag{5.14}$$

5.1.1 Non-chiral orbifold SPP/$\mathbb{Z}'_n$

Starting from the SPP geometry, one can construct additional models by considering abelian orbifolds SPP/Γ. A particular $\mathbb{Z}_2$ orbifold results in the PdP_{3c} geometry, which we are going to study in the next chapter. There is another $\mathbb{Z}_2$ involution that can be performed, resulting in the toric geometry denoted by $L^{2,4,2}$ in the literature, and whose toric diagram is given in Fig. 5.5a. As will be discussed in the next section, this geometry leads to two different toric phases, and we are interested in particular in the one corresponding to the quiver in Fig. 5.5b, which can be seen as arising from a $\mathbb{Z}_2$ involution on the SPP gauge theory. The resulting gauge theory has six unitary gauge groups, it is non-chiral, and we denote it by SPP/$\mathbb{Z}'_2$. The superpotential is

$$\begin{aligned}W_{\text{SPP}/\mathbb{Z}'_2}=&\,\phi_0\left(X_{05}X_{50}-X_{01}X_{10}\right)+\phi_3\left(X_{32}X_{23}-X_{34}X_{43}\right)+X_{10}X_{01}X_{12}X_{21}\\&-X_{21}X_{12}X_{23}X_{32}+X_{43}X_{34}X_{45}X_{54}-X_{54}X_{45}X_{50}X_{05}\,,\end{aligned} \tag{5.15}$$

and it can be explicitly obtained from the $\mathbb{Z}'_2$ action on the SPP superpotential in Eq. (5.5).
The non-chiral $\mathbb{Z}'_2$ orbifold discussed above belongs to an infinite family of non-chiral models SPP/$\mathbb{Z}'_n$, whose quivers correspond to a sequence on n copies of the structure of nodes and arrows in Fig. 5.6, giving in total $3n$ unitary gauge groups, n of which have matter in the adjoint.

[3] Observe that Tr $R=0$ at leading order in N for holographic theories.

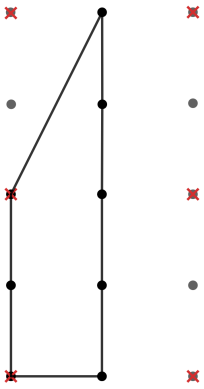

Figure 5.5a: The toric diagram of SPP/$\mathbb{Z}'_2$, a.k.a. $L^{(2,4,2)}$, where fixed points of the orientifold projection are drawn in red.

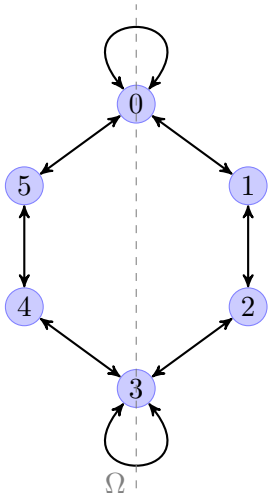

Figure 5.5b: The quiver of SPP/$\mathbb{Z}'_2$, a.k.a. $L^{(2,4,2)}$. The dashed line represents the orientifold projection.

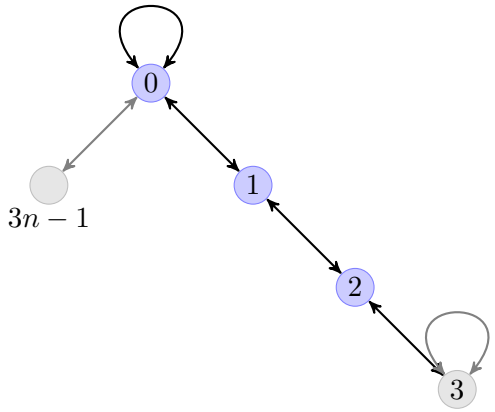

Figure 5.6. Blue nodes form the recursive structure of the quiver SPP/$\mathbb{Z}'_n$.

The associated geometry is known as $L^{n,2n,n}$ in the literature. The superpotential reads

$$\begin{aligned} W_{\text{SPP}/\mathbb{Z}'_n} &= \sum_{i=0}^{n-1} \phi_{3i} \left(X_{3i,\,3i-1} X_{3i-1,\,3i} - X_{3i,\,3i+1} X_{3i+1,\,3i} \right) \\ &+ \sum_{i=0}^{n-1} \left(X_{3i+1,\,3i} X_{3i,\,3i+1} X_{3i+1,\,3i+2} X_{3i+2,\,3i+1} \right. \\ &\left. - X_{3i+2,\,3i+1} X_{3i+1,\,3i+2} X_{3i+2,\,3i+3} X_{3i+3,\,3i+2} \right) , \end{aligned} \tag{5.16}$$

where it is understood that the group labels of the fields are defined modulo $3n$.
In order to determine the R charges and a charge of the SPP/$\mathbb{Z}'_n$ theory at the conformal fixed

point, we impose the constraints coming from the condition that the R charge of the superpotential be equal to 2.

$$\begin{aligned}
&r_{3i,3i+1} + r_{3i+1,3i} + r_{3i,3i} = -1 \ , \\
&r_{3i,3i-1} + r_{3i-1,3i} + r_{3i,3i} = -1 \ , \\
&r_{3i+1,3i} + r_{3i,3i+i} + r_{3i+1,3i+2} + r_{3i+2,3i+1} = -2 \ , \\
&r_{3i+2,3i+1} + r_{3i+1,3i+2} + r_{3i+2,3i+3} + r_{3i+3,3i+2} = -2 \ .
\end{aligned} \tag{5.17}$$

with $i = 0, ..., n-1$. As discussed in the previous subsection, $r_{3i,3i+1} = r_{3i+1,3i}$. The symmetry of the quiver also allows to impose various constraints on the charges. First of all, the charges are invariant under shifts in i. Besides, the $\mathbb{Z}_2$ symmetry around each adjoint node implies that $r_{3i-1,3i} = r_{3i+1,3i}$, $r_{3i,3i-1} = r_{3i,3i+1}$ and $r_{3i+1,3i+2} = r_{3i+2,3i+1}$. Finally, the condition that all the beta functions vanish is solved imposing that all the gauge groups have equal rank N. Putting all this together, one can show that the a charge is simply n times the a charge of the SPP theory. In particular, performing a maximization gives [117]

$$r_{3i,3i} = 1 - \frac{2}{\sqrt{3}} \ , \qquad r_{3i+1,3i+2} = -\frac{1}{\sqrt{3}} \ , \qquad r_{3i,3i+1} = -1 + \frac{1}{\sqrt{3}} \tag{5.18}$$

as in Eq. (5.13), and the corresponding maximized a-charge reads

$$a_{\mathrm{SPP}/\mathbb{Z}'_n} = n\, a_{\mathrm{SPP}} = n \frac{3\sqrt{3}}{8} N^2 \ . \tag{5.19}$$

As a consequence of the orbifold involution, we see that the d.o.f. of the field theory increase with n.

5.2 Mass Deformation of $\mathbb{C}^3/\mathbb{Z}'_{3n}$

As we have already seen, the SPP theory can be obtained via mass deformation of $\mathbb{C}^3/\mathbb{Z}'_3$, giving mass to two of the adjoints. This is more general and we can recover $\mathrm{SPP}/\mathbb{Z}'_n$ via mass deformation of $\mathbb{C}^3/\mathbb{Z}_{3n}$, giving mass to more pairs of adjoints. In particular, starting with the superpotential

$$W_{\mathbb{C}^3/\mathbb{Z}'_{3n}} = \sum_{i=0}^{3n-1} \phi_i \left(X_{i,\,i-1} X_{i-1,\,i} - X_{i,\,i+1} X_{i+1,\,i} \right) \tag{5.20}$$

and deforming it with

$$\Delta W_{\mathbb{C}^3/\mathbb{Z}'_{3n}} = \sum_{i=0}^{n-1} \frac{M}{2} \left(\phi_{3i+1}^2 - \phi_{3i+2}^2 \right) \ , \tag{5.21}$$

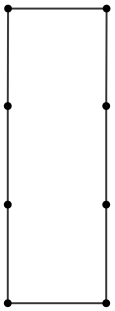

Figure 5.7a: The toric diagram for $L^{3,3,3}$.

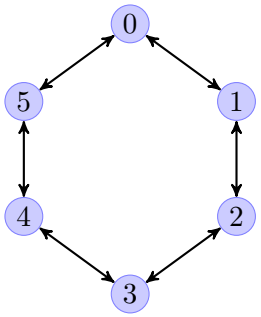

Figure 5.7b: The quiver for $L^{3,3,3}$, obtained by mass deformation of all of the adjoints in $\mathbb{C}^3/\mathbb{Z}'_6$.

below the scale M the effective theory reads

$$\begin{aligned} W = &\sum_{i=0}^{n-1} \phi_{3i} \left(X_{3i,\,3i-1} X_{3i-1,\,3i} - X_{3i,\,3i+1} X_{3i+1,\,3i} \right) \\ &+ \sum_{i=0}^{n-1} \left(X_{3i+1,\,3i} X_{3i,\,3i+1} X_{3i+1,\,3i+2} X_{3i+2,\,3i+1} \right. \\ &\left. - X_{3i+2,\,3i+1} X_{3i+1,\,3i+2} X_{3i+2,\,3i+3} X_{3i+3,\,3i+2} \right) \ , \end{aligned} \tag{5.22}$$

which is the superpotential of SPP$/\mathbb{Z}'_n$. Recall that SPP is the toric geometry $L^{1,2,1}$. In [70], it is pointed out that giving mass to contiguous k pair of adjoint fields in $\mathbb{C}^3/\mathbb{Z}'_{3n}$, one obtains the toric theory $L^{k,3n-k,k}$.

If we perform a mass deformation such that the highest number of pairs of adjoints are integrated out, the resulting theory depends on whether n is even or odd. In fact, for n even we can integrate out all the adjoint fields, with $k = 3n/2$, to obtain $L^{\frac{3n}{2},\frac{3n}{2},\frac{3n}{2}}$, whose toric diagram is a rectangle. In Fig. 5.7b-5.7a we show an example for $n = 2$. The final superpotential reads

$$\begin{aligned} W_{\frac{3n}{2},\frac{3n}{2},\frac{3n}{2}} = &\sum_{i=0}^{3n-1} \left(X_{i+1,\,i} X_{i,\,i+1} X_{i+1,\,i+2} X_{i+2,\,i+1} \right. \\ &\left. - X_{i+2,\,i+1} X_{i+1,\,i+2} X_{i+2,\,i+3} X_{i+3,\,i+2} \right) \ . \end{aligned} \tag{5.23}$$

On the other hand, for n odd at most we can integrate out $\frac{n-1}{2}$ pair of adjoints and we are left with a single adjoint field, which we can choose to be on node 0 without loss of generality. In this case we are left with $L^{\frac{3n-1}{2},\frac{3n+1}{2},\frac{3n-1}{2}}$, whose toric diagram is a trapezoid, see Fig. 5.8a. The resulting

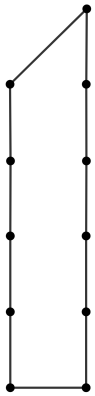

Figure 5.8a: The toric diagram for $L^{4,5,4}$.

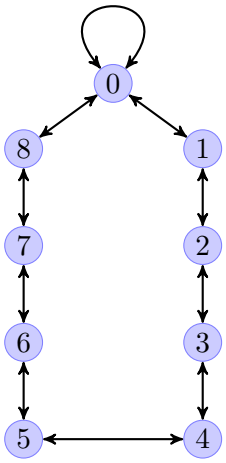

Figure 5.8b: The quiver for $L^{4,5,4}$, obtained by mass deformation of all but one of the adjoints in $\mathbb{C}^3/\mathbb{Z}'_9$.

superpotential reads

$$\begin{aligned} W_{\frac{3n-1}{2},\frac{3n+1}{2},\frac{3n-1}{2}} &= \phi_0 \left(X_{0,\,3n-1} X_{3n-1,\,0} - X_{01} X_{10} \right) \\ &+ \sum_{i=0}^{3n-3} \left(X_{i+1,\,i} X_{i,\,i+1} X_{i+1,\,i+2} X_{i+2,\,i+1} \right. \\ &\left. - X_{i+2,\,i+1} X_{i+1,\,i+2} X_{i+2,\,i+3} X_{i+3,\,i+2} \right) . \end{aligned} \tag{5.24}$$

5.2.1 Web of Seiberg dualities

As we have just shown, from $\mathbb{C}^3/\mathbb{Z}'_{3n}$ we can reach $\mathrm{SPP}/\mathbb{Z}'_n$ by mass deforming pairs of adjoint fields in a particular pattern, which is the one given in Eq. (5.21). On the other hand, toricity is preserved as long as we give mass to an adjacent pair of adjoint fields, that is two adjoint fields whose gauge groups are connected in the quiver. As an example, for the case of $\mathbb{C}^3/\mathbb{Z}'_6$ (*i.e.* $n = 2$) if we give mass to two adjacent pairs of adjoints we have two possibilities, up to symmetries: we can either give mass to the adjoints of the groups 1,2,4 and 5 or to the adjoints of 1,2,3 and 4. The resulting theories are two different toric phases of $L^{2,4,2}$, with the former being $\mathrm{SPP}/\mathbb{Z}'_2$. If instead we give mass to a single pair or to all the adjoints, there is clearly only one possibility in each case, corresponding to $L^{1,5,1}$ and $L^{3,3,3}$ respectively.
This can be generalized to any n. Starting from $\mathbb{C}^3/\mathbb{Z}'_{3n}$, we have one possibility if we give mass to a single pair, which corresponds to $L^{1,3n-1,1}$, while if we give mass to two pairs we have $\left[\frac{3n}{2}\right] - 1$ different $L^{2,3n-2,2}$ gauge theories. It is a combinatorial exercise to determine all possible theories that one obtains giving mass to k pairs. If $k = n$ one gets $L^{n,2n,n}$, which contains $\mathrm{SPP}/\mathbb{Z}'_n$. If n is even, one can remove all adjoint fields giving mass to $\frac{3n}{2}$ pairs, which gives the $L^{\frac{3n}{2},\frac{3n}{2},\frac{3n}{2}}$ theory.

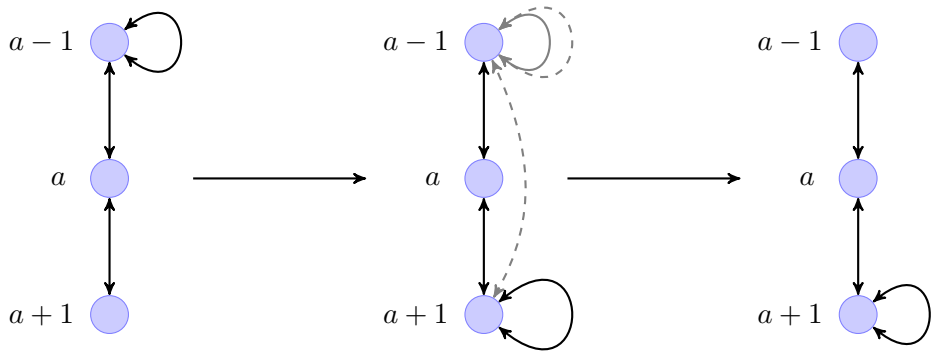

Figure 5.9. Performing Seiberg duality on node (a), while node $(a-1)$ has an adjoint, results in moving the adjoint from $(a-1)$ to $(a+1)$. Dashed lines are mesons, while gray lines represent fields that have been integrated out in the process.

If n is odd, one reaches the $L^{\frac{3n-1}{2},\frac{3n+1}{2},\frac{3n-1}{2}}$ theory giving mass to $\frac{3n-1}{2}$ adjacent pairs.
We now explicitly show that these $L^{k,3n-k,k}$ gauge theories for a given k are related by Seiberg duality, which in turn means that they are dual phases of the same toric diagram. In particular, we perform Seiberg duality on a gauge group with no adjoint fields. Suppose that (a) is such a node. There are two possibilities: either both nodes $(a-1)$ and $(a+1)$ have no adjoint, or one of the two, say $(a-1)$, has an adjoint. In the former case, Seiberg duality gives a theory with an adjoint on both the $(a-1)$ and the $(a+1)$ node. The latter case is the interesting one. Suppose the group at node a has rank N_a. The usual rules for the Seiberg dual give $\widetilde{N}_a = N_{a+1} + N_{a-1} - N_a$ and if $N_a = N$ for all a then $\widetilde{N}_a = N$. The matter content includes dual bifundamental fields and mesons. Integrating the massive fields out one obtains the dual magnetic theory. Note that the net result is to move an adjoint field from node $(a-1)$ to $(a+1)$, as displayed in Fig. 5.9. This is represented as the operation in Fig. 5.10 from the dimer perspective. Repeating the process, one can construct all possible theories with $3n-2k$ adjoints and non-adjoint nodes all in pairs. In particular, one can choose to dualise both nodes (a) and $(n-a)$, realizing a theory that is $\mathbb{Z}_2$-symmetric. This will be useful in the case of orientifold projections.

5.3 Orientifold of SSP/$\mathbb{Z}'_n$

In this section we study the orientifold projection Ω of the non-chiral orbifold SSP/$\mathbb{Z}'_n$ and in particular we seek the conformal point of the unoriented theory. We first discuss the cases with $n = 1$ and $n = 2$ and then general n.

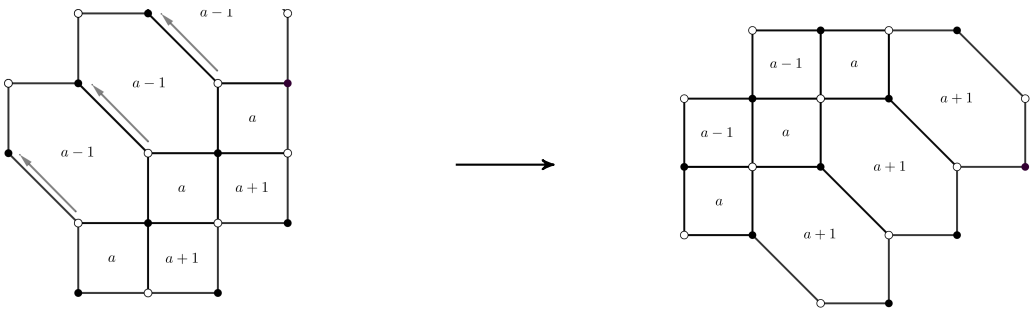

Figure 5.10. Seiberg duality on node (a), whereas node $(a-1)$ has an adjoint field, from the perspective of the dimer. As a result of integration of massive fields, the exagon $(a-1)$ collapses into a square, while the a pair of extra edges transform the square $(a+1)$ into an exagon, generating the adjoint fields.

5.3.1 Unoriented SPP

Let us perform the orientifold projection Ω with four fixed points, see Fig. 5.3b, whose signs are denoted by τ_0 and τ_{00} for the gauge group and the adjoint field, and τ_{12} and τ_{21} for the projected bifundamental fields. The anomaly cancellation condition imposes $\tau_{12} = \tau_{21}$. Since half the number of terms in the supepotential is even, the sign rule requires $\prod \tau = +1$. The superpotential of the unoriented theory reads

$$W^{\Omega}_{\text{SPP}} = -\phi_0 X_{01} X_{10} + X_{12} X_{21} X_{10} X_{01} \ . \tag{5.25}$$

The condition $R(W) = 2$ remains as in Eq. (5.10), while the cancellation of the R-symmetry anomaly gives

$$\begin{aligned} r_{00}\,(N_0 - N_1 + 2\tau_0) &= -\,(N_0 - N_1 - 2\tau_0) \ , \\ r_{00}\,(N_0 - N_1 - 2\tau_{12}) &= -\,(N_0 - N_1 + 2\tau_{12}) \ . \end{aligned} \tag{5.26}$$

At the conformal point of the parent theory, $N_0 = N_1 = N$, the orientifold projection gives $r_{00} = +1$, violating unitarity. On the other hand, imposing $N_1 = N_0 - 2\tau_0 = N_0 + 2\tau_{12}$ we obtain

$$r_{00} = 0 \ , \qquad \tau_0 = -\tau_{12} \ , \tag{5.27}$$

fixing $r_{01} = r_{12} = -1/2$. The superconformal R-charges are already determined, as the only remaining global abelian factors are baryonic and, since $\text{Tr}\, U(1)_B = 0$, they do not mix with the R-symmetry, see Tab. 5.1. Hence, the a-charge at large $N = N_0 \simeq N_1$ reads

$$a^{\Omega}_{\text{SPP}} = \frac{81}{256} N^2 \ . \tag{5.28}$$

	$USp/SO(N_0)$	$SU(N_1)$	$U(1)_R$	$U(1)_{B_1}$	$U(1)_{B_2}$
ϕ_0	$\square\!\!\square/\square\square$	**1**	1	0	0
X_{01}	$\square$	$\overline{\square}$	$\frac{1}{2}$	1	0
X_{10}	$\overline{\square}$	$\square$	$\frac{1}{2}$	-1	0
$X_{12}^{S/A}$	**1**	$\square\square/\square\!\!\square$	$\frac{1}{2}$	0	+1
$X_{21}^{S/A}$	**1**	$\overline{\square\square}/\overline{\square\!\!\square}$	$\frac{1}{2}$	0	-1

Table 5.1. The matter content and relative charges of $(\mathrm{SPP})^{\Omega}$.

The ratio between the a-charge of the parent and of the unoriented theory

$$\frac{a^{\Omega}_{\mathrm{SPP}}}{a_{\mathrm{SPP}}} = \frac{9\sqrt{3}}{32} \simeq 0.4871 \tag{5.29}$$

is less than a half. From a geometrical perspective, the volume of the horizon is less than halved, if compared with the parent one with the same radius

$$\frac{V^{\Omega}_{\mathrm{SPP}}}{V_{\mathrm{SPP}}} = \frac{8\sqrt{3}}{27} \simeq 0.5132\ . \tag{5.30}$$

The third scenario occurs here, where the R-charges after the orientifold projection are different from those of the parent theory already at leading order, in contrast with the first scenario. This can be traced back to the fact that the number of abelian symmetries that mix with the R-symmetry is less than in the parent theory, for the r_{00} being already fixed, which in turn fixes all the r_{ij} before a-maximization. In contrast, in the parent theory the r_{ij} are determined by a-maximization. The same mechanism, the breaking of an abelian symmetry, is discussed in [2]. This is the reason behind the values in Eqs. (5.29) and (5.30): since the R-charges are related to the Reeb vector, the consequence is that the geometry of the horizon is different between the first and the third scenario. One last solution is allowed for the R-charges. Imposing in Eq. (5.26) that $N_0 - N_1 + 2\tau_0 \neq 0$ and $N_0 - N_1 - 2\tau_{12} \neq 0$ and $N_0 - N_1 = p \neq 0$, we have

$$r_{00} = -\frac{p-2\tau_0}{p+2\tau_0} = -\frac{p+2\tau_{12}}{p-2\tau_{12}}\ , \qquad r_{01} = -\frac{2\tau_0}{p+2\tau_0}\ , \qquad r_{12} = -\frac{p}{p+2\tau_0}\ . \tag{5.31}$$

which requires $\tau_0 = -\tau_{12}$. They yields

$$a^{\Omega}_{\mathrm{SPP}} = \frac{27}{8}N^2\frac{p\tau_0}{(p+2\tau_0)^3}\,(p+\tau_0)\ , \tag{5.32}$$

for $\tau_0 = -1$ and $-N_1 < p < 0$, or $\tau_0 = +1$ and $N_0 > p > 0$, considering unitarity and $a^{\Omega} > 0$, $N_0 > 0$, $N_1 > 0$. Note that if $p = 2\tau_0$ we recover the previous case, then this is a more general

solution.
To sum up, for the unoriented SPP the result would seem to naively suggest the existence of a whole family of conformal theories with $\tau_0 = \tau_{00} = -\tau_{12} = -\tau_{21}$ and parametrized by p, the shift between ranks N_0 and N_1, i.e. the number of fractional branes. They would all belong to the third scenario, since a $U(1)$ is anomalous and at the fixed point the R-charges differ from those of the parent already at leading order. The fact that any value of p could in principle yield a conformal point is somewhat surprising, so the existence of this family of solution must be investiged more. We are going to discuss this point further.
We should worry about operators that may become free and decouple before the theory reaches the conformal point and correct the central charge a as in Eq. (2.13). In applying this analysis, we look at several operators potentially dangerous. Operators which contain mesons in the superpotential never become free, however other can be constructed. Since $\tau_0 = \tau_{00}$

$$\begin{aligned}
&\mathcal{O}_{0,j} = \mathrm{Tr}\ \phi_0^j \ , \quad j > 1 \ , \\
&\mathcal{M}_m = (X_{12}X_{21})^m \ , \quad m \geq 1 \ , \\
&\widetilde{\mathcal{M}}_{0,lk} = \phi_0^l \, (X_{01}X_{10})^k \ , \quad l \geq 0 \ , \quad k \geq 1
\end{aligned} \tag{5.33}$$

are allowed and their R-charge reads

$$\begin{aligned}
R_{\mathcal{O}}^{(j)} &= j\frac{4\tau_0}{p+2\tau_0} \ , \\
R_{\mathcal{M}}^{(m)} &= m\frac{4\tau_0}{p+2\tau_0} \ , \\
R_{\widetilde{\mathcal{M}}}^{(lk)} &= \frac{4\tau_0}{p+2\tau_0}(l-k) + 2k \ .
\end{aligned} \tag{5.34}$$

The singlet with $j = 1$ vanishes in the unoriented theory. In the parent theory this parametrizes the movement of fractional branes along a curve of singularity, but this mode is projected out by the orientifold plane since fractional branes are stuck at the orientifold singularity. The configuration will be explicit in the elliptic model (see Sec. 5.5).
Clearly, these operators may decouple depending on the value of p. We stress that each value of p defines an independent theory and we are not describing an RG-flow parametrized by p.[4] Let us focus on the case with $\tau_0 = \tau_{00} = +1$ and $0 < p < N_0$, the opposite choice is similar. The operator $\mathcal{O}_j$ becomes free for

$$j\frac{4}{p+2} \leq \frac{2}{3} \ , \tag{5.35}$$

[4]In principle, one could perform a duality cascade, under which the theory is self-similar and after a number of Seiberg dualitites it goes back to its original structure. This is not possible in this case, as one eventually needs to dualize a gauge group with tensorial matter and the superpotential does not meet the known dualities.

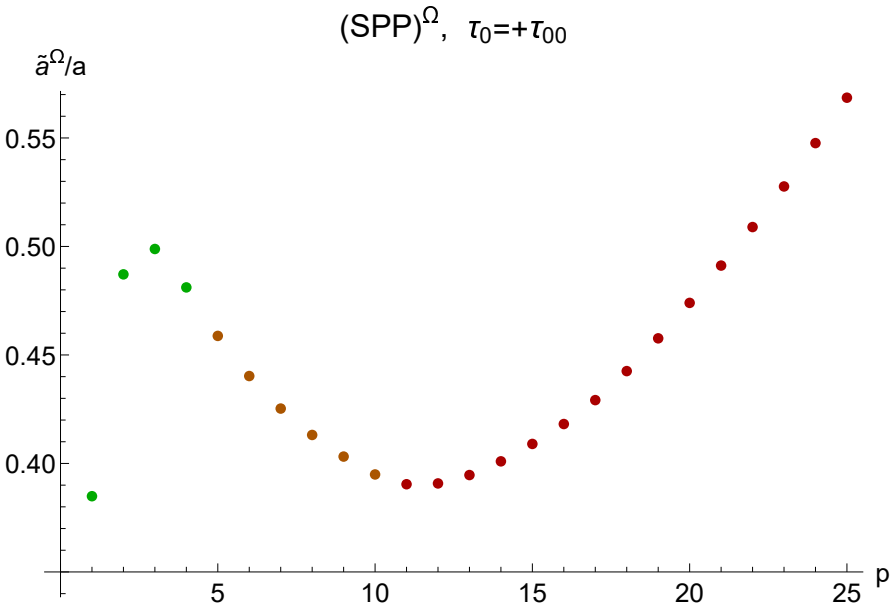

Figure 5.11. The ratio $\widetilde{a}^{\Omega}_{\text{SPP}}/a_{\text{SPP}}$ vs $p = N_0 - N_1$. The green points signal that there are no correction to the central charge, on orange points $(X_{12}X_{21})^m$ becomes free, while on red ones operators Tr ϕ_0^j start to decouple.

so, for all integers $j \leq \bar{j} = (p+2)/6$ an operator decouples and the a-charge gets corrected. For example, Tr ϕ_0^2 decouples for $p = 10$ (at which the correction is zero though), while for $p = 16$ both Tr ϕ_0^2 and Tr ϕ_0^3 decouple. As for $\widetilde{\mathcal{M}}_{0,lk}$ hits $R^{(lk)}_{\widetilde{\mathcal{M}}} = 2/3$ only for $p = 1$ and the correction to the a-charge is zero. On the other hand, $\mathcal{M}_m$ is free for $m \leq (p+2)/6$ and the first correction enters for $p = 4$, where it is zero. In Fig. 5.11 we can see that the corrected ratio $\widetilde{a}^{\Omega}_{\text{SPP}}/a_{\text{SPP}}$. It increases and approaches the value 0.5, beyond which we doubt the existence of the conformal theory at all: it is the $\mathbb{Z}_2$ projection of SPP. From Eq. (2.13), we also note that for $p > 4$ Tr $R \neq 0$ at leading order, due to the correction itself. Hence, beyond this point the holographic duality may not hold or perhaps not in its simple form. The existence of the conformal point can be bound to $p \leq 4$, for which the third scenario always occurs. Moreover, applying the analysis of [118] we find that for $p = 1$ all terms in the superpotential should be removed, posing doubts on the existence of the conformal point. We exclude $p = 1$ from the allowed range.
A hypothetical magnetic theory could confirm the existence of the conformal point and maybe select only one value of p. Unfortunately, for this case there is no known Seiberg duality compatible with the superpotential of the unoriented toric theory. As we shall see, this is not the case when $n > 1$.

5.3.2 Unoriented SPP/$\mathbb{Z}'_2$

Let us now focus on the case with $n = 2$, the first with unitary nodes with no tensorial matter, as can be seen from the quiver in Fig. 5.5b. Depending on the τ's, gauge groups at node zero are orthogonal or symplectic, with a bifundamental hypermultiplet and tensorial matter. The

superpotential reads

$$W^{\Omega}_{\mathrm{SPP}/\mathbb{Z}_2'} = -\phi_0 X_{01} X_{10} + X_{12} X_{21} X_{10} X_{01} - X_{21} X_{12} X_{23} X_{32} + \phi_3 X_{32} X_{23} \ . \tag{5.36}$$

Proceeding as before, we solve the constraints for the R-charges. Along with Eq. (5.10), $r_{00} = r_{33}$ and $2r_{01} = 2r_{23} = -1 - r_{00}$, we have

$$\begin{aligned} r_{00}\,(N_0 - N_1 + 2\tau_{00}) &= -\,(N_0 - N_1 - 2\tau_0)\ , \\ r_{00}\,(N_0 - N_2) &= 2N_1 - N_0 - N_2\ , \\ r_{00}\,(N_3 - N_1) &= 2N_2 - N_3 - N_1\ , \\ r_{00}\,(N_3 - N_2 + 2\tau_{33}) &= -\,(N_3 - N_2 - 2\tau_3)\ . \end{aligned} \tag{5.37}$$

From the projected nodes we may either have $\tau_0 = -\tau_{00}$ and $\tau_3 = -\tau_{33}$ and shift between the first and last pair of ranks determined, or $\tau_0 = \tau_{00}$ and $\tau_3 = \tau_{33}$. We denote them as solution A and B, respectively.

Solution A

	$USp/SO(N_0)$	$SU(N_1)$	$SU(N_2)$	$SO/USp(N_3)$	$U(1)_R$
ϕ_0	$\square\!\square/\begin{smallmatrix}\square\\\square\end{smallmatrix}$	$\mathbf{1}$	$\mathbf{1}$	$\mathbf{1}$	1
X_{01}	$\square$	$\overline{\square}$	$\mathbf{1}$	$\mathbf{1}$	$\frac{1}{2}$
X_{10}	$\overline{\square}$	$\square$	$\mathbf{1}$	$\mathbf{1}$	$\frac{1}{2}$
X_{12}	$\mathbf{1}$	$\square$	$\overline{\square}$	$\mathbf{1}$	$\frac{1}{2}$
X_{21}	$\mathbf{1}$	$\overline{\square}$	$\square$	$\mathbf{1}$	$\frac{1}{2}$
X_{23}	$\mathbf{1}$	$\mathbf{1}$	$\square$	$\overline{\square}$	$\frac{1}{2}$
X_{32}	$\mathbf{1}$	$\mathbf{1}$	$\overline{\square}$	$\square$	$\frac{1}{2}$
ϕ_3	$\mathbf{1}$	$\mathbf{1}$	$\mathbf{1}$	$\begin{smallmatrix}\square\\\square\end{smallmatrix}/\square\!\square$	1

Table 5.2. The matter content and the superconformal R-charges of $(\mathrm{SPP}/\mathbb{Z}_2')^{\Omega}$ solution A.

Consider the case $\tau_0 = -\tau_{00}$ and $\tau_3 = -\tau_{33}$. Denoting rank shifts as $N_0 - N_2 = p$, $N_1 - N_2 = q$ requires that $q = p - 2\tau_0$ and $\tau_0 = -\tau_3$. Then one gets

$$\begin{aligned} N_1 &= N_0 - 2\tau_0\ , \\ N_2 &= N_0 - p\ , \\ N_3 &= N_0 - p - 2\tau_0\ , \end{aligned} \tag{5.38}$$

along with

$$r_{00} = 1 - 4\frac{\tau_0}{p} \ , \qquad r_{01} = -\frac{p - 2\tau_0}{p} \ , \qquad r_{12} = -2\frac{\tau_0}{p} \ . \tag{5.39}$$

Thus, at large N

$$a^{\Omega}_{\text{SPP}/\mathbb{Z}'_2} = \frac{27}{8}N^2 \left(-\frac{\tau_0}{p^3}\right)\left(4 - p^2\right) \tag{5.40}$$

and the ratio w.r.t. the parent reads

$$\frac{a^{\Omega}_{\text{SPP}/\mathbb{Z}'_2}}{a_{\text{SPP}/\mathbb{Z}'_2}} = \frac{3\sqrt{3}}{2}\left(-\frac{\tau_0}{p^3}\right)\left(4 - p^2\right) \ , \tag{5.41}$$

with $\tau_0 = +1$ and $2 < p < N_0 - 2$, or $\tau_0 = -1$ and $2 < -p < N_3 - 2$, from unitarity and positivity of N_a.
Some operators are dangerous, in the sense that may decouple and correct the computation of the central charge a. Since $\tau_0 = -\tau_{00}$ there are no operators of the form Tr ϕ_0^j or Tr ϕ_3^j. However, the following gauge-invariant operators

$$\begin{aligned} &\mathcal{M}_m = (X_{12}X_{21})^m \ , \quad m \geq 1 \ , \\ &\widetilde{\mathcal{M}}_{0,lk} = \phi_0^l \, (X_{01}X_{10})^k \ , \quad l \geq 0 \ , \quad k \geq 1 \\ &\widetilde{\mathcal{M}}_{3,lk} = \phi_3^l \, (X_{32}X_{23})^k \ , \quad l \geq 0 \ , \quad k \geq 1 \end{aligned} \tag{5.42}$$

with R-charges

$$\begin{aligned} R^{(m)}_{\mathcal{M}} &= 2m\frac{p - 2\tau_0}{p} \ , \\ R^{(lk)}_{\widetilde{\mathcal{M}}} &= 2\frac{p - 2\tau_0}{p}(l - k) + 2k \end{aligned} \tag{5.43}$$

may decouple. Operator $\mathcal{M}_m$ becomes free only for $m = 1$ and $p = 3$, where the correction to a vanish. Instead, operators $\widetilde{\mathcal{M}}_{0,lk}$ and $\widetilde{\mathcal{M}}_{3,lk}$ become free for $l = 0$, $k \leq p/6$ and $p \geq 6$ and the a-charge gets corrected for $p > 6$. The final ratio $a^{\Omega}_{\text{SPP}/\mathbb{Z}'_2}/a_{\text{SPP}/\mathbb{Z}'_2}$ is displayed in Fig. 5.12. As before, the existence of the conformal point is bound to $p \leq 6$, where holography still holds and the third scenario occurs.

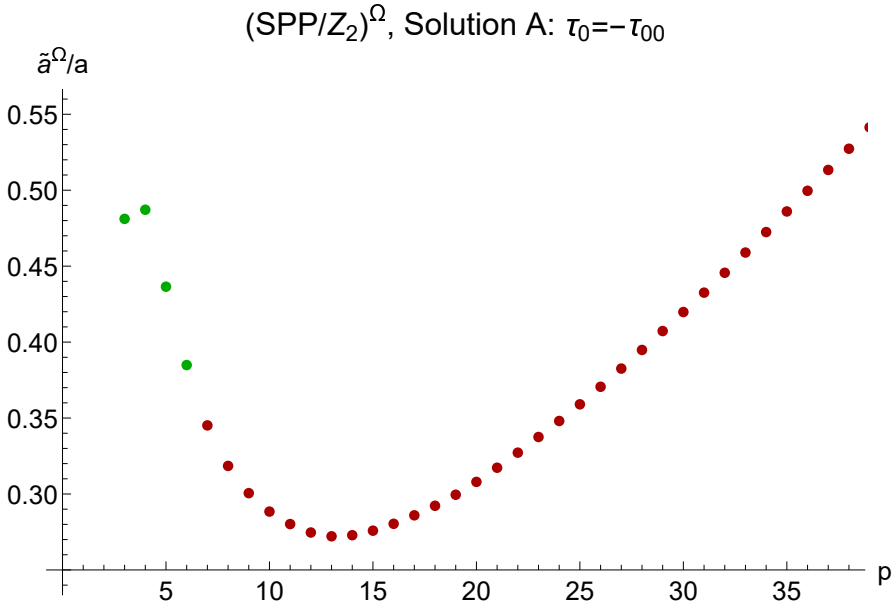

Figure 5.12. The ratio $\tilde{a}^{\Omega}_{\mathrm{SPP}/\mathbb{Z}_2'}/a_{\mathrm{SPP}/\mathbb{Z}_2'}$ vs $p = N_0 - N_2$ in Solution A. The green points signal that there are no correction to the central charge, while on red points operators $\phi_0^l\,(X_{01}X_{10})^k$ and $\phi_3^i\,(X_{32}X_{23})^k$ start to decouple.

Solution B

	$USp/SO(N_0)$	$SU(N_1)$	$SU(N_2)$	$SO/USp(N_3)$	$U(1)_R$
ϕ_0	$\square\!\!\square/\square\square$	**1**	**1**	**1**	1
X_{01}	$\square$	$\overline{\square}$	**1**	**1**	$\frac{1}{2}$
X_{10}	$\overline{\square}$	$\square$	**1**	**1**	$\frac{1}{2}$
X_{12}	**1**	$\square$	$\overline{\square}$	**1**	$\frac{1}{2}$
X_{21}	**1**	$\overline{\square}$	$\square$	**1**	$\frac{1}{2}$
X_{23}	**1**	**1**	$\square$	$\overline{\square}$	$\frac{1}{2}$
X_{32}	**1**	**1**	$\overline{\square}$	$\square$	$\frac{1}{2}$
ϕ_3	**1**	**1**	**1**	$\square\square/\square\!\!\square$	1

Table 5.3. The matter content and the superconformal R-charges of $(\mathrm{SPP}/\mathbb{Z}_2')^{\Omega}$ solution B.

This solution is obtained for $\tau_0 = \tau_{00}$ and $\tau_3 = \tau_{33}$ and $N_0 \neq N_1 - 2\tau_0$, $N_3 \neq N_2 - 2\tau_3$. Denoting

the shifts as $N_0 - N_1 = p$, $N_1 - N_2 = q$, $N_2 - N_3 = s$ leads to $q = 2\tau_0$, $p = s$, $\tau_0 = -\tau_3$ and

$$\begin{aligned} N_1 &= N_0 - p \,, \\ N_2 &= N_0 - p - 2\tau_0 \,, \\ N_3 &= N_0 - 2p - 2\tau_0 \,, \end{aligned} \tag{5.44}$$

along with

$$r_{00} = -\frac{p - 2\tau_0}{p + 2\tau_0} \,, \qquad r_{01} = -2\frac{\tau_0}{p + 2\tau_0} \quad , \qquad r_{12} = -\frac{p}{p + 2\tau_0} \,. \tag{5.45}$$

This family of solutions generalizes the one discussed for SPP and for $p = 2\tau_0$ it gives $r_{00} = 0$, and it will appear again for general $\mathbb{Z}'_n$. In order to impose unitarity, $-1 < r_{00} < 1$ holds for $\tau_0 = +1$ and $0 < p < (N_0 - 2)/2$, or for $\tau_0 = -1$ and $-(N_3 - 2)/2 < p < 0$.
The a-charge and the ratio read

$$\begin{aligned} a^{\Omega}_{\mathrm{SPP}/\mathbb{Z}'_2} &= \frac{27}{4} N^2 \frac{p\tau_0}{(p + 2\tau_0)^3} (p + \tau_0) \,, \\ \frac{a^{\Omega}_{\mathrm{SPP}/\mathbb{Z}'_2}}{a_{\mathrm{SPP}/\mathbb{Z}'_2}} &= \frac{3\sqrt{3}}{(p + 2\tau_0)^3} p\tau_0 (p + \tau_0) \,. \end{aligned} \tag{5.46}$$

In this case operators of the form

$$\begin{aligned} &\mathcal{O}_{0,j} = \mathrm{Tr}\ \phi_0^j \,, && j \geq 1 \,, && \\ &\mathcal{O}_{3,j} = \mathrm{Tr}\ \phi_3^j \,, && j \geq 1 \,, && R^{(j)}_{\mathcal{O}} = j\tfrac{4\tau_0}{p+2\tau_0} \,, \\ &\mathcal{M}_m = (X_{12}X_{21})^m \,, && m \geq 1 \,, && R^{(m)}_{\mathcal{M}} = m\tfrac{4\tau_0}{p+2\tau_0} \,, \\ &\widetilde{\mathcal{M}}_{0,lk} = \phi_0^l \,(X_{01}X_{10})^k \,, && l \geq 0 \,, \quad k \geq 1 \,, && \\ &\widetilde{\mathcal{M}}_{3,lk} = \phi_3^l \,(X_{32}X_{23})^k \,, && l \geq 0 \,, \quad k \geq 1 \,, && R^{(lk)}_{\widetilde{\mathcal{M}}} = \tfrac{4\tau_0}{p+2\tau_0}(l-k) + 2k \,, \end{aligned} \tag{5.47}$$

may decouple and the central charge must be corrected as in Eq. (2.13). The corrections are the same as those discussed in SPP/Ω and the corrected central charge is displayed in Fig. 5.13. As in the Ω projection of SPP and its solution with $r_{00} \neq 0$, for $p > 4$ it turns out that $\mathrm{Tr}\ R \neq 0$ and the conformal theory may exist only for $p \leq 4$, where it realises the third scenario, as can be seen from Fig. 5.13.

Seiberg duality for SPP/$\mathbb{Z}'_2$

The solutions with $r_{00} \neq 0$ discussed in the previous subsections are somewhat difficult to interpret. The central charge a must be corrected by the contribution of those operators which decouple along

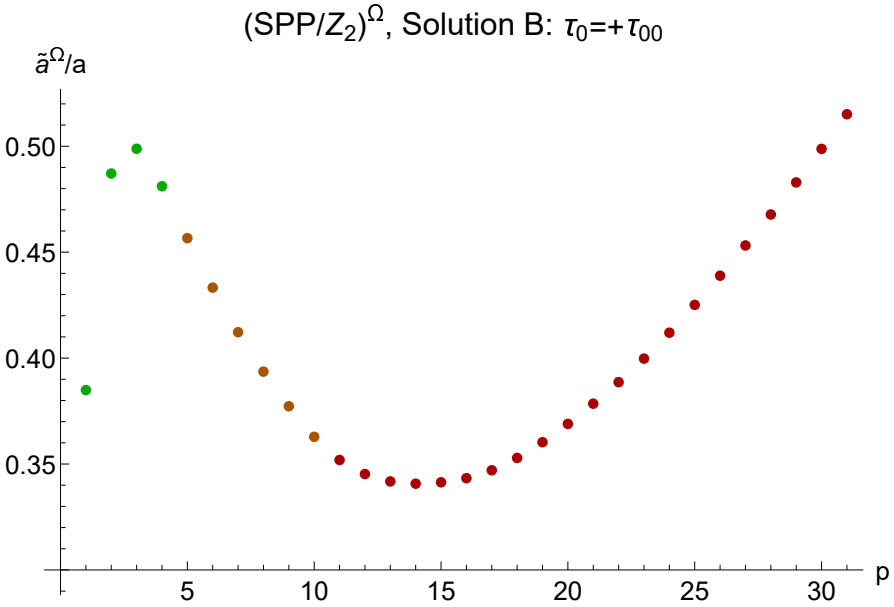

Figure 5.13. The ratio $\tilde{a}^{\Omega}_{\mathrm{SPP}/\mathbb{Z}_2}/a_{\mathrm{SPP}/\mathbb{Z}_2}$ vs $p = N_0 - N_1$ in solution B. The green points signal that there are no correction to the central charge, on orange points $(X_{12}X_{21})^m$ becomes free, while on red points operators Tr ϕ_0^j and Tr ϕ_3^j start to decouple.

the flow towards the IR, where the conformal point in the third scenario stays. A side-effect of these corrections is that Tr $R \neq 0$ at leading order, then once they contribute, the holographic duality may not hold anymore. All one can say is that this reasoning bounds the number of fractional branes p, up to 6 in solution A and up to 4 in solution B (as in the SPP case), for the theory to have a gravity dual. Beyond this limiting value, the ratio between the corrected a-charge and the parent one in no more significative for the existence of the conformal point. As a consequence, the distinction between first and third scenario no longer holds.

It is puzzling that the conformal point exists only for a range of number of fractional branes. Seiberg duality may help in finding a clear evidence for the very existence of the conformal point. From this point of view, we perform Seiberg duality on an SU node in SPP/$\mathbb{Z}'_2$ and look for the conformal point in the magnetic theory, then compare it with the electric theory. The two must be the same.

First, let us focus on the quiver theory in Fig. 5.5b with solutions A for the r-charges, $\tau_0 = -\tau_{00} = -\tau_3 = \tau_{33}$, with ranks given in Eq. (5.38). Performing Seiberg duality on gauge group $SU(N_1)$, the resulting magnetic node has rank

$$\widetilde{N}_1 = N_0 + N_2 - N_1 = N_0 - p + 2\tau_0 \,, \tag{5.48}$$

while mesons and dual quarks are constructed as discussed in Sec. 5.2.1. The final quiver is shown

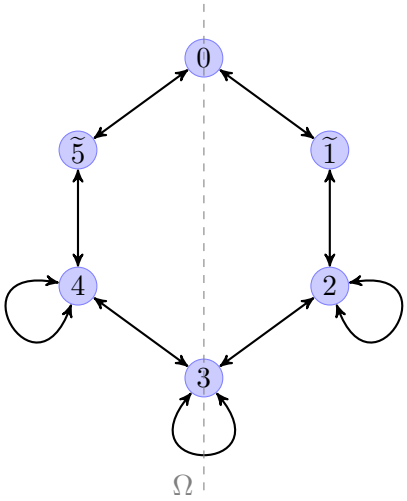

Figure 5.14. The quiver for the orientifold projection of magnetic SPP/$\mathbb{Z}_2'$.

in Fig. 5.14 and the superpotential reads

$$\widetilde{W}^{\Omega}_{\mathrm{SPP}/\mathbb{Z}_2'} = \phi_3 X_{32} X_{23} - \widetilde{X}_{12}\widetilde{X}_{21}\widetilde{X}_{10}\widetilde{X}_{01} + M_2\left(\widetilde{X}_{21}\widetilde{X}_{12} - X_{23}X_{32}\right) . \tag{5.49}$$

The conformal point is given by $r_{22} = 0$ and $p = 4\tau_0$. At these values, none of the gauge invariant operators decouples, neither in the electric nor in the magnetic theory. The a-charge does not change in the magnetic theory, hence, there is only one value for the number of fractional branes so that the conformal point exists and it features the third scenario.
The matter content and superpotential for solution B remains unchanged, while orientifold signs are $\tau_0 = \tau_{00} = -\tau_3 = -\tau_{33}$ and ranks given in Eq. (5.44) and the dual gauge node has rank $\widetilde{N}_1 = N_0 - 2\tau_0$. For the fixed point, it must be $r_{22} = 0$ and $p = 2\tau_0$ and, again, the central charge a gets no correction both in the electric and magnetic theory. We conclude that this is the conformal point, in third scenario, we looked for. We notice that in both cases the fixed point exists only for $r_{00} = 0$.

5.3.3 Unoriented SPP/$\mathbb{Z}_n'$

As we have seen in Sec. 5.1.1, the parent gauge theory SPP/$\mathbb{Z}_n'$ has a recursive structure that allows us to solve the set of equation for the R-charges. The computation for the unoriented theory is similar, with some modifications due to the Ω projection. The $\mathbb{Z}_2$ maps two sides of the quiver and we keep nodes from 0 to $\bar{n}$, the latter being

$$\begin{aligned} \bar{n} &= \frac{3}{2}n \quad n \text{ even} , \\ \bar{n} &= \frac{3n-1}{2} \quad n \text{ odd} . \end{aligned} \tag{5.50}$$

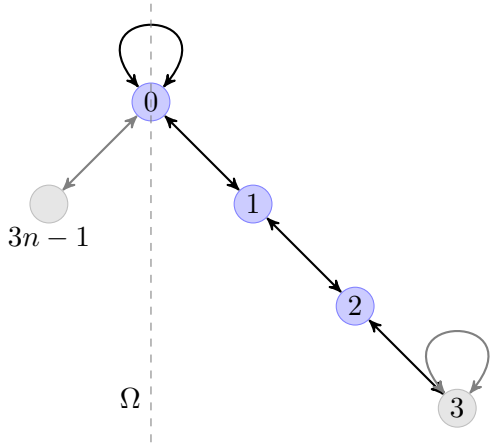

Figure 5.15. Blue nodes form the recursive structure of the quiver SPP/$\mathbb{Z}'_n$.

Half the superpotential is projected out and it reads

$$\begin{aligned} W^{\Omega}_{SPP/\mathbb{Z}'_n} = &-\phi_0 X_{01} X_{10} + \sum_{i=1}^{\lfloor \frac{n}{2} \rfloor} \phi_{3i} \left(X_{3i,\,3i-1} X_{3i-1,\,3i} - X_{3i,\,3i+1} X_{3i+1,\,3i} \right) \\ &+ \sum_{i=0}^{\bar{n}-1} \left(X_{3i+1,\,3i} X_{3i,\,3i+1} X_{3i+1,\,3i+2} X_{3i+2,\,3i+1} \right. \\ &\left. - X_{3i+2,\,3i+1} X_{3i+1,\,3i+2} X_{3i+2,\,3i+3} X_{3i+3,\,3i+2} \right) \\ &+ \begin{cases} \phi_{\bar{n}} X_{\bar{n},\bar{n}-1} X_{\bar{n}-1,\bar{n}} & , \quad n \text{ even} \\ X^{S/A}_{\bar{n},\bar{n}+1} X^{S/A}_{\bar{n}+1,\bar{n}} X_{\bar{n},\bar{n}-1} X_{\bar{n}-1,\bar{n}} & , \quad n \text{ odd} \end{cases} \end{aligned} \tag{5.51}$$

The gauge group at node 0 and its adjoint field are projected by the orientifold involution, with signs τ_0 and τ_{00}, respectively. Depending on the parity of n, the other projected elements are the gauge group at node $\bar{n}$ and its adjoint if n is even, with signs $\tau_{\bar{n}}$ and $\tau_{\bar{n},\bar{n}}$. On the other hand, if n is odd, fields $X_{\bar{n},\bar{n}+1}$ and $X_{\bar{n}+1,\bar{n}}$ are projected onto symmetric or anti-symmetric representations by $\tau_{\bar{n},\bar{n}+1}$ and $\tau_{\bar{n}+1,\bar{n}}$. In this case, the anomaly-cancellation condition is not trivial and requires that $\tau_{\bar{n},\bar{n}+1} = \tau_{\bar{n}+1,\bar{n}}$. From the sign rule, this means that $\tau_0 = \tau_{00}$.
Let us look at the constraints on the R-charges. Eq. (5.10) still holds and recursion yields

$$\begin{aligned} &r_{00} = r_{3i,3i} \ , \\ &2r_{3i,3i+1} + r_{00} = -1 \ , \\ &2r_{3i+1,3i+2} - r_{00} = -1 \ . \end{aligned} \tag{5.52}$$

Using Eq. (5.52), anomaly-free R-symmetry gives

$$r_{00}\left(N_0 - N_1 + 2\tau_{00}\right) = -\left(N_0 - N_1 - 2\tau_0\right) \ , \tag{5.53}$$

$$r_{00}\left(2N_{3i} - N_{3i-1} - N_{3i+1}\right) = -\left(2N_{3i} - N_{3i-1} - N_{3i+1}\right) \ , \tag{5.54}$$

$$r_{00}\left(N_{3i} - N_{3i+2}\right) = 2N_{3i+1} - N_{3i} - N_{3i+2} \ , \tag{5.55}$$

$$r_{00}\left(N_{3i+3} - N_{3i+1}\right) = 2N_{3i+2} - N_{3i+3} - N_{3i+1} \ , \tag{5.56}$$

$$r_{00}\left(N_{\bar{n}} - N_{\bar{n}-1} + 2\tau_{\bar{n}\bar{n}}\right) = -\left(N_{\bar{n}} - N_{\bar{n}-1} - 2\tau_{\bar{n}}\right) \ , \tag{5.57}$$

$$r_{00}\left(N_{\bar{n}} - N_{\bar{n}-1} + 2\tau_{\bar{n},\bar{n}+1}\right) = -\left(N_{\bar{n}} - N_{\bar{n}-1} - 2\tau_{\bar{n},\bar{n}+1}\right) \ . \tag{5.58}$$

If we impose that $N_i = N$ for all i, we obtain

$$r_{00} = \frac{\tau_0}{\tau_{00}} = \pm 1 \ , \tag{5.59}$$

but both choices of signs would violate unitarity. Thus, the conformal point of the parent theory is excluded. Allowing for different ranks gives, from the second equation,

$$r_{00} = -1 \ , \quad \text{if} \quad 2N_{\bar{n}} - N_{\bar{n}-1} + N_{\bar{n}+1} \neq 0 \tag{5.60}$$

and again $R_{00} = 0$, violating unitarity. On the other hand, if we impose the right hand sides to vanish, we get

$$r_{00} = 0 \ , \tag{5.61}$$

$$N_i = N_0 - i\, 2\tau_0 \ , \quad 0 \leq i \leq \bar{n} \ ,$$

$$\tau_0 = -\tau_{\bar{n}} \ , \quad n \text{ even} \ ,$$

$$\tau_0 = -\tau_{\bar{n},\bar{n}+1} \ , \quad n \text{ odd} \ . \tag{5.62}$$

Note that the sign rule restricts the possible choices for the τ signs, such that only $(\tau_0, \tau_{00}, \tau_{\bar{n}}, \tau_{\bar{n},\bar{n}}) = (\pm, \pm, \mp, \mp)$ are allowed, both for n even and, *mutatis mutandis*, for n odd. Before the orientifold projection there are $3n$ nodes, while all R-charges can be expressed in terms of one of them, say r_{01}, due to the recursive structure. In case of n even (the odd case is similar), after the $\mathbb{Z}_2$ involution there are 2 projected nodes and $3n/2 - 1$ not projected. The condition $r_{00} = 0$ ensures that $r_{01} = r_{12} = -1/2$, then there are $3n$ fields carrying r-charge $(-1/2)$. We obtain, at large N,

$$a^{\Omega}_{\mathrm{SPP}/\mathbb{Z}'_n} = \frac{81}{256} n N^2 \ , \tag{5.63}$$

which holds also for n odd. The volume of the horizon is

$$V^{\Omega}_{\mathrm{SPP}/\mathbb{Z}'_n} = \frac{\pi}{n}\frac{64}{81} \ . \tag{5.64}$$

The ratio with the a-charge at the conformal point before the orientifold projection is

$$\frac{a^{\Omega}_{\mathrm{SPP}/\mathbb{Z}'_n}}{a_{\mathrm{SPP}/\mathbb{Z}'_n}} = \frac{9\sqrt{3}}{32} \simeq 0.4871 \ . \tag{5.65}$$

This solution exists for all non-chiral orbifold $\mathbb{Z}'_n$ with $n \geq 1$, where for $n = 1$ and $n = 2$ it is part of the more general family of solution we found. Note that a solution with $\tau_0 = -\tau_{00}$ is allowed only for $n = 2$, because for $n > 2$ nodes with adjoint fields prevent the solution to exist.

5.3.4 Seiberg duality for Unoriented SPP/$\mathbb{Z}'_n$

The a-maximization procedure for unoriented SPP/$\mathbb{Z}'_n$ shows that there is a conformal point for $r_{00} = 0$. For this value of the R-charges, none of the gauge-invariant operators decouples. Then, the conformal point is determined without any ambiguities in the electric theory. As a further check, we study the dual magnetic theory and look for the conformal point. Due to the recursive structure, we have two options: first, for $n > 1$, we can dualize only the first unitary gauge group and compute the maximal central charge a. Second, we can dualize the first node of each fundamental structure, along all the quiver for even n or all but the last unitary group for odd n. This is because the last unitary group has tensorial matter and we do not know how Seiberg duality works in this case with the toric superpotential, the same problem as in SPP. However, in this second method we just obtain the first one recursively repeated. Note that for all dualized node the rank remains the same, as

$$\widetilde{N}_i = N_{i-1} + N_{i+1} - N_i = N_i \ , \tag{5.66}$$

where we have used Eq.(5.61).
Then, proceeding as in the first case, the resulting gauge groups, matter and superpotential is the same as for the magnetic SPP/$\mathbb{Z}'_2$, with the remaining quiver and superpotential unchanged:

$$\widetilde{W}^{\Omega}_{\mathrm{SPP}/\mathbb{Z}'_n} = M_2\left(\widetilde{X}_{21}\widetilde{X}_{12} - X_{23}X_{32}\right) - \widetilde{X}_{12}\widetilde{X}_{21}\widetilde{X}_{10}\widetilde{X}_{01} + \phi_3\left(X_{32}X_{23} - X_{34}X_{43}\right) + \dots \ . \tag{5.67}$$

Solving the constraints for the R-charges, we find that for those bifudamental fields transforming under gauge groups which have also an adjoint field

$$r_{i,\,i+1} + r_{i+1,\,i} = -1 - r_{22} \ , \tag{5.68}$$

for example $r_{12}+r_{21}=-1-r_{22}$, since in the magnetic theory the second node has an adjoint. For the adjoints along the quiver $r_{i,i}=r_{22}$. On the other hand, for those bifundamental transforming under gauge groups which do not have an adjoint

$$r_{i,\,i+1}+r_{i+1,\,i}=-1+r_{22}\ , \tag{5.69}$$

for example $r_{01}+r_{10}=-1+r_{22}$ in the magnetic theory. For the R-symmetry to be anomaly-free, the only solution is $r_{22}=0$, as for the electric theory. The central charge a gets no correction, since no operators decouple. We conclude that the conformal point of $\mathrm{SPP}/\mathbb{Z}'_n$ is the one with $r_{22}=0$, $\tau_0=\tau_{00}=-\tau_3=-\tau_{33}$ and central charge, in the third scenario,

$$\begin{aligned} a^{\Omega}_{\mathrm{SPP}/\mathbb{Z}'_n} &= \frac{81}{256}nN^2\ , \\ \frac{a^{\Omega}_{\mathrm{SPP}/\mathbb{Z}'_n}}{a_{\mathrm{SPP}/\mathbb{Z}'_n}} &= \frac{9\sqrt{3}}{32}\simeq 0.4871\ , \end{aligned} \tag{5.70}$$

as for the electric theory.

5.4 Orientifold projection of $\mathbb{C}^3/\mathbb{Z}'_{3n}$ and deformations

All parent theories we have been studying in this chapter can be obtained from $\mathbb{C}^3/\mathbb{Z}'_{3n}$ by mass deformation. As we are interested in the conformal point after the orientifold projection and to compare it with the parent one, we should analyze the orientifold of $\mathbb{C}^3/\mathbb{Z}'_{3n}$ to get insights on the RG flow to the unoriented $(\mathrm{SPP}/\mathbb{Z}'_n)^{\Omega}$ and the unoriented $\left(L^{k,n-k,k}\right)^{\Omega}$. The strategy for the computation of the fixed point follows closely the one adopted in the previous sections. The only difference is that in this case adjoint fields are present at all nodes and the superpotential has only cubic interactions. Then one finds

$$r_{00}=r_{ii}\ ,\qquad 2r_{01}=2r_{i,i+1}=-1-r_{00}\ ,\qquad \forall i\ . \tag{5.71}$$

For the parent theory, the constraints on the R-charges give $N_i=N$ for all i and

$$a_{\mathbb{C}^3/\mathbb{Z}'_{3n}}=\frac{3}{4}nN^2\ . \tag{5.72}$$

The orientifold projection we want to study is given by four fixed points, but their signs depend on n being even or odd. If n is even $\prod\tau=(-1)^{N_W/2}=+1$, whereas if n is odd $\prod\tau=-1$. Let us first focus on the case with n odd. The anomaly cancellation condition imposes $\tau_{\bar{n},\bar{n}+1}=\tau_{\bar{n}+1,\bar{n}}$, where $\bar{n}=(3n-1)/2$ is the last node in the orientifolded quiver. Then, it follows that $\tau_0=-\tau_{00}$.

One finds a solution for the R-charges at $N_i = N_0 - i\,2\tau_0$, $0 \leq i \leq \bar{n}$, $\tau_0 = -\tau_{\bar{n},\bar{n}+1}$, with

$$\begin{aligned} r_{00} &= r_{01} = -\frac{1}{3}\,, \\ a^{\Omega}_{\mathbb{C}^3/\mathbb{Z}'_{3n}} &= \frac{3}{8} n N^2\,, \end{aligned} \tag{5.73}$$

so the theory belongs to the first scenario.
We turn to n even, in which case the last node $\bar{n} = 3n/2$ is projected by the orientifold plane. There is no condition for anomaly cancellation, thus two distinct choices are allowed: solution A with $\tau_0 = -\tau_{00}$ and solution B with $\tau_0 = \tau_{00}$.[5] For solution A, one finds that $N_i = N_0 - i\,2\tau_0$, $0 \leq i \leq \bar{n}$, $\tau_0 = \tau_{\bar{n}}$ and the same values of Eq. (5.73), so again the theory realises the first scenario. On the other hand, for solution B one gets $N_i = N_0 - i\,p$, $0 \leq i \leq \bar{n}$, $\tau_0 = -\tau_{\bar{n}}$, $p\tau_0 > 0$ and

$$\begin{aligned} a^{\Omega}_{\mathbb{C}^3/\mathbb{Z}'_{3n}} &= \frac{81}{16} n N^2 \frac{p^2\tau_0}{(p+2\tau_0)^3}\,, \\ \left(\frac{a^{\Omega}}{a}\right)_{n\ \text{even}} &= \frac{27}{4} \frac{p^2\tau_0}{(p+2\tau_0)^3}\,, \end{aligned} \tag{5.74}$$

which is always less than $1/2$, hence the theory belongs to the third scenario. For some values of p there are gauge-invariant operators that decouple before reaching the conformal point. In this case, they are

$$\begin{aligned} &\mathcal{O}_{i,j} = \text{Tr}\ \phi_i^j\,, \qquad j > 1\,, \\ &\widetilde{\mathcal{M}}_{i,lk} = \phi_i^l \left(X_{i,i+1} X_{i+1,i}\right)^k\,, \qquad l \geq 0\,, k \geq 1\,, \end{aligned} \tag{5.75}$$

whose R-charges read

$$\begin{aligned} R^{(j)}_{\mathcal{O}} &= j \frac{4\tau_0}{p+2\tau_0}\,, \\ R^{(lk)}_{\widetilde{\mathcal{M}}} &= \frac{4\tau_0}{p+2\tau_0}(l-k) + 2k\,. \end{aligned} \tag{5.76}$$

While the second operator hits the unitary bound only for $p = 1$, $l = 0$ and $k = 1$ with vanishing correction to the central charge, operators $\mathcal{O}_{i,j}$ start to decouple at $p = 10$. The corrected central charge is shown in Fig. 5.16. Interestingly, at $p = 2\tau_0$, none of the gauge-invariant operators decouple and the central charge a^{Ω} results to be equal to that of SPP$/\mathbb{Z}'_n$, n even. Moreover, the pattern of mass deformation needed to flow from $\mathbb{C}^3/\mathbb{Z}'_{3n}$ to SPP$/\mathbb{Z}'_n$ enjoys the $\mathbb{Z}'_2$ required for the orientifold projection, so this flow is preserved under the orientifold involution. That is not the case for the Seiberg dual phases. In fact, the phases that are not $\mathbb{Z}_2$ symmetric are projected out

[5] Note that the same choices are allowed for $(\text{SPP}/\mathbb{Z}'_2)^{\Omega}$.

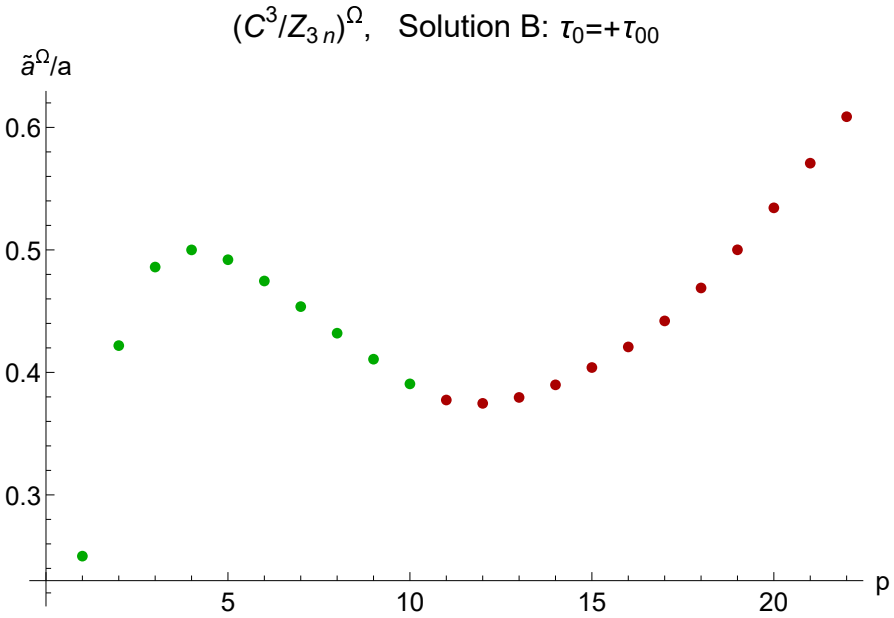

Figure 5.16. The corrected central charge a for the unoriented $\mathbb{C}^3/\mathbb{Z}'_{12}$ solution B, where operators Tr ϕ_i^j start to decouple at $p = 10$.

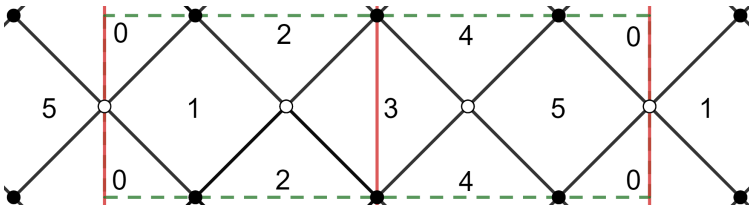

Figure 5.17. The brane tiling for $L^{3,3,3}$, where fixed lines represent the orientifold projection.

by the orientifold.

The deformation where the highest number of pairs of adjoints become massive allow for the orientifold involution, so the class of theories $\left(L^{\frac{3n}{2},\frac{3n}{2},\frac{3n}{2}}\right)$, $\left(L^{\frac{3n-1}{2},\frac{3n+1}{2},\frac{3n-1}{2}}\right)$ can be reached in presence of orientifold planes. Their difference in the toric diagrams is crucial, since for n even we can perform the orientifold projection we are interested in only with fixed lines[6]. See Fig. 5.17 for the brane tiling of $n = 2$, namely $L^{3,3,3}$. On the contrary, for n odd fixed lines are not allowed, as can be seen from the toric diagram. An example of such a case on the brane tiling is $n = 1$, namely SPP, in Fig. 5.3b.

Let us find and compare the conformal point both for the parent and the unoriented theories. Consider first the case with n even, where all adjoints have been integrated out. The constraints

[6]The related brane tiling is made only of squares and a fixed point can not lie on a square, because it must map nodes with different colors.

for the R-charges [117] read

$$\begin{aligned} r_{i,\,i+1} &= -\frac{1}{2}\,, \\ N_i &= N\,, \quad i = 0,\,\ldots,\,n-1\,, \end{aligned} \tag{5.77}$$

and the central charge a is

$$a_{n\ \text{even}} = \frac{81}{128} n N^2\,. \tag{5.78}$$

Performing the orientifold projection, with fixed lines, we find $N_i = N_0 - i\,2\tau_0$, $0 \leq i \leq \bar{n}$, $\tau_0 = -\tau_3$, where τ_0 and τ_3 are the sign of the two fixed lines. At large N, the a-charge reads

$$a^{\Omega}_{n\ \text{even}} = \frac{81}{256} n N^2\,. \tag{5.79}$$

Clearly, for n even the theory realizes the first scenario, since $a^{\Omega}/a = 0.5$ and the R-charges are the same both for parent and unoriented ones, at leading order.

	$USp/SO(N_0)$	$SU(N_1)$	$SU(N_2)$	$SO/USp(N_3)$	$U(1)_R$
X_{01}	$\square$	$\overline{\square}$	$\mathbf{1}$	$\mathbf{1}$	$\frac{1}{2}$
X_{10}	$\overline{\square}$	$\square$	$\mathbf{1}$	$\mathbf{1}$	$\frac{1}{2}$
X_{12}	$\mathbf{1}$	$\square$	$\overline{\square}$	$\mathbf{1}$	$\frac{1}{2}$
X_{21}	$\mathbf{1}$	$\overline{\square}$	$\square$	$\mathbf{1}$	$\frac{1}{2}$
X_{23}	$\mathbf{1}$	$\mathbf{1}$	$\square$	$\overline{\square}$	$\frac{1}{2}$
X_{32}	$\mathbf{1}$	$\mathbf{1}$	$\overline{\square}$	$\square$	$\frac{1}{2}$

Table 5.4. The matter content and the superconformal R-charges of $(L^{3,3,3})^{\Omega}$, dual to $(\text{SPP}/\mathbb{Z}'_2)^{\Omega}$.

However, for $\mathbb{C}^3/\mathbb{Z}'_{3n}$ with n odd, after mass deformation the presence of the adjoint field ϕ_0 in the parent theory gives [117]

$$\begin{aligned} 2r_{2i,\,2i+1} &= -1 - r_{00}\,, \\ 2r_{2i+1,\,2i+2} &= -1 + r_{00}\,, \\ N_i &= N \quad, \quad i = 0, \ldots, n-1\,. \end{aligned} \tag{5.80}$$

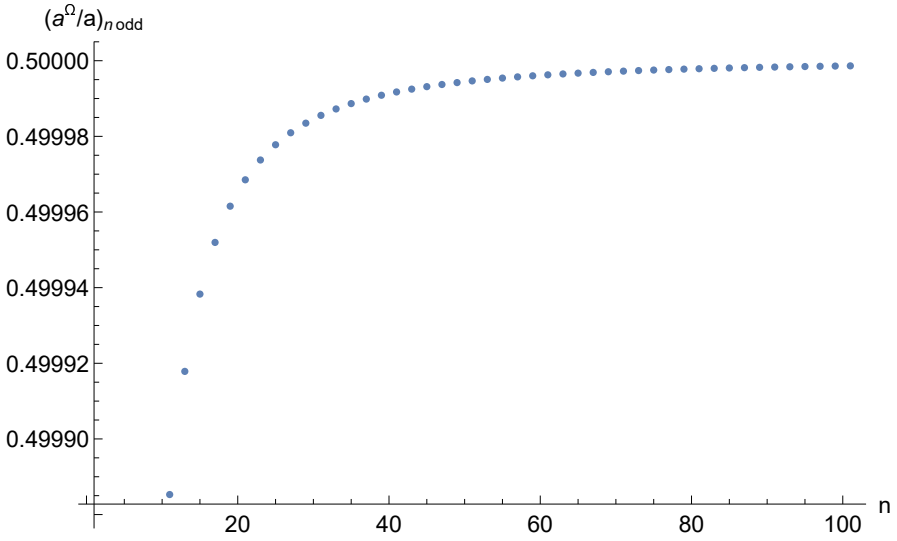

Figure 5.18. The ratio $\left(\frac{a^\Omega}{a}\right)$ for n odd, which asymptotically approaches 0.5 .

Maximization of the central charge yields

$$r_{00} = n - \sqrt{\frac{1+3n^2}{3}}\ ,$$
$$a_{n\ \text{odd}} = \frac{9}{64}\left[3n\left(1-n^2\right) + \left(1+3n^2\right)\sqrt{\frac{1+3n^2}{3}}\right]\ . \tag{5.81}$$

For the orientifold projection, $N_i = N_0 - i\,2\tau_0$, $0 \leq i \leq \bar{n}$, $\tau_0 = \tau_{00} = -\tau_{\bar{n},\bar{n}+1} = -\tau_{\bar{n}+1,\bar{n}}$. Since it is required that $r_{00} = 0$, the R-charges and the central charge a are the same of n even in Eq. (5.79). The ratio between the central charges reads

$$\left(\frac{a^\Omega}{a}\right)_{n\ \text{odd}} = \frac{9}{4}n\left[3n\left(1-n^2\right) + \left(1+3n^2\right)\sqrt{\frac{1+3n^2}{3}}\right]^{-1}\ , \tag{5.82}$$

which asymptotically tends to 0.5, as shown in Fig. 5.18. This case belongs to the third scenario. Hence, for the unoriented case there is no distinction between n even or odd and both show the same central charge a of the unoriented SPP/$\mathbb{Z}'_n$. But, for n odd $L^{\frac{3n-1}{2},\frac{3n+1}{2},\frac{3n-1}{2}}$ features the third scenario and the orientifold projection is performed with fixed points. For n even $L^{\frac{3n}{2},\frac{3n}{2},\frac{3n}{2}}$ features the first scenario and its orientifold projection is performed with fixed lines. In $L^{\frac{3n}{2},\frac{3n}{2},\frac{3n}{2}}$ the fact that fixed lines are needed for the orientifold projection is crucial: fixed lines breaks a $U(1)$ mesonic symmetry, part of the toric $U(1)^2 \times U(1)_R$. On the contrary, the orientifold projection with fixed points does not break toricity, but at the conformal point $r_{00} = 0$ and, as a consequence, $r_{01} = r_{122} = -1/2$. Thus, the number of nodes and flavour symmetries matches, and 't Hooft anomalies do as well.

Figure 5.19. Two dual theories: on the left, SPP$/\mathbb{Z}'_2$ with fixed points and, on the right, $L^{3,3,3}$ with fixed lines.

The superpotential and the matter content are however different and equivalence of the superconformal index must be checked. Contributions to the index come from matter fields X_{ij} and vector multiplets V_i as[7]

$$\begin{aligned} i_X(t,s) &= \sum \frac{t^{R_{ij}}\chi_{X_{ij}} - t^{2-R_{ij}}\chi_{\overline{X}_{ij}}}{(1-ts)\,(1-ts^{-1})}\,, \\ i_V(t,s) &= \sum_{i=0}^{3n-1} \frac{\left[2t^2 - t\,(s+s^{-1})\right]}{(1-ts)\,(1-ts^{-1})}\chi_{\mathrm{adj}_i}\,, \end{aligned} \tag{5.83}$$

where the first sum runs over all matter fields, $\chi_{X_{ij}}$, $\chi_{\overline{X}_{ij}}$ are the characters of the representation of X_{ij} and its conjugate, t and s are the fugacities for R-charge and (twice the) spin, respectively. When matter fields ϕ_i are present, either in the adjoint or in the anti/symmetric representation, in the unoriented models $R_{ii} = 1$ at the conformal fixed point and their contributions to the superconformal index vanish. The remaining contributions are equal for unoriented model with the same number of gauge groups.

Hence, the central charge a^Ω, 't Hooft anomalies and the superconformal index of $(SPP/\mathbb{Z}'_n)^\Omega$ match that of $\left(L^{\frac{3n}{2},\frac{3n}{2},\frac{3n}{2}}\right)^\Omega$ and of $(\mathbb{C}^3/\mathbb{Z}'_{3n})^\Omega$ with $p = 2\tau_0$ for n even, while for n odd the same quantities match between $(SPP/\mathbb{Z}'_n)^\Omega$ and $\left(L^{\frac{3n-1}{2},\frac{3n+1}{2},\frac{3n-1}{2}}\right)^\Omega$. We want to stress that, for n even, the former theory is an orientifold with fixed points in the third scenario, while the latter is an orientifold with fixed lines in the first scenario, as shown in Fig. 5.19. The reader is invited to go back to Fig. 5.1, where the full web of relations that we find is summarized.

[7]Recall that $R_{ij} = r_{ij} + 1$ in our notation.

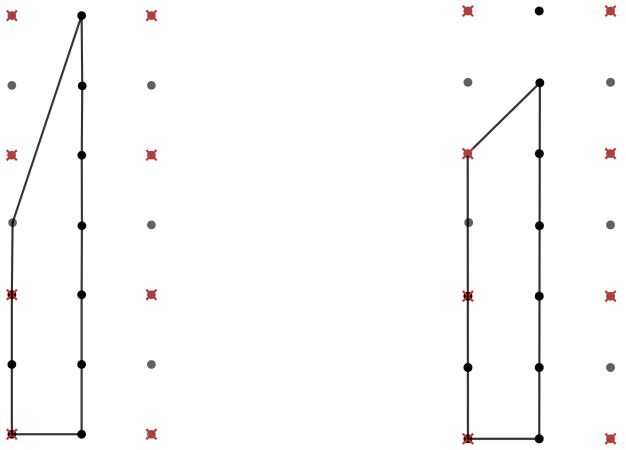

Figure 5.20. Two dual theories: on the left, SPP/$\mathbb{Z}_3'$ and, on the right, $L^{4,5,4}$, both with fixed points.

5.5 Elliptic models

The models described above arise as the supersymmetric gauge field theory living on the world-volume (WV) of D3-branes at a toric CY singularity. We mentioned that, after two T-dualities, one may recover a system of NS5-branes and D5-branes wrapped along a torus and generating the brane tiling. Both descriptions are defined in type IIB string theory. However, performing one T-duality one can construct another useful description of the brane system in type IIA, as D4-branes suspended between NS5 branes. In particular, the D4-branes are wrapped along a compact direction, say x^6, while NS5s can extend along directions x^4, x^5 or x^8, x^9. In the former case they are called simply NS5, in the latter NS5′. Both types split the WV of D4-branes. See [107] for the construction of such theories. The configuration is summarized in Tab. 5.5, where also O6-planes are included, yielding the Ω projection.

	0 1 2 3	4	5	6	7	8	9
D4	– – – –			–			
NS5	– – – –	–	–				
NS5′	– – – –					–	–
O6$^{\pm}$	– – – –				–	–	–

Table 5.5. The T-dual picture with D4-branes, NS5 and NS5′-branes. The direction x^6 is compact.

A simple example that can be obtained from this configuration is the SPP, where two NS and one NS′ 5-branes, located at different positions on x^6, divide the WV of D4-branes into three stacks, which we label by 0,1 and 2, see Fig. 5.21. Bifundamental fields X_{01}, X_{01}, X_{12}, X_{12} and X_{20}, X_{02} arise at the intersections between D4s and a 5-brane. The stack denoted by 0 is suspended between two parallel NS5 branes and D4-branes can be moved along them. This generates an adjoint field $X_{00} = \phi_0$, which completes an $\mathcal{N} = 2$ vector multiplet. In fact, locally the physics resembles

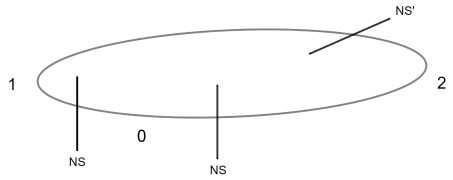

Figure 5.21. The brane system in type IIA which corresponds to the SPP singularity. The circular direction is x^6.

$\mathcal{N} = 2$. D4-branes between two orthogonal 5-branes generate a quartic superpotential term of the form $\pm X_{ij}X_{ji}X_{ij'}X_{j'i}$, taken with positive sign if an NS5 lies at the left of the D4. When D4s are suspended between two parallel 5-branes, a cubic term as $\phi_i \left(X_{ij}X_{ji} - X_{ij'}X_{j'i}\right)$ is generated.
The geometry of the singularity can be described in $\mathbb{C}^4$ as the locus

$$xy = zw^2 \ . \tag{5.84}$$

This construction can be generalized to the case of r NS5 and s NS5$'$, whose geometry reads

$$xy = z^s w^r \ . \tag{5.85}$$

Adjoint fields arise between parallel 5-branes of the same type, but a relative rotation corresponds to giving them a mass, and the effective field theory is obtained below the mass scale. Thus, we can start with a system of $3n$ NS5s, corresponding to $\mathbb{C}^3/\mathbb{Z}'_{3n}$, and rotate the NS5 in an alternating scheme. If $3n$ is even, we can give mass to all the adjoints fields and integrate them out, whereas in case of $3n$ odd two 5-branes remain always parallel. This is exactly the process we have described in the previous section, and we end up with $L^{\frac{3n}{2},\frac{3n}{2},\frac{3n}{2}}$ or $L^{\frac{3n-1}{2},\frac{3n+1}{2},\frac{3n-1}{2}}$, see for example $L^{3,3,3}$ in Fig. 5.22.
When a pair of O6$^{\pm}$ planes is present in the system, it induces a $\mathbb{Z}_2$ indentification among 5-branes and stacks of D4. For n odd, one of the orientifold planes lies in correspondence of a 5-brane which separates a stack of D4 labelled by i and another one labelled by j. In this case, fields X_{ij}, X_{ji} are projected onto symmetric or antisymmetric representations, both in the same one in case of an NS5, in opposite ones for an NS5$'$[8]. The other O6$^{\pm}$ lies on a stack of D4, projecting the gauge group onto SO/Sp and the adjoint field onto a symmetric or antisymmetric representation. This happens also for n even, where both orientifold planes act in this way. Note that the mode of fractional branes along parallel 5-branes is projected out, since the D4s are stuck at the orientifold singularity: they can not be moved along x^4, x^5 since the orientifold plane does not wrap these directions.
In these elliptic models, Seiberg duality is described as the reordering of the 5-branes [107, 119]. Consider, for example, the situation in which node $(a-1)$ has an adjoint and we want to dualize

[8] This is because the NS5$'$ divide the O6 into two regions. Crossing the 5-branes, the RR-charge changes sign.

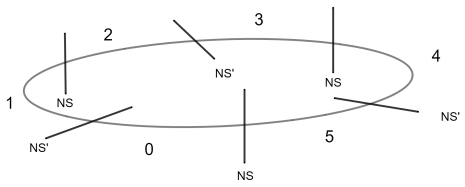

Figure 5.22. The brane system in type IIA which corresponds to the $L^{3,3,3}$ singularity. The circular direction is x^6.

node (a). As described in Sec. 5.2.1 and Figs. 5.9-5.10 the adjoint moves from node $(a-1)$ to $(a+1)$, while the rest of the quiver remains untouched. Let us look at the process in the ellipctic model, where the same configuration corresponds to a stack of D4 labelled by $(a-1)$ delimited by two parallel 5-branes, say two NS5. The stack (a) is delimited then by an NS5 and an NS5$'$, and finally $(a+1)$ by an NS5$'$ and an NS5, in this order. Seiberg duality on (a) means that one exchanges the 5-branes at its ends, so no adjoint field is generated. On the other hand, the 5-branes delimiting $(a-1)$ are now orthogonal, whereas for $(a+1)$ the 5-branes are parallel, explaining the presence of the adjoint field in the magnetic theory.

This construction explains why Seiberg duality picks the conformal point of $(\mathrm{SPP}/\mathbb{Z}_2')^\Omega$ at $p = 4\tau_0$ for solution A ($\tau_0 = -\tau_{00}$) and at $p = 2\tau_0$ for solution B ($\tau_0 = +\tau_{00}$). In fact, moving the NS5 towards the NS5$'$ and eventually crossing it, results in the dual configuration where the number of D4 does not change [107, 119], since in the system no D6 are present[9]. For the field theory associated to $(\mathrm{SPP}/\mathbb{Z}_2')^\Omega$, this means that dualizing either node 1 or 2 yields $N_1 = \widetilde{N}_1$ or $N_2 = \widetilde{N}_2$, which is true only for $p = 4\tau_0$ in solution A (see Eq. (5.38)) and $p = 2\tau_0$ in solution B (see Eq. (5.44)). The same mechanism of reordering of 5-branes occurs in dualizing a gauge node in $(\mathrm{SPP}/\mathbb{Z}_n')^\Omega$, which results in $\widetilde{N}_i = N_i$, as already noted in Sec. 5.3.4. For $n > 2$ the electric theory has the unique solution at $r_{00} = 0$, value obtained also for solution B of $(\mathrm{SPP}/\mathbb{Z}_2')^\Omega$ at $p = 2\tau_0$. Note that this solution has the same choice for τ signs as for $n > 2$.

In theories without an orientifold plane and each gauge node connected to the adjacents by a chiral and an anti-chiral field, the condition that, after Seiberg duality, the rank of the gauge group remains the same is quite natural. In fact, the electric theory is conformal when all ranks of the gauge factors are equal, hence, in the conformal window $\widetilde{N}_i = N_i$ for the magnetic theory. On the other hand, the presence of an orientifold plane shifts the ranks of gauge factors, for anomaly cancellation, and the condition for the ranks to remain equal is no longer obvious.

The message from $(\mathrm{SPP}/\mathbb{Z}_n')^\Omega$ with $n \geq 2$ is that for theories where each gauge factor has both chiral and anti-chiral matter and in presence of orientifold planes, the conformal window is given by the condition that the magnetic dual theory yields $\widetilde{N}_i = N_i$, as for theories without orientifold. Moreover, it seems that in this class of unoriented theories at the conformal point $r_{00} = 0$.

Checking these statements for SPP^Ω is quite complicated, both on the elliptic model and on the field

[9] If we add D6-branes along directions 0123789 in between the 5-branes, new D4-branes are created while exchanging the position of the 5-branes, in order to preserve supersymmetry [119].

theory side. In the former, we can either move an NS5′ brane and its image towards the orientifold plane or deal with an NS5 at the position of the orientifold plane. From the field theory perspective, we may construct a magnetic dual theory by means of the deconfinement trick [84, 120–123], in which the tensorial matter is deconfined into fundamental fields of an auxiliary gauge group, leaving the original unitary group with only (anti)fundamental fields. Applying this technique in SPP^{Ω} with antisymmetric matter, the extra gauge group is symplectic. Indeed, for $r_{00} = 0$ the rank of the Seiberg dual of $SU(N_1)$ remains unchanged, as in the previous cases, while this does not happen with symmetric matter and an orthogonal extra group. However, after the duality the auxiliary group can not be confined back. While most of the family $(\mathrm{SPP}/\mathbb{Z}'_n)^{\Omega}$ have the conformal point at $r_{00} = 0$, all we can say for SPP^{Ω} is that we are not able to exclude fixed points with $r_{00} \neq 0$. From the result we got for $(\mathrm{SPP}/\mathbb{Z}'_n)^{\Omega}$, in which we have analytical tools, we expect that the same should hold also for SPP^{Ω}, namely, that the conformal point exists only for a specific value of p for which $r_{00} = 0$.

5.6 Discussion

In this chapter we have found an infinite class of pairs of non-chiral unoriented theories whose conformal fixed points have the same central charge a^{Ω}, 't Hooft anomalies and superconformal index. These theories are $(\mathrm{SPP}/\mathbb{Z}'_n)^{\Omega}$ and the orientifold Ω of $L^{\frac{3n-1}{2},\frac{3n+1}{2},\frac{3n-1}{2}}$ for n odd or $L^{\frac{3n}{2},\frac{3n}{2},\frac{3n}{2}}$ for n even, whose parent theories can be constructed from the non-chiral orbifold $\mathbb{C}^3/\mathbb{Z}'_{3n}$ by mass deformation of pairs of adjoint fields [39].

For n odd, we find that both theories in each pair belong to the third scenario, whereby the orientifold projections, realised with fixed points on the dimer, break the conformal invariance of the parent theories even at large N, and they flow to a new conformal fixed point in the infrared. For $n = 1$ the two theories are actually the same, namely $(\mathrm{SPP})^{\Omega}$. Imposing that all β-functions vanish, it seems that for any value of the number of fractional branes p the theory has a fixed point. However, for some values of p, the central charge a must be corrected taking into account operators that decouple before reaching the conformal point. The effect is that the ratio a^{Ω}/a tends to increase. Considering that the Ω projection is a $\mathbb{Z}_2$ involution of the parent theory, any point at which $a^{\Omega}/a > 1/2$ seems difficult to interpret. Moreover, for $p \geq 5$, $\mathrm{Tr}\, R \neq 0$ already at leading order, spoiling the holographic duality, at least in its simple form. Being the parent theory a holographic theory, beyond this value the comparison with the a charge of the parent theory is unreliable. A possibility is that for $p \geq 5$ the field theory has a conformal point, with no gravity dual. Furthermore, following the prescription in [118], for $p = 1$ all the terms in the superpotential must be eliminated. Eventually, for $n = 1$ all we can say from the field theory side is that in the range $2 \leq p \leq 4$ a-maximization yields a maximum in the third scenario.

For n even, while for $\mathrm{SPP}/\mathbb{Z}'_n$ the orientifold involution is performed with fixed points and belongs to the third scenario, for $L^{\frac{3n}{2},\frac{3n}{2},\frac{3n}{2}}$ it is performed by fixed lines and belongs to the first scenario. This is a stronger evidence of the fact that the conformal points that we find are physically relevant.

For $n = 2$, apparently conformal invariance does not fix the relative rank p of the gauge groups, but Seiberg duality selects the value of $p = 2\tau_0$, which yields $r_{00} = 0$. Interestingly, for n even the orientifold projection of the theory $\mathbb{C}^3/\mathbb{Z}'_{3n}$ belongs to the third scenario and only for $p = 2\tau_0$ it shares the same central charge a^Ω, 't Hooft anomalies and superconformal index of the unoriented $\mathrm{SPP}/\mathbb{Z}'_n$ and, in turn, $L^{\frac{3n}{2},\frac{3n}{2},\frac{3n}{2}}$.

On the gravity side, all these theories can be described in Type IIA by means of elliptic models [107] where the geometry of the singularity depends on the configuration of NS5-branes, while stacks of D4-branes suspended between them provide the field theory. Rotating the 5-brane, one gives a geometric meaning to mass deformation and the flow to $\mathrm{SPP}/\mathbb{Z}'_n$ and $L^{k,n-k,k}$ mentioned above. In this context, Seiberg duality gives a clearer picture of the conformal point. Reordering the 5-branes does not change the number of D4, since no D6-branes are present. Back on the field theory side, this means that the ranks in the magnetic theory remain unchanged, and this happens only for the unique value of p that gives $r_{00} = 0$. Nonetheless, we have not been able to fully understand why one should pick that unique value in the case of $n = 1$, an issue related to the presence of tensorial matter. We leave this as an open problem.

The fact that each pair of theories share the same central charge a^Ω, 't Hooft anomalies and superconformal index, along with the fact that they share the same global symmetries, may imply that they are connected by an exactly marginal deformation. Since the endpoints of this exactly marginal deformation are orientifold projections of toric theories, one can conjecture that the two theories are actually dual and the two unoriented geometries are the same. The actual geometric interpretation of this infrared duality is presently lacking, but having found an infinite class of non-chiral theories in which this duality is realised gives hope that a geometric picture could emerge. In particular, the metrics of the parent theories of all these models are known. In the next chapter, we are going to discuss the only chiral example, at the best of our knowledge, that shows this mechanism. The metric for the associated geometry is not known.

Chapter 6

Infrared duality in unoriented Pseudo del Pezzo

The study of orientifold projection of brane tiling and toric theories has lead us to a new infrared duality between unoriented theories, descendants via mass deformation of the non-chiral orbifold of $\mathbb{C}^3$. We have constructed two infinite families that are in some sense dual and part of them belong to the third scenario. The importance of the results presented in the previous chapter is then two-fold. However, all of these families are non-chiral and up to this point one could think that perhaps those results are possible only for non-chiral models.
Searching for a chiral example is computationally hard, as one usually loose the recursive structure of the systems of anomaly-free conditions, for gauge and global symmetries, so examples with large quiver are difficult to solve analytically after the orientifold projection, whereas most of the small do not belong to the third scenario. We can restrict the models we should look for noticing that one of the families in the last chapter is $L^{a,b,a}$ and their non-chiral orbifolds, so maybe the answer is among their chiral orbifold involutions.
In this chapter, based on [2], we discuss the only chiral example we could find that belongs to the third scenario and that is dual to an unoriented theory in first scenario. It is the case of the chiral orbifold $\mathrm{SPP}/\mathbb{Z}_2$, known also as Pseudo del Pezzo 3c, PdP_{3c}. It is obtained by successive blow-ups [107, 124–126] of del Pezzo singularities. In particular, from dP_2, corresponding to the complex cone over the del Pezzo surface obtained by the blow-up of two generic points pf $\mathbb{P}^2$, we obtain dP_3 or, if the blow-up is non-generic [125, 126], either PdP_{3b} or PdP_{3c}. The latter two theories, whose toric diagrams are drawn in Fig. 6.1, are the ones we are interested in. In Fig. 6.3-6.4 we draw the dimers of these two theories. By looking at the diagrams we see that the two theories have different superpotentials but share the same quivers, given in Fig. 6.2.

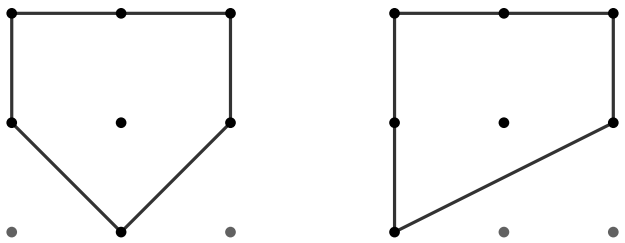

Figure 6.1. The toric diagram of PdP_{3b} on the left and the toric diagram of PdP_{3c} on the right.

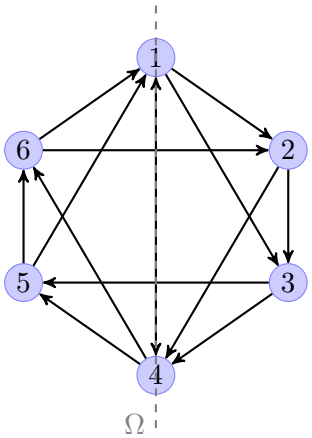

Figure 6.2. The quiver of theories PdP_{3b} and PdP_{3c}. The dashed gray line labelled as Ω represents the orientifold projection, which identifies the two sides of the quiver and projects fields and gauge groups that lie on top of it.

6.1 Parent Pseudo del Pezzo $3b$ and $3c$

Let us introduce the parent gauge theories of interest. We begin with PdP_{3b} [32, 125, 126], whose quiver and dimer are drawn in Fig. 6.2 and 6.3. There are 6 gauge groups $\prod_{a=1}^{6} SU(N_a)$ and the matter fields are bifundamentals X_{ab} corresponding to the edges in the dimer. For instance, X_{12} transforms in the fundamental representation of $SU(N_1)$ and in the anti-fundamental of $SU(N_2)$ and is the edge between faces 1 and 2 in the dimer. The global symmetries of this model are $\mathrm{U}(1)^2 \times \mathrm{U}(1)_R$ as mesonic symmetry and $\mathrm{U}(1)^5$ as baryonic one, of which $\mathrm{U}(1)^2$ is anomalous. The superpotential of the theory reads

$$\begin{aligned} W_{3b} = & X_{13}X_{34}X_{41} - X_{46}X_{61}X_{14} + X_{45}X_{51}X_{14} \\ & - X_{24}X_{41}X_{12} + X_{62}X_{24}X_{46} - X_{35}X_{51}X_{13} \\ & + X_{23}X_{35}X_{56}X_{61}X_{12} - X_{23}X_{34}X_{45}X_{56}X_{62} \ . \end{aligned} \tag{6.1}$$

The gauge anomalies vanish imposing the following relation between the ranks of the gauge groups:

$$\begin{aligned} N_1 + N_6 - N_3 - N_4 = 0 \ , \\ N_2 + N_3 - N_5 - N_6 = 0 \ . \end{aligned} \tag{6.2}$$

We find the superconformal fixed point and the corresponding R-charges R_{ab} for the fields X_{ab} maximizing the a-charge. Requiring that the β-functions vanish, equivalent to non-anomalous R-symmetry, we have

$$\sum_a (R_{ab} - 1)N_a = -2N_b \ , \tag{6.3}$$

where the sum is over gauge groups a connected to b by a bifundamental field X_{ab}. Together with the condition that the R-charge of the superpotential is $R(W) = 2$, we have a system of equations with a priori eight independent R-charges. This can be seen also from the quiver, which enjoys a $\mathbb{Z}_2$ symmetry. The a-charge is a two-variable function, namely, a global symmetry $\mathrm{U}(1)^2$ mixes

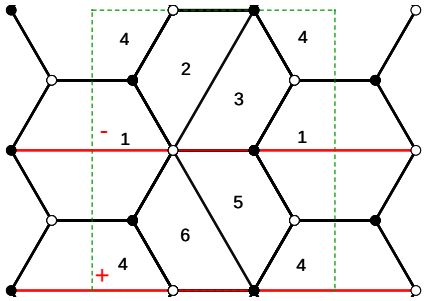

Figure 6.3. The dimer of PdP_{3b}, where the dashed green line delimits the fundamental cell. The two red fixed lines and their signs represent the orientifold projection that yields the unoriented $\mathrm{PdP}_{3b}^{\Omega}$.

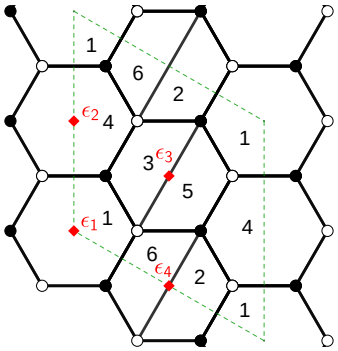

Figure 6.4. The dimer of PdP_{3c}, where the dashed green line delimits the fundamental cell. The four red fixed points $(\tau_1, \tau_2, \tau_3, \tau_4)$ represent the orientifold projection, where $(+,-,-,+)$ corresponds to $\mathrm{PdP}_{3c}^{\Omega_1}$ and $(-,+,-,+)$ corresponds to $\mathrm{PdP}_{3c}^{\Omega_2}$.

with the R-symmetry. The local maximum yields [32]

$$\begin{aligned} R^b_{23} &= 7 - 3\sqrt{5}\,, \\ R^b_{13} &= R^b_{14} = R^b_{24} = 3 - \sqrt{5}\,, \\ R^b_{12} &= R^b_{34} = R^b_{35} = R^b_{62} = 2\sqrt{5} - 4\,, \end{aligned} \tag{6.4}$$

$$\begin{aligned} a_{3b} &= \frac{27}{4} N^2 \left(5\sqrt{5} - 11\right)\,, \\ \mathrm{Vol}(\mathrm{PdP}_{3b}) &= \frac{\pi^3}{27\left(5\sqrt{5} - 11\right)}\,, \end{aligned} \tag{6.5}$$

where $N_a = N\ \forall a = 1, \ldots, 6$ since this condition gives the only solution that respects the unitarity bound. Note that the expression of the a-charge is given at leading order in N.
The second theory we study is PdP_{3c} [32, 125, 126], whose dimer is drawn in Fig. 6.4. As in the previous case, the gauge group is $\prod_{a=1}^{6} SU(N_a)$ and the global symmetries are $\mathrm{U}(1)^2 \times \mathrm{U}(1)_R$ as mesonic symmetry and $\mathrm{U}(1)^5$ as baryonic one, of which $\mathrm{U}(1)^2$ is anomalous. The matter fields are also the same of the PdP_{3b} theory and indeed the two models share the same quiver in Fig. 6.2. Nonetheless, they have a different dimer and therefore interact differently. In fact, the superpotential reads

$$\begin{aligned} W_{3c} = {} & X_{12}X_{24}X_{41} + X_{45}X_{51}X_{14} - X_{13}X_{34}X_{41} \\ & - X_{46}X_{61}X_{14} + X_{13}X_{35}X_{56}X_{61} + X_{46}X_{62}X_{23}X_{34} \\ & - X_{12}X_{23}X_{35}X_{51} - X_{45}X_{56}X_{62}X_{24}\,. \end{aligned} \tag{6.6}$$

The gauge anomalies vanish imposing the condition in Eq. (6.2) as before. Computing the R-charges

which maximize the a-charge we find [32]

$$\begin{aligned} R^c_{14} &= 2 - \frac{2\sqrt{3}}{3} \,, \\ R^c_{23} &= R^c_{35} = R^c_{62} = 1 - \frac{\sqrt{3}}{3} \,, \\ R^c_{12} &= R^c_{13} = R^c_{24} = R^c_{34} = \frac{\sqrt{3}}{3} \,, \end{aligned} \tag{6.7}$$

$$\begin{aligned} a_{3c} &= \frac{3\sqrt{3}}{4} N^2 \,, \\ \mathrm{Vol}(\mathrm{PdP}_{3c}) &= \frac{\pi^3}{3\sqrt{3}} \,, \end{aligned} \tag{6.8}$$

where again $N_a = N \ \forall a = 1, \ldots, 6$ is the only solution that respects the unitarity bound. Note that the difference in the R-charges arises from the condition $R(W) = 2$. It is crucial to note that in this case the a-charge is a three-variable function, namely, the non-R symmetry which mixes with the R-charge is $\mathrm{U}(1)^3$.

6.2 Unoriented $\mathbf{PdP}_{3b}$ and $\mathbf{PdP}_{3c}$

The orientifold projection of a quiver gauge theory is represented as a line which identifies the two sides of the quiver and projects the groups and the fields that are mapped onto themselves, as discussed in Chapter 3. For the PdP_{3b} and PdP_{3c} theories, the involution is the Ω line in Fig. 6.2.

6.2.1 Unoriented $\mathbf{PdP}_{3b}$

We consider the orientifold involution of PdP_{3b} with two fixed lines and we choose the configuration with signs $(-,+)$, as in Fig. 6.3. As a consequence, the gauge group $SU(N_5)$ is identified with $SU(N_3)$ and $SU(N_6)$ with $SU(N_2)$, while $SU(N_1)$ becomes $USp(N_1)$ and $SU(N_4)$ becomes $SO(N_4)$ since they lie on top of the fixed lines. The resulting theory has gauge groups $USp(N_1) \times SU(N_2) \times SU(N_3) \times SO(N_4)$, where the fields X^A_{35} and X^S_{62} belong to the antisymmetric and symmetric representations of the gauge groups $SU(N_3)$ and $SU(N_2)$ respectively. The superpotential reads

$$\begin{aligned} W^{\Omega}_{3b} = {} & X_{13}X_{34}X_{41} - X_{24}X_{41}X_{12} + X^S_{62}X_{24}X_{46} \\ & - X^A_{35}X_{51}X_{13} + X_{23}X^A_{35}X_{56}X_{61}X_{12} \\ & - X_{23}X_{34}X_{45}X_{56}X^S_{62} \end{aligned} \tag{6.9}$$

and the anomaly cancellation condition is

$$N_1 + N_2 - N_3 - N_4 + 4 = 0 \, . \tag{6.10}$$

As in the parent theory, there are eight a priori independent R_{ab}. The condition for the β-functions to vanish changes slightly due to the orientifold involution. In fact, one has

$$\sum_a (R_{ab} - 1)N_a = -(N_b \pm 2) \, , \tag{6.11}$$

if the group labelled by b is orthogonal $(-)$ or symplectic $(+)$. Likewise, for unitary gauge groups one has

$$\sum_a (R_{ab} - 1)N_a + (R_b - 1)(N_b \pm 2) = -2N_b \, , \tag{6.12}$$

where R_b is the R-charge of the symmetric $(+)$ or the antisymmetric $(-)$ field charged under $SU(N_b)$. Imposing conformal invariance, consistency with the unitarity bound requires $N_2 = N_3 = N_1 + 2 = N_4 - 2 = N$. One then finds the flavour symmetry is $\mathrm{U}(1)^2$ and the R-charges are the same as the ones of the parent theory in Eq. (6.4) up to $O(1/N)$ corrections. This implies that this orientifold realizes what we have described in the introduction as the 'second scenario', in which there is a fixed point, and the orientifold induces corrections to the R-charges that vanish at large N. Taking this limit, the value of the a-charge is

$$a_{3b}^{\Omega} = \frac{27}{8} N^2 \left(5\sqrt{5} - 11\right) \, . \tag{6.13}$$

Note that the central charge a is half the one of the parent theory. This is expected since the degrees of freedom have been halved. Besides, also the volume of the PdP_{3b} after the orientifold is half the volume of the parent space. To see this, consider that the orientifold acts as a $\mathbb{Z}_2$ projection on the geometry. As a consequence, the number of units of 5-form flux is $N/2$ [116]. Thus, the proper ratio between the volumes reads

$$\frac{\mathrm{Vol}(\mathrm{PdP}_{3b}^{\Omega})}{\mathrm{Vol}(\mathrm{PdP}_{3b})} = \frac{1}{2} \, . \tag{6.14}$$

This is similar to the case of the $\mathbb{Z}_n$ orbifold of flat space, where the volume is a fraction n of the volume of the sphere S^5.

6.2.2 Unoriented $\mathbf{PdP}_{3c}$

Let us turn to the orientifold of PdP_{3c}. As shown in Fig. 6.4, the dimer admits only the projection with fixed points, whose signs $(\tau_1, \tau_2, \tau_3, \tau_4)$ project the group $SU(N_1)$, the group $SU(N_4)$, the field X_{35} and the field X_{62}, respectively. The parent theory has $N_W = 8$, thus $\prod_{i=1}^4 \tau_i = +1$. The two

inequivalent choices are $\Omega_1 = (+,-,-,+)$ and $\Omega_2 = (-,+,-,+)$.
First, we focus on Ω_1. The unoriented theory has gauge groups $SO(N_1) \times SU(N_2) \times SU(N_3) \times USp(N_4)$, where fields X_{35}^A and X_{62}^S are antisymmetric and symmetric representations of $SU(N_3)$ and $SU(N_2)$ respectively. The superpotential reads

$$\begin{aligned} W_{3c}^{\Omega_1} = & X_{13}X_{35}^A X_{56}X_{61} - X_{45}X_{56}X_{62}^S X_{24} \\ & + X_{12}X_{24}X_{41} - X_{13}X_{34}X_{41} \end{aligned} \tag{6.15}$$

and the anomaly cancellation condition remains as Eq. (6.10). The superconformal fixed point of this unoriented model has the same R-charges of the parent theory in Eq. (6.7) up to $O(1/N)$ corrections, with the flavour $\mathrm{U}(1)^3$ symmetry mixing with R-symmetry, and thus the second scenario described in the introduction is again realized as in the PdP_{3b} case. In the large N limit, the a-charge is

$$a_{3c}^{\Omega_1} = \frac{3\sqrt{3}}{8} N^2 \,, \tag{6.16}$$

where $N_1 = N_2 = N_3 - 2 = N_4 - 2 = N$ is the only consistent solution. Again, the a-charge is halved because of the orientifold projection, and the ratio between the volumes is $1/2$ as before.
The unoriented theory obtained from $\Omega_2 = (-,+,-,+)$ has gauge groups $USp(N_1) \times SU(N_2) \times SU(N_3) \times SO(N_4)$, where fields X_{35}^A and X_{62}^S are unchanged w.r.t. the previous case. The superpotential $W_{3c}^{\Omega_2}$ is formally identical to $W_{3c}^{\Omega_1}$ in Eq. (6.15) and again the anomaly cancellation condition remains as Eq. (6.10). The a-maximization in this case is more subtle. If one took naively the limit $N \to \infty$ before solving the equation for vanishing β-functions and $R(W) = 2$, one would obtain the R-charges and half the a-charge of the parent theory, with non-R flavour $\mathrm{U}(1)^3$. On the other hand, we find that for any *finite* value of N, the only consistent solution is $N_2 = N_3 = N_1 + 2 = N_4 - 2 = N$ exactly as in $\mathrm{PdP}_{3b}^{\Omega}$, with one flavour U(1) broken and the remaining $\mathrm{U}(1)^2$ mixing with R-symmetry. This has the crucial effect of giving at leading order in $1/N$ the value of the superconformal R-charges as

$$\begin{aligned} & R_{23}^{\Omega_2} = 7 - 3\sqrt{5} \,, \\ & R_{13}^{\Omega_2} = R_{14}^{\Omega_2} = R_{24}^{\Omega_2} = 3 - \sqrt{5} \,, \\ & R_{12}^{\Omega_2} = R_{34}^{\Omega_2} = R_{35}^{\Omega_2} = R_{62}^{\Omega_2} = 2\sqrt{5} - 4 \,, \end{aligned} \tag{6.17}$$

which are different from the R-charges of the parent theory in Eq. (6.7), and the $a_{3c}^{\Omega_2}$-charge takes the value

$$a_{3c}^{\Omega_2} = \frac{27}{8} N^2 \left(5\sqrt{5} - 11\right) \,, \tag{6.18}$$

which is smaller than the value of $a_{3c}^{\Omega_1}$ in Eq. (6.16). Consequently, the ratio between $a_{3c}^{\Omega_2}$ and that

of the parent theory is

$$\frac{a_{3c}^{\Omega_2}}{a_{3c}} = \frac{3\sqrt{3}}{2}\left(5\sqrt{5}-11\right) \simeq 0.47\,, \tag{6.19}$$

while the ratio between the volumes is

$$\frac{\mathrm{Vol}(\mathrm{PdP}_{3c}^{\Omega_2})}{\mathrm{Vol}(\mathrm{PdP}_{3c})} \simeq 0.53\,. \tag{6.20}$$

The fact that $a_{3c}^{\Omega_2}$ is less than halved w.r.t. the central charge a_{3c} of the parent theory can be taken as a sign of an RG flow towards the IR. Thus, a natural question is what is the endpoint of this RG flow. Surprisingly, the R-charges and the a-charge in Eqs. (6.17) and (6.18) are exactly those of $\mathrm{PdP}_{3b}^{\Omega}$ given in Eqs. (6.4) and (6.13). This suggests the two theories are dual at the conformal fixed point. In other words, the RG flow is going from $\mathrm{PdP}_{3c}^{\Omega_2}$ in the UV to $\mathrm{PdP}_{3b}^{\Omega}$ in the IR.
To further support this conjecture we investigate the $1/N$ corrections to the R-charges. Remarkably, imposing that the β-functions vanish yields exactly the same solutions at any finite N, which implies that the charges w.r.t. all the global symmetries of the two theories are the same. The values of these charges are reported in Tab. 6.1, where Q_1 and Q_2 are associated to the flavour symmetry $U(1)_1 \times U(1)_2$, while R_0 is an allowed non-superconformal choice of the R-charge.

	Q_1	Q_2	R_0
X_{12}	$-\frac{N+2}{N}$	$\frac{1}{2}$	$\frac{1}{2}$
X_{13}	0	$-\frac{1}{2}$	$\frac{1}{2}$
X_{24}	$\frac{1}{N}$	$-\frac{1}{2}$	$\frac{1}{2}$
X_{62}^{S}	$-\frac{4}{N}$	1	1
X_{23}	$\frac{N+2}{N}$	-1	0
X_{34}	-1	$\frac{1}{2}$	$\frac{1}{2}$
X_{41}	1	0	1
X_{35}^{A}	0	1	1

Table 6.1. The values of the charges Q_1, Q_2 and R_0 for the fields of $\mathrm{PdP}_{3b}^{\Omega}$ and $\mathrm{PdP}_{3c}^{\Omega_2}$, which are the same. Q_1 and Q_2 refer to the charges under the flavour symmetry $U(1)_1 \times U(1)_2$, while R_0 is an allowed non-superconformal choice of the R-charge.

6.3 Discussion

We have shown that the value of the a-charge of the superconformal fixed point of the unoriented $\mathrm{PdP}_{3c}^{\Omega_2}$ is smaller than expected and this gives strong evidence that there is an RG flow from the UV to the IR. On the fixed point in the IR, the R-charges and a-charge are exactly those of the unoriented $\mathrm{PdP}_{3b}^{\Omega}$. Moreover, the two theories share the same field content and have identical

charges under the same global symmetry for any finite N. As a consequence, 't Hooft anomalies match in the IR as well as the superconformal index and thus we conjecture that in the IR the two unoriented theories describe the same physics.

A natural question that one can ask is whether the $\mathrm{PdP}_{3b}^{\Omega}$ and $\mathrm{PdP}_{3c}^{\Omega_2}$ theories are connected by an exactly marginal deformation. A hint in this direction comes from the fact that the two theories differ only because of superpotential terms. This implies that if one turns on in the $\mathrm{PdP}_{3c}^{\Omega_2}$ theory a deformation $\alpha(W_{3b}^{\Omega} - W_{3c}^{\Omega_2})$, the resulting theory must have a superconformal fixed point for any value of α, with the same value of the R-charges. While for $\alpha = 0$ and $\alpha = 1$ the theory results from an orientifold projection, it would be very interesting to investigate the origin of the other superconformal theories.

As far as the gravity side of the AdS/CFT correspondence is concerned, the mechanisms known in the literature to produce RG flows in the context of holographic field theories do not seem to explain our result. In particular, the flow described above is not due to mass deformations [1, 70], to a Higgs mechanism [125] or to the introduction of fractional branes [127]. We can expect some kind of kink solution interpolating between two asymptotic geometries like in [128], but the metrics of the CY complex cones over PdP_{3b} and PdP_{3c} are unknown and thus we do not have control of the bulk theory. Progress on the gravity side of the orientifold theories discussed in this letter would also allow one to investigate holographically the marginal deformation discussed above.

The picture from the orientifold analysis is thus that the configuration of branes and orientifold planes in the $\mathrm{PdP}_{3c}^{\Omega_2}$ theory breaks the conformal symmetry in the UV, but makes the theory flow to a different IR fixed point that is the one of the $\mathrm{PdP}_{3b}^{\Omega}$ theory, with which $\mathrm{PdP}_{3c}^{\Omega_2}$ shares all the symmetries. In the bulk, we can thus expect form fluxes that make the volume increase so that only asymptotically the metric is AdS. The scale associated to the flow might be identified with the size of the cycles wrapped by the branes that generate the fluxes.

Another direction that can be explored is the possibility that the duality is a consequence of the PdP_{3b} and PdP_{3c} parent theories being connected by specular duality [32, 129], which in general is a map between theories with the same master space. In the case of theories whose toric diagram has only one internal point, like the ones we are discussing, specular duality exchanges mesonic and anomalous baryonic symmetries. The chain of maps that relate the two parent theories is more precisely a specular duality followed by a Seiberg duality [58] and again another specular duality. One could even investigate the possibility that a chain of Seiberg dualities relates the two unoriented theories. Seiberg dualities in the case in which (anti-)symmetric fields are present have been considered in [120, 121], where one describes them as mesons of a new confining symplectic or orthogonal gauge group. The problem of this approach is that one needs to add a gauge group going towards the UV and that can not describe the flow from $\mathrm{PdP}_{3b}^{\Omega}$ to $\mathrm{PdP}_{3c}^{\Omega_2}$.

Finding other chiral examples would allow us to understand the physical origin of this infrared duality. However, as the number of gauge groups increases, it becomes computationally harder to find the exact local maximum of the a-charge. To give more evidence that the unoriented $\mathrm{PdP}_{3c}^{\Omega_2}$ flows to $\mathrm{PdP}_{3b}^{\Omega}$ in the IR, we plan to study the moduli spaces of the two unoriented theories. Another possible line of investigation would be to check whether S-duality and strong coupling

effects are involved, along the lines of [82–85].

Conclusions

Over the previous chapters, we have constructed $\mathcal{N} = 1$ gauge theories from orientifold projections of toric models and used the tools for supersymmetric theories in order to determine their conformal point, if any. In Chapter 4, we saw that the relevant mass deformation triggers a flow in the parent toric theory A, which ends on a different toric model B. In principle, the orientifold may spoil the relation between the two models, as its action is non-trivial, both on geometry and field theory. It introduces fixed points and both A^Ω and B^Ω will have real groups and/or tensor representations, not present in the parent models. First of all, the orientifold requires a $\mathbb{Z}_2$ symmetry and this already projects out some connections and models. But even when this $\mathbb{Z}_2$ symmetry is preserved, the orientifold involutions change the properties from A to A^Ω and any connection to B and B^Ω is not granted. An example is given by Seiberg duality cascade from A to a confined phase B, as happens for the conifold or its chiral orbifold [64, 65]. In presence of orientifold, the duality cascade from A^Ω to B^Ω has different features than in A to B, both in the UV and in the IR [88]. Thus, there is no reason to expect a priori that A^Ω and B^Ω are still connected. Nonetheless, in Chapters 4 and 5 mass deformations of pairs of fields, in suitable chosen patterns, preserve the connection in presence of orientifold and we are able to move from A^Ω to B^Ω. However, this flow is qualitatively different than in the parent theories, as before the orientifold a relevant deformation triggers the flow, whereas for the unoriented models symmetry requires that they are connected by an exactly marginal deformation, and we conclude that they live on the same conformal manifold.

Going more into details, in Chapter 5 we have focused on $L^{a,b,a}$ theories and this entire non-chiral family can be obtained by mass deforming the orbifold theory $\mathbb{C}^2/\mathbb{Z}_{3n} \times \mathbb{C}$. A precise pattern of mass deformation leads to $\mathrm{SPP}/\mathbb{Z}'_n$, instead another one to $L^{\overline{n},\overline{n},\overline{n}}$ with $\overline{n} = 3n/2$ or $L^{\overline{n},\overline{n}+1,\overline{n}}$ with $\overline{n} = (3n-1)/2$. This is preserved by the orientifold projection, as long as the pattern is $\mathbb{Z}_2$ symmetric. After the orientifold projection, $(\mathrm{SPP}/\mathbb{Z}'_n)^\Omega$ and $\left(L^{\overline{n},\overline{n}+1,\overline{n}}\right)^\Omega$ belong to the so-called third scenario. For these models, the orientifold projection breaks the conformal point of the parent theory, meaning that the R-charges of the parent, at leading order, yield an anomalous symmetry. In the flow towards the infrared, a new conformal point is developed, where the R-charges are modified already at leading order in N. In principle, this mechanism could be dangerous, as it may happen that accidental symmetries are generated. We took into account that gauge-invariant operators may decouple and it turns out that, at least for $n > 1$, they do not spoil the new conformal point. However, something else might happen, over which we dot have control.

The case for n even is interesting, let us discuss why starting from the mother $\left(\mathbb{C}^2/\mathbb{Z}_{3n}\times\mathbb{C}\right)^{\Omega}$. We found two possible orientifold projections, Ω^A that yields a $\mathcal{N}=2$ and Ω^B that gives a $\mathcal{N}=1$ instead. The ratio between the central charges a^{Ω} is 27/32 and this usually happens by mass deforming a $\mathcal{N}=2$ that eventually flows to a $\mathcal{N}=1$ in the IR [130]. However, if we mass deform Ω^A, depending on the precise pattern we choose we end up with $\left(\text{SPP}/\mathbb{Z}'_n\right)^{\Omega}$ or $\left(L^{\overline{n},\overline{n},\overline{n}}\right)^{\Omega}$, modulo Seiberg dualities. We found that these two have the same central charges a^{Ω}, 't Hooft anomaly and superconformal indices as Ω_B, for which it is crucial the presence of fields with superconformal $R=1$. Hence, we conjecture that these unoriented theories are dual, in the sense that they live on the same conformal manifold. The fact that $\left(L^{\overline{n},\overline{n},\overline{n}}\right)^{\Omega}$ actually belongs to the first scenario and its R-charges are the same as its parent model, at leading order, puts the existence of the conformal manifold and of the duality on more solid grounds.

An enlightening description of what is the nature of the duality is given in [131], where they use the IIA elliptic models with orientifold planes to enlarge the family of theories that enjoys this duality, which in turn manifests itself as an inherited S-duality at work. The picture they give is clear: starting from $\mathcal{N}=2$ elliptic model with orientifold planes, one can give mass to pairs of adjoint fields, and the theory flows to a $\mathcal{N}=1$ SCFT. This can be marginally deformed thanks to the fields with $R=1$, whose quadratic term is marginal and S-duality acts on the coupling, exploring the same conformal manifold.

While for non-chiral models the field theory description of the duality seems quite clear, the unique chiral example described in Chapter 6 is somewhat cryptic, as mass deformation does not seem to be involved and none of the fields carry $R=1$. More cases should allow us to generate a picture also for chiral models. Along this line, we are already analyzing orbifold $\mathbb{C}^3/\left(\mathbb{Z}_m\times\mathbb{Z}_n\right)$ and their orientifold projections, and this will lead us to the construction of more chiral examples, with a similar mechanism that exploits the interplay between mass deformation and orientifold for $\mathbb{C}^3/\left(\mathbb{Z}_2\times\mathbb{Z}_{2n}\right)$ and $\left(L^{a,b,a}/\mathbb{Z}_2\right)$. In the future, we will consider the orientifold projection of [87] with no fixed loci.

In light of the AdS/CFT correspondence we expect that for all of these unoriented cases, both chiral and non-chiral, a geometric counterpart of the duality exists, explaining how different oriented geometries are the same after the orientifold projection. While this is still unclear to us, we are confident that in the future a picture will emerge.

Bibliography

[1] M. Bianchi, D. Bufalini, S. Mancani, and F. Riccioni, "Mass deformations of unoriented quiver theories," *JHEP*, vol. 07, 2020.

[2] A. Antinucci, S. Mancani, and F. Riccioni, "Infrared duality in unoriented Pseudo del Pezzo," *Phys. Lett. B*, vol. 811, p. 135902, 2020.

[3] A. Antinucci, M. Bianchi, S. Mancani, and F. Riccioni, "Suspended fixed points," *Nucl. Phys. B*, vol. 976, p. 115695, 2022.

[4] J. D. Bekenstein, "Black holes and entropy," *Phys. Rev. D*, vol. 7, pp. 2333–2346, 1973.

[5] G. 't Hooft, "Dimensional reduction in quantum gravity," *Conf. Proc. C*, vol. 930308, pp. 284–296, 1993.

[6] L. Susskind, "The World as a hologram," *J. Math. Phys.*, vol. 36, pp. 6377–6396, 1995.

[7] J. M. Maldacena, "The Large N limit of superconformal field theories and supergravity," *Int. J. Theor. Phys.*, vol. 38, pp. 1113–1133, 1999. [Adv. Theor. Math. Phys.2,231(1998)].

[8] E. Witten, "Anti-de Sitter space and holography," *Adv. Theor. Math. Phys.*, vol. 2, pp. 253–291, 1998.

[9] S. S. Gubser, I. R. Klebanov, and A. M. Polyakov, "Gauge theory correlators from noncritical string theory," *Phys. Lett.*, vol. B428, pp. 105–114, 1998.

[10] O. Aharony, S. S. Gubser, J. M. Maldacena, H. Ooguri, and Y. Oz, "Large N field theories, string theory and gravity," *Phys. Rept.*, vol. 323, pp. 183–386, 2000.

[11] M. Ammon and J. Erdmenger, *Gauge/gravity duality: Foundations and applications*. Cambridge: Cambridge University Press, 4 2015.

[12] D. R. Morrison and M. R. Plesser, "Nonspherical horizons. 1.," *Adv. Theor. Math. Phys.*, vol. 3, pp. 1–81, 1999.

[13] O. Aharony, S. Kachru, and E. Silverstein, "New N=1 superconformal field theories in four-dimensions from D-brane probes," *Nucl. Phys.*, vol. B488, pp. 159–176, 1997.

[14] U. Bruzzo, A. Fino, and P. Fré, "The Kähler Quotient Resolution of $\mathbb{C}^3/\Gamma$ Singularities, the McKay Correspondence and $D = 3$ $\mathcal{N} = 2$ Chern–Simons Gauge Theories," *Commun. Math. Phys.*, vol. 365, no. 1, pp. 93–214, 2019.

[15] V. Bouchard, "Lectures on complex geometry, Calabi-Yau manifolds and toric geometry," 2007.

[16] N. C. Leung and C. Vafa, "Branes and toric geometry," *Adv. Theor. Math. Phys.*, vol. 2, pp. 91–118, 1998.

[17] C. Closset, "Toric geometry and local Calabi-Yau varieties: An Introduction to toric geometry (for physicists)," 1 2009.

[18] D. A. Cox, J. B. Little, and H. Schenk, *Toric Varieties*. Graduate Studies in Mathematics, 2011.

[19] M. Yamazaki, "Brane tilings and their applications," *Fortschritte der Physik*, vol. 56, no. 6, pp. 555–686, 2008.

[20] A. Hanany and K. D. Kennaway, "Dimer models and toric diagrams," 3 2005.

[21] S. Franco, A. Hanany, K. D. Kennaway, D. Vegh, and B. Wecht, "Brane dimers and quiver gauge theories," *JHEP*, vol. 01, p. 096, 2006.

[22] B. Feng, A. Hanany, Y.-H. He, and A. M. Uranga, "Toric duality as Seiberg duality and brane diamonds," *JHEP*, vol. 12, p. 035, 2001.

[23] S. Franco, A. Hanany, F. Saad, and A. M. Uranga, "Fractional branes and dynamical supersymmetry breaking," *JHEP*, vol. 01, p. 011, 2006.

[24] A. Hanany and D. Vegh, "Quivers, tilings, branes and rhombi," *JHEP*, vol. 10, p. 029, 2007.

[25] A. Hanany, C. P. Herzog, and D. Vegh, "Brane tilings and exceptional collections," *JHEP*, vol. 07, p. 001, 2006.

[26] A. Butti, D. Forcella, A. Hanany, D. Vegh, and A. Zaffaroni, "Counting Chiral Operators in Quiver Gauge Theories," *JHEP*, vol. 11, p. 092, 2007.

[27] K. D. Kennaway, "Brane Tilings," *Int. J. Mod. Phys. A*, vol. 22, pp. 2977–3038, 2007.

[28] J. Davey, A. Hanany, and R.-K. Seong, "Counting Orbifolds," *JHEP*, vol. 06, p. 010, 2010.

[29] A. Hanany and R.-K. Seong, "Symmetries of Abelian Orbifolds," *JHEP*, vol. 01, p. 027, 2011.

[30] J. Davey, A. Hanany, and R.-K. Seong, "An Introduction to Counting Orbifolds," *Fortsch. Phys.*, vol. 59, pp. 677–682, 2011.

[31] A. Hanany, V. Jejjala, S. Ramgoolam, and R.-K. Seong, "Calabi-Yau Orbifolds and Torus Coverings," *JHEP*, vol. 09, p. 116, 2011.

[32] A. Hanany and R. Seong, "Brane tilings and reflexive polygons," *Fortsch. Phys.*, vol. 60, pp. 695–803, 2012.

[33] A. Hanany and R.-K. Seong, "Brane Tilings and Specular Duality," *JHEP*, vol. 08, p. 107, 2012.

[34] M. R. Douglas and G. W. Moore, "D-branes, quivers, and ALE instantons," 3 1996.

[35] M. R. Douglas, B. R. Greene, and D. R. Morrison, "Orbifold resolution by D-branes," *Nucl. Phys. B*, vol. 506, pp. 84–106, 1997.

[36] C. Beasley, B. R. Greene, C. I. Lazaroiu, and M. R. Plesser, "D3-branes on partial resolutions of Abelian quotient singularities of Calabi-Yau threefolds," *Nucl. Phys. B*, vol. 566, pp. 599–640, 2000.

[37] F. Fucito, J. F. Morales, and R. Poghossian, "Instantons on quivers and orientifolds," *JHEP*, vol. 10, p. 037, 2004.

[38] M. Bianchi, F. Fucito, and J. F. Morales, "Dynamical supersymmetry breaking from unoriented D-brane instantons," *JHEP*, vol. 08, p. 040, 2009.

[39] M. Bianchi, G. Inverso, J. F. Morales, and D. Ricci Pacifici, "Unoriented Quivers with Flavour," *JHEP*, vol. 01, p. 128, 2014.

[40] Y. Imamura, "Anomaly cancellations in brane tilings," *JHEP*, vol. 06, p. 011, 2006.

[41] A. Butti, "Deformations of Toric Singularities and Fractional Branes," *JHEP*, vol. 10, p. 080, 2006.

[42] R. Argurio, M. Bertolini, S. Franco, E. García-Valdecasas, S. Meynet, A. Pasternak, and V. Tatitscheff, "Dimers, Orientifolds and Anomalies," *JHEP*, vol. 02, p. 153, 2021.

[43] S. Franco and A. M. . Uranga, "Dynamical SUSY breaking at meta-stable minima from D-branes at obstructed geometries," *JHEP*, vol. 06, p. 031, 2006.

[44] Y. Imamura, K. Kimura, and M. Yamazaki, "Anomalies and O-plane charges in orientifolded brane tilings," *JHEP*, vol. 03, p. 058, 2008.

[45] S. Franco, "Bipartite Field Theories: from D-Brane Probes to Scattering Amplitudes," *JHEP*, vol. 11, p. 141, 2012.

[46] S. Franco and A. Uranga, "Bipartite Field Theories from D-Branes," *JHEP*, vol. 04, p. 161, 2014.

[47] V. A. Novikov, M. A. Shifman, A. I. Vainshtein, and V. I. Zakharov, "Exact Gell-Mann-Low Function of Supersymmetric Yang-Mills Theories from Instanton Calculus," *Nucl. Phys. B*, vol. 229, pp. 381–393, 1983.

[48] K. A. Intriligator and B. Wecht, "The Exact superconformal R symmetry maximizes a," *Nucl. Phys.*, vol. B667, pp. 183–200, 2003.

[49] D. Anselmi, D. Z. Freedman, M. T. Grisaru, and A. A. Johansen, "Nonperturbative formulas for central functions of supersymmetric gauge theories," *Nucl. Phys. B*, vol. 526, pp. 543–571, 1998.

[50] D. Anselmi, J. Erlich, D. Z. Freedman, and A. A. Johansen, "Positivity constraints on anomalies in supersymmetric gauge theories," *Phys. Rev. D*, vol. 57, pp. 7570–7588, 1998.

[51] M. Henningson and K. Skenderis, "The Holographic Weyl anomaly," *JHEP*, vol. 07, p. 023, 1998.

[52] V. Balasubramanian and P. Kraus, "A Stress tensor for Anti-de Sitter gravity," *Commun. Math. Phys.*, vol. 208, pp. 413–428, 1999.

[53] W. Mueck and K. S. Viswanathan, "Counterterms for the Dirichlet prescription of the AdS / CFT correspondence," 5 1999.

[54] Z. Komargodski and A. Schwimmer, "On Renormalization Group Flows in Four Dimensions," *JHEP*, vol. 12, p. 099, 2011.

[55] H. Osborn, "N=1 superconformal symmetry in four-dimensional quantum field theory," *Annals Phys.*, vol. 272, pp. 243–294, 1999.

[56] D. Kutasov, A. Parnachev, and D. A. Sahakyan, "Central charges and U(1)(R) symmetries in N=1 superYang-Mills," *JHEP*, vol. 11, p. 013, 2003.

[57] T. Banks and A. Zaks, "On the Phase Structure of Vector-Like Gauge Theories with Massless Fermions," *Nucl. Phys. B*, vol. 196, pp. 189–204, 1982.

[58] N. Seiberg, "Electric - magnetic duality in supersymmetric nonAbelian gauge theories," *Nucl. Phys.*, vol. B435, pp. 129–146, 1995.

[59] K. A. Intriligator and P. Pouliot, "Exact superpotentials, quantum vacua and duality in supersymmetric SP(N(c)) gauge theories," *Phys. Lett.*, vol. B353, pp. 471–476, 1995.

[60] K. A. Intriligator and N. Seiberg, "Duality, monopoles, dyons, confinement and oblique confinement in supersymmetric SO(N(c)) gauge theories," *Nucl. Phys. B*, vol. 444, pp. 125–160, 1995.

[61] D. Kutasov and A. Schwimmer, "On duality in supersymmetric Yang-Mills theory," *Phys. Lett. B*, vol. 354, pp. 315–321, 1995.

[62] K. A. Intriligator, "New RG fixed points and duality in supersymmetric SP(N(c)) and SO(N(c)) gauge theories," *Nucl. Phys. B*, vol. 448, pp. 187–198, 1995.

[63] K. A. Intriligator, R. G. Leigh, and M. J. Strassler, "New examples of duality in chiral and nonchiral supersymmetric gauge theories," *Nucl. Phys. B*, vol. 456, pp. 567–621, 1995.

[64] I. R. Klebanov and M. J. Strassler, "Supergravity and a confining gauge theory: Duality cascades and chi SB resolution of naked singularities," *JHEP*, vol. 08, p. 052, 2000.

[65] M. J. Strassler, "The Duality cascade," in *Theoretical Advanced Study Institute in Elementary Particle Physics (TASI 2003): Recent Trends in String Theory*, pp. 419–510, 5 2005.

[66] C. E. Beasley and M. Plesser, "Toric duality is Seiberg duality," *JHEP*, vol. 12, p. 001, 2001.

[67] D. Martelli, J. Sparks, and S.-T. Yau, "The Geometric dual of a-maximisation for Toric Sasaki-Einstein manifolds," *Commun. Math. Phys.*, vol. 268, pp. 39–65, 2006.

[68] S. S. Gubser, "Einstein manifolds and conformal field theories," *Physical Review D*, vol. 59, no. 2, 1998.

[69] I. R. Klebanov and E. Witten, "Superconformal field theory on three-branes at a Calabi-Yau singularity," *Nucl. Phys.*, vol. B536, pp. 199–218, 1998.

[70] M. Bianchi, S. Cremonesi, A. Hanany, J. F. Morales, D. Ricci Pacifici, and R. Seong, "Mass-deformed Brane Tilings," *JHEP*, vol. 10, p. 027, 2014.

[71] B. Feng, S. Franco, A. Hanany, and Y.-H. He, "UnHiggsing the del Pezzo," *JHEP*, vol. 08, p. 058, 2003.

[72] M. Bianchi and A. Sagnotti, "On the systematics of open string theories," *Phys. Lett.*, vol. B247, pp. 517–524, 1990.

[73] M. Bianchi and A. Sagnotti, "Twist symmetry and open string Wilson lines," *Nucl. Phys. B*, vol. 361, pp. 519–538, 1991.

[74] M. Bianchi, "Open strings and dualities," *J. Korean Phys. Soc.*, vol. 33, pp. S510–S519, 1998.

[75] C. Angelantonj and A. Sagnotti, "Open strings," *Phys. Rept.*, vol. 371, pp. 1–150, 2002. [Erratum: Phys. Rept.376,no.6,407(2003)].

[76] C. Angelantonj, M. Bianchi, G. Pradisi, A. Sagnotti, and Ya. S. Stanev, "Chiral asymmetry in four-dimensional open string vacua," *Phys. Lett.*, vol. B385, pp. 96–102, 1996.

[77] A. M. Uranga, "The standard model in string theory from D-branes," *Nucl. Phys. Proc. Suppl.*, vol. 171, pp. 119–138, 2007.

[78] R. Blumenhagen, B. Kors, D. Lust, and S. Stieberger, "Four-dimensional String Compactifications with D-Branes, Orientifolds and Fluxes," *Phys. Rept.*, vol. 445, pp. 1–193, 2007.

[79] M. Wijnholt, "Geometry of Particle Physics," *Adv. Theor. Math. Phys.*, vol. 13, no. 4, pp. 947–990, 2009.

[80] M. Cicoli, I. n. G. Etxebarria, F. Quevedo, A. Schachner, P. Shukla, and R. Valandro, "The Standard Model quiver in de Sitter string compactifications," *JHEP*, vol. 08, p. 109, 2021.

[81] S. Franco, A. Hanany, D. Krefl, J. Park, A. M. Uranga, and D. Vegh, "Dimers and orientifolds," *JHEP*, vol. 09, p. 075, 2007.

[82] I. Garcia-Etxebarria, B. Heidenreich, and T. Wrase, "New N=1 dualities from orientifold transitions. Part I. Field Theory," *JHEP*, vol. 10, p. 007, 2013.

[83] I. García-Etxebarria, B. Heidenreich, and T. Wrase, "New N=1 dualities from orientifold transitions - Part II: String Theory," *JHEP*, vol. 10, p. 006, 2013.

[84] I. García-Etxebarria and B. Heidenreich, "Strongly coupled phases of $\mathcal{N} = 1$ S-duality," *JHEP*, vol. 09, p. 032, 2015.

[85] I. García-Etxebarria and B. Heidenreich, "S-duality in $\mathcal{N} = 1$ orientifold SCFTs," *Fortsch. Phys.*, vol. 65, no. 3-4, p. 1700013, 2017.

[86] I. n. G. Etxebarria, B. Heidenreich, M. Lotito, and A. K. Sorout, "Deconfining $\mathcal{N} = 2$ SCFTs, or the Art of Brane Bending," 11 2021.

[87] E. García-Valdecasas, S. Meynet, A. Pasternak, and V. Tatitscheff, "Dimers in a Bottle," *JHEP*, vol. 04, p. 274, 2021.

[88] R. Argurio and M. Bertolini, "Orientifolds and duality cascades: confinement before the wall," *JHEP*, vol. 02, p. 149, 2018.

[89] M. Bianchi and E. Kiritsis, "Non-perturbative and Flux superpotentials for Type I strings on the Z(3) orbifold," *Nucl. Phys.*, vol. B782, pp. 26–50, 2007.

[90] M. Bianchi, F. Fucito, and J. F. Morales, "D-brane instantons on the T**6 / Z(3) orientifold," *JHEP*, vol. 07, p. 038, 2007.

[91] Y. Ito and M. Reid, "The McKay correspondence for finite subgroups of SL(3,C)," 1994.

[92] U. Bruzzo, A. Fino, P. Fré, P. A. Grassi, and D. Markushevich, "Crepant resolutions of $\mathbb{C}^3/\mathbb{Z}_4$ and the generalized Kronheimer construction (in view of the gauge/gravity correspondence)," *J. Geom. Phys.*, vol. 145, p. 103467, 2019.

[93] M. Bianchi and J. F. Morales, "Anomalies and tadpoles," *Journal of High Energy Physics*, vol. 2000, no. 03, p. 030–030, 2000.

[94] G. Aldazabal, D. Badagnani, L. E. Ibáñez, and A. M. Uranga, "Tadpole versus anomaly cancellation in d = 4,6 compact iib orientifolds," *Journal of High Energy Physics*, vol. 1999, no. 06, p. 031–031, 1999.

[95] B. Feng, A. Hanany, and Y. He, "Phase structure of d-brane gauge theories and toric duality," *Journal of High Energy Physics*, vol. 2001, p. 040–040, Aug 2001.

[96] S. Franco, A. Hanany, D. Vegh, B. Wecht, and K. D. Kennaway, "Brane Dimers and Quiver Gauge Theories," *Journal of High Energy Physics*, vol. 2006, p. 096–096, Jan 2006.

[97] M. Bertolini, F. Bigazzi, and A. Cotrone, "New checks and subtleties for AdS/CFT and a-maximization," *JHEP*, vol. 12, p. 024, 2004.

[98] D. Berenstein, C. P. Herzog, P. Ouyang, and S. Pinansky, "Supersymmetry breaking from a Calabi-Yau singularity," *JHEP*, vol. 09, p. 084, 2005.

[99] M. Bertolini, F. Bigazzi, and A. L. Cotrone, "Supersymmetry breaking at the end of a cascade of Seiberg dualities," *Phys. Rev.*, vol. D72, p. 061902, 2005.

[100] M. Bianchi, F. Fucito, G. Rossi, and M. Martellini, "On the ADHM construction on ALE gravitational backgrounds," *Phys. Lett. B*, vol. 359, pp. 49–55, 1995.

[101] M. Bianchi, F. Fucito, G. Rossi, and M. Martellini, "Explicit construction of Yang-Mills instantons on ALE spaces," *Nucl. Phys. B*, vol. 473, pp. 367–404, 1996.

[102] A. Lawrence, N. Nekrasov, and C. Vafa, "On conformal field theories in four dimensions," *Nuclear Physics B*, vol. 533, p. 199–209, Nov 1998.

[103] A. Hanany and Y.-H. He, "Non-abelian finite gauge theories," *Journal of High Energy Physics*, vol. 1999, p. 013–013, Feb 1999.

[104] J. Park, R. Rabadan, and A. M. Uranga, "Orientifolding the conifold," *Nucl. Phys.*, vol. B570, pp. 38–80, 2000.

[105] D. Forcella, A. Hanany, and A. Zaffaroni, "Master space, hilbert series and seiberg duality," *Journal of High Energy Physics*, vol. 2009, p. 018–018, Jul 2009.

[106] S. Franco, A. Retolaza, and A. Uranga, "D-brane Instantons as Gauge Instantons in Orientifolds of Chiral Quiver Theories," *JHEP*, vol. 11, p. 165, 2015.

[107] A. M. Uranga, "Brane configurations for branes at conifolds," *JHEP*, vol. 01, p. 022, 1999.

[108] M. Billo, M. Frau, I. Pesando, F. Fucito, A. Lerda, and A. Liccardo, "Classical gauge instantons from open strings," *JHEP*, vol. 02, p. 045, 2003.

[109] M. Billo, M. Frau, F. Fucito, and A. Lerda, "Instanton calculus in R-R background and the topological string," *JHEP*, vol. 11, p. 012, 2006.

[110] R. Blumenhagen, M. Cvetic, S. Kachru, and T. Weigand, "D-Brane Instantons in Type II Orientifolds," *Ann. Rev. Nucl. Part. Sci.*, vol. 59, pp. 269–296, 2009.

[111] M. Bianchi and G. Inverso, "Unoriented D-brane instantons," *Fortsch. Phys.*, vol. 60, pp. 822–834, 2012.

[112] R. Argurio, M. Bertolini, G. Ferretti, C. Petersson, and A. Lerda, "Stringy instantons at orbifold singularities," *Journal of High Energy Physics*, vol. 2007, no. 06, p. 067–067, 2007.

[113] S. Franco, E. García-Valdecasas, and A. M. Uranga, "Bipartite field theories and D-brane instantons," *JHEP*, vol. 11, p. 098, 2018.

[114] E. García-Valdecasas Tenreiro and A. Uranga, "Backreacting D-brane instantons on branes at singularities," *JHEP*, vol. 08, p. 061, 2017.

[115] R. Argurio, M. Bertolini, S. Meynet, and A. Pasternak, "On supersymmetry breaking vacua from d-branes at orientifold singularities," *Journal of High Energy Physics*, vol. 2019, no. 12, 2019.

[116] E. Witten, "Baryons and branes in anti-de Sitter space," *JHEP*, vol. 07, p. 006, 1998.

[117] S. Franco, A. Hanany, D. Martelli, J. Sparks, D. Vegh, and B. Wecht, "Gauge theories from toric geometry and brane tilings," *JHEP*, vol. 01, p. 128, 2006.

[118] S. Benvenuti and S. Giacomelli, "Supersymmetric gauge theories with decoupled operators and chiral ring stability," *Phys. Rev. Lett.*, vol. 119, no. 25, p. 251601, 2017.

[119] S. Elitzur, A. Giveon, and D. Kutasov, "Branes and N=1 duality in string theory," *Phys. Lett. B*, vol. 400, pp. 269–274, 1997.

[120] M. Berkooz, "The Dual of supersymmetric SU(2k) with an antisymmetric tensor and composite dualities," *Nucl. Phys. B*, vol. 452, pp. 513–525, 1995.

[121] P. Pouliot, "Duality in SUSY SU(N) with an antisymmetric tensor," *Phys. Lett. B*, vol. 367, pp. 151–156, 1996.

[122] T. Sakai, "Duality in supersymmetric SU(N) gauge theory with a symmetric tensor," *Mod. Phys. Lett. A*, vol. 12, pp. 1025–1034, 1997.

[123] M. A. Luty, M. Schmaltz, and J. Terning, "A Sequence of duals for Sp(2N) supersymmetric gauge theories with adjoint matter," *Phys. Rev. D*, vol. 54, pp. 7815–7824, 1996.

[124] C. Beasley, B. R. Greene, C. Lazaroiu, and M. Plesser, "D3-branes on partial resolutions of abelian quotient singularities of calabi–yau threefolds," *Nuclear Physics B*, vol. 566, no. 3, 2000.

[125] B. Feng, S. Franco, A. Hanany, and Y. He, "Unhiggsing the del pezzo," *Journal of High Energy Physics*, vol. 2003, no. 08, 2003.

[126] B. Feng, Y. He, and F. Lam, "On correspondences between toric singularities and -webs," *Nuclear Physics B*, vol. 701, no. 1-2, 2004.

[127] S. S. Gubser and I. R. Klebanov, "Baryons and domain walls in an N=1 superconformal gauge theory," *Phys. Rev. D*, vol. 58, p. 125025, 1998.

[128] D. Freedman, S. Gubser, K. Pilch, and N. Warner, "Renormalization group flows from holography supersymmetry and a c theorem," *Adv. Theor. Math. Phys.*, vol. 3, 1999.

[129] A. Hanany and R. Seong, "Brane tilings and specular duality," *Journal of High Energy Physics*, vol. 2012, no. 8, 2012.

[130] Y. Tachikawa and B. Wecht, "Explanation of the Central Charge Ratio 27/32 in Four-Dimensional Renormalization Group Flows between Superconformal Theories," *Phys. Rev. Lett.*, vol. 103, p. 061601, 2009.

[131] A. Amariti, M. Fazzi, S. Rota, and A. Segati, "Conformal S-dualities from O-planes," *JHEP*, vol. 01, p. 116, 2022.